The effect of hygroscopicity on the delivery of salbutamol salts to the lung

Thompson, James Anthony

Award date:
2005

Awarding institution:
University of Bath

THE EFFECT OF HYGROSCOPICITY ON THE DELIVERY OF SALBUTAMOL SALTS TO THE LUNG

Submitted by:

James Anthony Thompson

For the degree of Doctor of Philosophy,

Of the University of Bath,

Department of Pharmacy and Pharmacology.

August 2005

ProQuest LLC
789 East Eisenhower Parkway
P.O. Box 1346
Ann Arbor, MI 48106-1346

ACKNOWLEDGEMENTS

I have to say thanks to many people over many years for help and support upon completion of this work.

Firstly I would to thank Jim Wells, my first academic tutor, for his guidance and passion for science. As well as a fine tutor he has become a person I am glad to call a friend even though time and distance has divided our paths. Our discussions in the Ship and Mitre are some of the happiest times I spent in Liverpool.

Following on the academic theme a lot of thanks and appreciation goes to Dr Rob Price, for helping me and encouraging me to complete this work. Also, special thanks to Dr Paul Young and Dr Dani Traini for help, support and friendship through this ordeal. A final thanks goes to the ever changing post grads in the pharmaceutics department: Dina, Sebastian, Philippe and Camille.

Thanks to two good mates from Liverpool for their friendship over many years: Mr G. Smyth for an education regarding an initial introduction into inhaled drug delivery, and Mr M. Bradley for his skill into the art of typing and formatting. I will be eternally grateful and forever in their debt.

Thanks to my wife Sam for her constancy throughout the whole of this journey. Her love and support have been an inspiration and without her this would not have been completed. She has been there for me when not only was there no light at the end of the tunnel, but the tunnel wasn't even in view. Hopefully it will be the Dr Jekyll and not Mr Hyde she sees from now on; sorry for the papers being everywhere!

Finally a thank you to my daughter, Jasmine Katie whom has taught me that it:

"Does not do to dwell on dreams and forget to live"

If I could, I would trade all of the work here and the same again so that she could meet my mother. Unfortunately this will never happen, a great tragedy, as I am sure they would have got on well together.

As I come to the end of something I have searched so long and hard for, and in passing thinking about all the events in between, in summary the words of a genius have an air of inevitability

There are only two tragedies in life: one is not getting what one wants, and the other is getting it.

(Oscar Wilde 1854-1900)

ABSTRACT

Since its inception, some 50 years ago, the pressurised metered dose inhaler has become the most widely prescribed medicament for a number of respiratory conditions. Unfortunately, the dosage form has remained virtually static in terms of pharmaceutical development, with success measured from clinical perspectives being largely viewed as an amelioration of the classic symptoms frequently exhibited.

The complexity of the dosage form has dictated that the fundamental processes of aerosol production are not totally characterised, nor fully understood. It was the intention, therefore, of this thesis to investigate and appropriate a better understanding of the fundamental pharmaceutics of pressurised HFA aerosol systems, resulting from the influence of environmental conditions on particle size distributions of the aerosol clouds generated.

To facilitate investigations, several, novel, model bronchodilator derivatives were synthesised, characterised and formulated as novel pressurised solution based inhalers. From the data generated, it was possible to formulate screening and production methodologies for both solution and suspension products, and of the derivatives synthesised the two chosen for study were the cis butenedioate (maleate), and the cis octadecenoate (oleate), as these were both ethanol soluble and were hydrophilic and hydrophobic in nature. Theoretically, calculated solubility levels correlated well with practical determinations, and, in conjunction, solubility was determined in HFA anti-solvent and a range of ethanol and co-solvent mixtures. In order to maintain solution stability, when formulated at a clinically therapeutic level, 15% w/w co solvent and 30% w/w co solvent levels were required for the maleate and oleate respectively. Ultimately, from the data generated, it presented a possible method to predict solution stability from a theoretical approach rather than purely visual empirical levels alone.

The effects of temperature, and thus vapour pressure, on the resulting particle size distributions of hydrophilic salt solutions, (formulated at 15 and 20% w/w) in pressurised formulations were investigated under a range of standard pharmacopeial testing conditions: 4 and 37ºC, respectively. Results indicated that particle size distribution patterns were not significantly different when compared on an intra formulation basis over the range, but stage depositions were statistically different when compared on an or inter formulation level, particularly at high temperatures.

Statistical differences were also noted in MMAD, GSD, and fine particle dose and throat deposition for a number of combinations. The data lead to the generation of a semi-empirical equation to predict the MMAD from the incorporation of inherent physicochemical characteristics: pressure, surface tension, viscosity, formulation composition and inhaler hardware tolerances.

Finally, a comprehensive matrix of testing was performed over a range of temperature and humidity profiles on both the hydrophobic and hydrophilic derivatives formulated as solution-based inhalers. The anticipated effects of hygroscopicity on the delivery of salbutamol salts to the lung were not as initially postulated. It was evident that cloud dynamics were modified depending on the salt derivative within both primary and secondary aerosolisation mechanisms. In conjunction, the hydrophilic salt gave a different distribution pattern to that of the hydrophobic, primarily due as hypothesised, to the chemistries of the molecules. It was also evident that the major particle parameters could be manipulated, standard lab conditions did not reflect those when tested under simulated *in-vivo* conditions in the lab, and particle deposition morphologies were substantially different. Statistical significances were evident for the major particle parameters when compared for both intra and inter formulations.

In conclusion it may be possible from the careful selection of drug derivative, formulation, and environmental conditions to preferentially deposit therapeutic drug particles to specific locations within the lung.

List of common Abbreviations

Abs.	Absorbance
ACI	Andersen Cascade Impactor
ACE	Angiotension Converting Enzyme
Act	Actuator
(c) AMP	(cyclic) Adenosine monophosphate
ANOVA	Analysis of Variation
BAD	Breath Actuated Device
BCD	Breath Coordinated Device
BOD	Breath Operated Device
b.p	Boiling Point
COMT	Catechol Ortho Methyl Transferase
Conc (c)	Concentration
COPD	Chronic Obstructive Pulmonary Disease
Cp	Heat Capacity (constant Pressure)
CFC	Chlorofluorocarbons
CLG	Compressed Liquefied Gas
CV	Coefficient of variation
Cv	Heat Capacity (constant volume)
d_o	Spray orifice diameter
D	Diameter
D (ρ)	Particle Density
d_{ae}	Aerodynamic diameter
DD	Delivered dose (Ex-device)
DPI	Dry Powder Inhaler
DSC	Differential scanning Calorimetry
DV (μ)	Dynamic viscosity
ECD_{50}	Effective Cut-Off Diameter: Equivalent mass of oversized to the mass of undersized particles in an ideal collection apparatus.
ED	Emitted Dosed
EGF	Epithelial Growth Factor
FEV_1	Forced expiratory volume in one second
FVC	Forced Vital Capacity

GM-CSF	Granulocyte Macrophage Colony Stimulating Factor
GRR	Growth rate ratio
GSD	Geometric Standard Deviation
HFA 134(a)	Hydrofluoroalkane 134(a): 1,1,1,2-Tetrafluoroethane
HPLC	High Performance liquid Chromatography
HRH	High Relative Humidity
5HT	5 Hydroxy Tryptamine
HT	High Temperature
I.R.	Infrared Spectroscopy
IL-1β	Interleukin 1 Beta
INT.	Intensity
LRH	Low Relative Humidity
LT	Low temperature
LPF	Large Particle Fraction
MAO	Monoamine Oxidase
m.p	Melting Point
MD	Metered Dose
MCP	Monocyte Chemotactic Peptide
MMAD	Mass Mean Aerodynamic diameter
ND	Not Determined
NSA	Novel Solubility Apparatus
NFκB	Nuclear factor Kappa Beta
NVC	Non volatile component
P	Pressure
pH	Potential of Hydrogen
pMDI	Pressurised metered dose inhaler
PEF	Peek Expiratory Flow
q	Charge
r	radius
RAO	Reversible Airway Obstruction
R.H.%	Percentage Relative Humidity
RSD	Relative Standard deviation
SD	Standard Deviation
SEM	Scanning Electron Microscopy
ST (σ)	Surface tension
Th_2	T helper cell
VMD	Volume mean diameter

We	Weber Number
XRC	X-RayCrystallography

1 INTRODUCTION 1

1.1 The Respiratory system: Structure and Function 1
1.2 Physiology and Pharmacology of the Airways 6
1.2.1 The epithelium 6
1.2.2 Smooth Muscle 7
1.2.3 Submucosal glands 8
1.2.4 Mucociliary Clearance 8
1.3 Asthma 9
1.3.1 Definition 9
1.3.2 Intrinsic and Extrinsic Asthma 9
1.3.3 Physiology and Pharmacology of an asthma attack 10
1.3.4 Prevalence 11
1.4 Salbutamol and the Bronchodilator family 11
1.4.1 Pharmacology and Mechanism of action 11
1.4.2 Receptors and receptor subtypes 12
1.4.3 Structure Activity Relationships 13
1.4.4 Enantiomers 14
1.4.5 Efficacy and Potency 15
1.5 Particle Deposition Mechanisms in Human Airways 15
1.5.1. Introduction 15
1.5.2. Inertial Impaction 16
1.5.3 Sedimentation 17
1.5.4 Brownian motion 18
1.6 Aerosol Characteristics and Definitions 18
1.6.1 Definition 18
1.6.2 Size Distribution 18
1.6.3 Geometric Mean Diameter (GMD) 19
1.6.4 The Mass Median Diameter (MMD) 19
1.6.5 Mass Mean Aerodynamic Diameter (MMAD) 19
1.6.7 Geometric Standard Deviation (GSD, σ_g) 20
1.7 Inhalation aerosol delivery devices 20
1.8 Selection of a Delivery System 21

1.8.1 Nebulisers 21
1.8.2 Dry Powder Inhalers 22
1.9 Metered Dose Inhalers 24
1.9.1 Introduction 24
1.9.1 (a) Basic Operation 25
1.9.1 (b) Disadvantages of Pressurised systems 26
1.10 Pressurised metered Dose Inhalers: The Current Situation 28
1.10.1 General Discussion 28
1.11 Solutions versus Suspensions (Pros and Cons) 28
1.11.1 General Discussion 28
1.12 Aims of the study 30
1.12.1 Discussion 30
1.12.2 Experimental Rationale 30
1.12.3 Salbutamol Derivatives: Synthsesis, practical solubility evaluation and predictive solubility theory of novel bronchodilators. 30
1.12.4 Pre-formulation Studies: Characterisation of Novel Derivatives 30
1.12.5 Formulation Variables: The effect of temperature, co-solvent level and drug structure on cloud formation and the semi-empirical prediction of particulate aerosol cloud size 31
1.12.6 Environmental Variables: The effect of temperature, humidity, drug structure and formulation on cloud formation 31
2 METHODS AND MATERIALS 32
2.1 Materials 32
2.2 Salbutamol Salts: Selection criteria and synthesis. 32
2.2.1 Rational Drug Salt Selection 32
2.2.2 Salt Characteristics 33
2.2.3 Counter Anion and its effects on Salt Character 35
2.2.4 Acid Selection: Solubility Considerations 36
2.2.5 Synthesis of Salt Derivatives 37
2.2.6 Final Salt Selection 38
2.3 *In-Vitro* Particle Size Analysis 39
2.3.1 Particle Size Distribution Analysis 39
2.3.2 The Andersen Cascade Impactor 40

2.3.3 Impactor Calibration and In Study Use 42
2.4 Statistical Analysis 43
2.5 Differential Scanning Calorimetry. (DSC) 44
2.5.1 Materials and Methods 44
2.5.2 Results and Discussion 44
2.6 Infrared Spectroscopy 46
2.6.1 Methods and Materials 46
2.6.2 Results and Discussion 46
2.7 X-Ray Crystallography 48
2.7.1 Materials and Methods 48
2.7.2 Results and Discussion 48
2.8 Fluorescence Spectroscopy 50
2.8.1 Materials and Methods 50
2.8.2 Results and Discussion 51
2.9 High Performance Liquid chromatography 52
2.9.1 Materials and Methods 52
2.9.2 Results and Discussion. 52
3 THE EFFECTIVE SOLUBILITY OF SALBUTAMOL SALT DERIVATIVES IN PMDI MEDIA 53
3.1 General Overview 53
3.2 Initial solubility and stability investigations via visual assessment 53
3.2.1 Methods and Materials 55
3.2.2 Results and Discussion 55
3.2.3 Conclusion 56
3.3 Theoretical Evaluation of derivative solubility as a function of the Co-solvent. 59
3.3.1 General Discussion 59
3.3.2 Theoretical Determination of Solubility 61
3.2.3. Conclusion 62
3.4 Experimentally Determined Solubility of Salt Derivatives as a Function of Co-solvent. 62
3.4.1 Introduction 62
3.4.2 Methods and Materials 62

3.4.3 Results and Discussion 63
3.4.4 Conclusion.....64
3.5 Experimentally Determined Solubility of Salt Derivatives as a Function of 134(a) the Anti-solvent. 66
3.5.1 Introduction.....66
3.5.2 Methods and materials 66
3.5.3 Results and Discussion 68
3.6 Experimentally Determined Solubility of Salt Derivatives as a Function of Ethanol and 134(a) Mixtures. 71
3.6.1 Methods and Materials 71
3.7 Introduction to a novel model for Predicting Solubility in pMDI systems: A Theoretical Approach. 72
3.8 Solubility Data: Comparison of intra-formulation solubility profiles. 73
3.8.1 Intra-formulation evaluation: Data Discussion 73
3.9 Application of the novel solubility concept: Theoretical vs. visual stability correlation.....74
3.9.1 Conclusion.....76

4.0 *IN VITRO* EVALUATION OF NOVEL SOLUTION FORMULATIONS UNDER NON-STANDARD LABORATORY TESTING CONDITIONS.....80

4.1 Aerosols: An Introduction.....80
4.2 Overview of Droplet Formation Mechanisms. 81
4.3 Practical Evaluation of Droplet Formation: Previous Studies.....83
4.4 Multi-component Aerosol Systems 84
4.5 Aerosol Device performance 85
4.6 Aerosol Device Optimisation.....86
4.7 In-vitro determination of PSD's emitted from a novel solution pMDI.....86
4.7.1 Introduction.....86
4.7.2 Methods and Materials 87
4.7.3 Results and Discussion 89
4. 7.4 Conclusion.....97
4.8 Current Semi-Empirical Methods to Predict MMAD's of pMDI's. 100
4.8.1 Derivation of an equation to predict MMAD's generated from solution based pressurized metered dose inhalers. 101

4.8.2 Evaluation of the Geometric Standard Deviation. 104
4.8.3 Conclusion 104

5 THE EFFECTS OF ENVIRONMENTAL CONDITIONS ON THE AEROSOL CHARACTERISTICS OF NOVEL SOLUTION PMDI'S 106

5.1 Introduction 106
5.2 Overview of the Thermodynamic Properties of Inhaled Aerosol Particles 107
5.2.1 Present Theoretical models: A brief review 107
5.2.2 Improved theoretical models. 108
5.2.3 Experimental investigations of environmental influences on aerosol behaviour: An overview of laboratory systems 109
5.2.4 Experimental Set-up: In-vitro environmental control in this study .. 110
5.3 Methods and Materials 110
5.4 Results and Discussion 114
5.4.1 Introduction 114
5.4.2 Primary and secondary mechanisms of particle formation and associated aerosol fractions: A brief summary of definitions 115
5.4.3 Tabulated Data Summaries 116
5.4.4. The effect of temperature variation and constant relative low humidity testing conditions on the deposition patterns of salbutamol salt formulations. 120
5.4.5. The effect of temperature variation and constant high relative humidity testing conditions on the deposition patterns of salbutamol salt formulations. 122
5.4.6. The effect of relative humidity variation and constant low temperature testing conditions on the deposition patterns of salbutamol salt formulations. 125
5.4.7 The effect of relative humidity variation and constant high temperature testing conditions on the deposition patterns of salbutamol salt formulations. 128
5.4.8 The effect of environmental testing conditions on the MMAD and of salbutamol salt formulations. 130

5.5. Inter formulation comparisons of the Particle Size Distributions produced from Novel solution pMDI's.....133
5.5.1 General Discussion 135
5.5.2 Inter formulation comparisons: The effects of environmental testing conditions on particle deposition patterns from novel solution pMDI's.....135
5.6 The effect of environmental testing condition on the major primary and secondary particle production mechanisms.....137
5.7 Data evaluation and discussion of the possible mechanisms resulting in the particle size deposition patterns of novel solution pMDI' formulations.....142
The Effects of Environmental Conditions on Drug Delivery 147
6 CONCLUSIONS AND RECOMMENDATION FOR FUTURE WORK 149
APPENDICES FOR CHAPTER 1.....156
APPENDICES FOR CHAPTER 2.....158
APPENDICES FOR CHAPTER 3.....165
APPENDICES FOR CHAPTER 4.....171
APPENDICES FOR CHAPTER 5.....177
REFERENCES 180

1 INTRODUCTION

1.1 The Respiratory system: Structure and Function

The delivery of aerosol particles to the respiratory tract is a complex process highly dependent upon a number of multifaceted and intrinsically related parameters: the composition of the formulation, the method of generation (pMDI, DPI, nebuliser), the patient's ventilatory parameters (e.g. whether sedentary, light or heavy breathing rates and inspiratory volumes) and, ultimately, the respiratory system itself (related to the structure and unique environmental profiles, i.e. branching patterns, temperature gradients and humidity profiles). A schematic representation of the respiratory system, together with approximate penetration power of aerosol particles of varying particle size, is shown in figure 1.0.

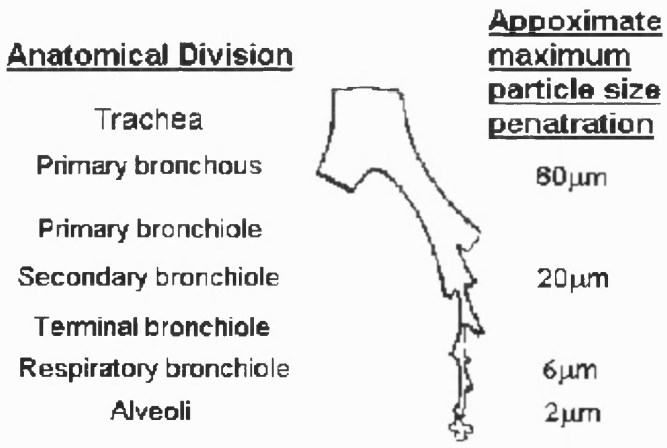

Figure 1.0 ***A schematic representation of the human respiratory system.***

The respiratory system has been described within numerous texts; and, perhaps the principal treatise describing its physical structure was proposed by the anatomist Weibel, (Weibel, 1963). The main functionality of lungs can be divided into two principal categories: those of the respiratory and non-respiratory respectively; respiratory functions include gas exchange mechanisms and the maintenance of acid base balance, and the non-respiratory functions include modulation of both the endocrine and metabolic activities. Respiration, *per se*, requires gas exchange facilitating the transport of oxygen into the blood and the removal of carbon dioxide from the circulation. The airways, themselves, provide the path of least resistance to airflow during both inhalation and

exhalation, and, so, allow gas exchange to take place in the alveoli. Further, the lungs themselves, from an anatomical perspective, are divided into two zones or compartments namely the conducting zone and the respiratory zone.

Both zones are divided for clarity into "generations", which describe the major airway brancheing patterns. The airway generations commence at the trachea designated arbitrarily generation 0, and terminate at the alveolar sacs culminating at generation number 23. The conducting zones consist of the first 16 of the aforementioned generations, initiating at the trachea, and dichotomously branch into smaller bronchi and bronchioles, ending in the terminal bronchioles.

The respiratory zone is defined as the "architectural portion" of the respiratory tract participating in gas exchange beginning with the respiratory bronchioles containing the alveoli, and these airways further subdivide into additional respiratory bronchioles, eventually giving rise to the alveolar ducts and sacs respectively.

The branching patterns of the airways of the respiratory tract have been described previously (Horsfield et al 1971 and Menkes et al. 1986), with two primary characteristic properties of the branching airways being shown to have a major impact on lung function: the decrease airway of calibre and the subsequent increase in surface area. The bifurcating airways concomitantly decrease in diameter and length, but their increase in number leads to a greater cross sectional area. Thus, the ratio for each bifurcation is 2, and with N representing the number branches in each generation, then the number of respiratory airways (z) is dictated by the following equation:

$$N(z) = 2^z \qquad \textit{Equation 1.0}$$

Where N is the number of branches and z is the airway generation.

The constant decrease of airway diameter and increase in surface area ensures optimal flow of bulk air through the system. Couple this with fact that the respiratory bronchioles and alveolar ducts change very little with new generations, then the cross sectional area effectively doubles with each new airway generation beyond generation 16. The relative physical dimensions, cross sectional areas and volumes are given in appendix A 1.1.

Other structural modifications also assist in airway function. As one descends the lung, distal to the oropharynx, the amount of supporting cartilage decreases, and the posterior aligned "C " shaped rings located at the trachea to provide physical support diminish, and such reductions facilitate airway compliance and patency.

Ancillary morphological features, of the distal airways, which assist in airflow, are the collateral channels. These structures namely the pores of Kohn facilitate and allow airflow between neighboring acini and alveoli (Menkes et al. 1986), and were once thought to be artifacts resulting from microscopic fixation procedures. Their exact physiological significance has not been evaluated. In conjunction, other connections exist. For example, Martin has demonstrated inter bronchiolar channels in canine lungs (Martin 1966), and both Lambert and Boyden have described channels connecting respiratory bronchioles, alveolar ducts and sacs in adjacent lung acini found in human tissues (Lambert 1955, Boyden 1971). All of these structures provide an alternative pathway for air to flow in the event of occlusions occurring, as in diseased states. It is unlikely, however, whether these would be of great importance if a major bronchus were obstructed. As well as the structures described, other changes occur in histology and morphology throughout the respiratory tract that may impart influence on both lung function and pathophysiology. These can be summarised briefly as variations in cell types such as epithelial cells, which line the airway lumen, mucus secreting glands, airway smooth muscle, respiratory nerves and blood vessels

Blood supply to the lungs is divided between the pulmonary and systemic circulations (Fishman 1985 and Grover et al 1984). The pulmonary circulation consists of a highly vascularised bed that exits the right side of the heart via the pulmonary artery, and, subsequently, branches into a vascular capillary bed encasing the alveoli. These finally, reconnect to form the pulmonary veins that drain into the left side of the heart. The whole cardiac output, therefore, flows through the pulmonary circulation, which operates under both low pressure and resistance. The vessels contain very little, if no, arterial smooth muscle tone resulting in a mean pressure of 15mm Hg (c.f. systemic circulatory pressures of 100mmHg), and, in conjunction, can distend and collapse. The properties of low pressure, distensible vessels and the alveolar pressure of the interstices result in asymmetric flow of blood, sensitive to the effects of gravity. The pressure gradients resulting from arterial, venous and alveolar pressures result in blood flow independence on alveolar pressure depending on cardiovascular parameters (pressure, geometry and smooth muscle tone).

Gas exchange occurs at the alveolar-capillary boundary by diffusion. The concentration and partial pressures that exist between the alveolus and the surrounding capillary bed dictate this passive transport. Within the alveolus, the partial pressure of oxygen is approximately 104 mmHg as compared to that of deoxygenated capillary blood that is 40mmHg, providing the driving force of oxygen exchange. In conjunction, carbon dioxide experiences the opposite concentration gradient having a greater capillary to alveolar pressure of 5mmHg, driving transport in the opposite direction.

Blood flow is regulated by both active and passive mechanisms. The passive involves dilation of micro-vessels, which accommodates increased blood flow without any large changes in pressure; and, the major active mechanism involves the response to alveolar hypoxia. In certain circumstances, alveoli may become poorly ventilated resulting in low oxygen tension and pulmonary artery constriction, which reduces blood flow to poorly ventilated areas redirecting them to areas of higher oxygen tension.

Other functions of the pulmonary circulation involve metabolic processes. For example, the conversion of inactive to active hormones i.e. angiotensin II from I by ACE on endothelial cells, catabolic processes including molecules such as bradykinin, 5HT, tryptamine, peptides and hormones and the release of bioactive mediators into the system.

As well as the pulmonary circulation, the lungs receive blood supply from the systemic circulation, commonly refered to as the bronchial circulation. The bronchial fraction of the pulmonary circulation serves to deliver essential nutrients to the tracheobronchial portion of the respiratory tree incorporating tissues, muscle cells, nerves and glands as well as the associated arteries, veins and pleura. However, this is separate from the respiratory zone, which receives its sustenance from the pulmonary circulation, and, functionally, performs several essential tasks:

(a) It assists in the heating and humidification of inspired air,
(b) It assists in gas exchange and essential nutrient support when the pulmonary circulation is obstructed (by dilation and connections with capillaries helping with blood flow),
(c) It is a major player in inflammatory conditions in the lung, being involved in oedema and transportation of inflammatory cells and mediators to the airways.

Finally, the bronchial circulation provides the only angiogenic section of the lung that provides new blood vessels requisite to vascularise new tissue

1.2 Physiology and Pharmacology of the Airways

1.2.1 The epithelium

The entire respiratory tree is covered with a layer of epithelial cells, which have a varied and, consequently, wide range of functions as illustrated in table 1.0.

Cell	Situation	Function
Columnar	Trachea toTerminal respiratory bronchioles	Mucocilary escalator Glycoprotein secretion
Basal	Trachea and main Bronchi	Progenitor cell. Aid in attachment of columnar cell to basement membrane
Goblet	Trachea and main Bronchi	Progenitor cell line for ciliated cells; mucus secretor
Clara	Bronchioles	Glycoprotein secretion, Progenitor for ciliated and Clara cells, Serous Xenobiotic metabolism
Brush	Infrequent	Transitional cell
Serous	Infrequent	Transitional cell
Intermediate	Bronchi	Paracrine Non-endocrine chemoreceptor function
Alveolar Airways		
Type I Pneumocyte	Alveoli	Gas exchange media up to 97% of alveolar surface
Type II Pneumocyte	Alveoli	Surfactant secretion, Type I progenitor cell

Table 1.0: The structure and function of cells associated with the airway epithelium.

In essence, the epithelial lining acts as a "barrier" in preventing interaction between aeroallergens and the sub-mucosa of the lungs (Holgate 2003), including particulate contaminats such as dusts, bacteria, smoke and noxious chemicals. Indeed, pharmacologic agents, from a physiologic sense, fall into this category. The structure of the lining is enhanced via mucus secretions and from the highly specialised tight

intercellular junctions. These junctions substantially reduce the amount of material reaching sub-epithelial airway structures (Sturgess 1989).

The most prominent cells identified within the epithelium are those of the ciliated columnar cells. These line the complete airway from the trachea through to the respiratory bronchioles and concomitantly diminish in size and proportion as the airways are penetrated. Their primary function is to remove mucus from the lower airways to the upper where it is either expectorated or swallowed accordingly. In addition, ciliated cells secrete glycoproteins, which contribute to the mucus layer. Epithelial goblet cells also secrete mucus and are abundant within the conducting airways, but are absent in the bronchiole, and have been implicated as the progenitors for ciliated cells (Evans et al 1986). Other cell types found include the basal and clara cells. Basal cells also predominate within the epithelium, and act as attachments for columnar cells to the basement membrane (Evans et al 1989). Clara cells can be situated within the bronchioles and like other counterparts secrete mucus but also participate in the metabolism of Xenobiotic substances.

Within the alveoli, two cell types are found: type I and type II pneumocytes. Type I are responsible for gas diffusion and gas exchange, and type II are responsible for surfactant production.

1.2.2 Smooth Muscle

Smooth muscle is distributed through the entire tracheobronchial tree and is separated from the epithelium via a layer containing nerves, blood vessels and connective tissue commonly known as the lamina propia. And, muscle phenotype depending on location exhibits different spatial arrangements. For example, in the trachea it covers the posterior surface, while it completely surrounds the centralized bronchi and bronchioles and, acts like a sphincter, which contracts when stimulated. The amount and distribution of the smooth muscle, like the epithelium, decreases within the lower airways, but strands of smooth muscle can be found as far as the terminal bronchioles and have even been observed down to the level of the alveolar ducts. During contraction, smooth muscle can cause extensive narrowing of the lumen, and when coupled with deposition of mucus plugs and cellular debris can cause severe airflow restrictions (As depicted in equation 1.1). In diseased states, smooth muscle can be stimulated to increase in size and number, and hypertrophy and hyperplasia may ensue.

1.2.3 Submucosal glands

Present in cartilaginous airways, but absent in non-cartilaginous counterparts, these structures display four distinct morphological regions extending from their distal to proximal ends, which in turn exhibit associated functionality: serous tubules lined with secreting cells terminating in acini, mucus tubules with associated secreting cells, columnar collecting ducts, and, finally, a ciliary excretory duct. Excreted serous fluid carries mucus from the mucus tubules post migration, and travels into the collecting ducts, which is finally expelled with the mucus onto the airway epithelial surface. (Meyrick et al 1969)

1.2.4 Mucociliary Clearance

The chemistry of the mucus secreted onto the epithelial surface is a complex cocktail of compounds including glycoproteins, immunoglobulins, surfactants and a variety of other components. Physically, it is biphasic in nature, and has a low viscosity sol layer in contact with the epithelial surface, and conversely a high viscosity gel layer that sits on the surface top of the sol layer, separated by a biphospholipid layer; functionally, it facilitates several important functions

(a) It prevents dehydration,
(b) It saturates incoming air to equilibrate to saturated water vapour content,
(c) It provides a protective barrier through physical 'trapping', antimicrobial, and metabolic action (Basbaum and Finkbeiner 1989).

For example, when an aerosol particle is deposited within the airways, it is carried by coordinated cilia beats, transporting foreign particulates upwards to the tracheobronchial region, and as the size of the airway increases so does the rate of clearance.

1.3 Asthma

1.3.1 Definition

There is no single, universal and all encompassing definition of asthma. Indeed bronchial asthma and chronic obstructive pulmonary disease are generally considered two respiratory maladies that share functional abnormalities. The separation of the two respiratory conditions relies upon the force of the expiratory flow rates, specifically the FEV_1 value from total lung capacity. Utilising this reliable and non-invasive measurement allows subsequent classification of the two syndromes. In asthma the airflow limitation is reversible whereas, in COPD the situation is poorly reversible or irreversible (Romagnoli et al 1999).

1.3.2 Intrinsic and Extrinsic Asthma

Asthma can be divided into two categories from aetiology: intrinsic and extrinsic. Intrinsic asthma tends to occur later in life, and its mechanism of action is not completely understood. Extrinsic asthma, which is the more common form of the disease, results from an allergic response mediated by Immunoglobulin E (IgE), which results from the invasion of foreign proteins, and these present themselves as aeroallergens to those atopic and highly susceptible individuals (Finnerty and Holgate 1989). Other extrinsic agents such as chemicals such as toluene diisocyante (Maestrelli et al 1995) have also been implicated in non-IgE mechanisms, but display a T helper cell Th_2/Tc_2 profile. In these cases, it is difficult to explain what links asthma with atopy and the ability to generate IgE as a direct response to commonly recognized environmental allergens that predispose only one-seventh of those subjected to develop this disease.

1.3.3 Physiology and Pharmacology of an asthma attack

At the onset an acute asthma attack both bronchial smooth muscle contraction, and hypertrophy of the bronchial muscle occur in chronic conditions, which, in turn, reduces the size of the bronchial lumen thus restricting airflow. This restriction in airflow can be related to Poiseuille's law for laminar flow of a fluid through a pipe. Although the bronchial tree does not meet all the requirements of the law *per se*, it provides a useful approximation of the resistance to the airflow. The mathematical expression for Poiseuille's law is described in equation (1.1) below:

$$F = \frac{\pi \Delta \mathrm{Pr}^4}{\eta.8.L} \qquad \text{Equation 1.1}$$

Where F is the laminar flow of the fluid, ΔP is the driving pressure, r is the vessel radius, η the fluid viscosity and L is the vessel length.

From this relationship it can be seen, as the radius of an airway decreases, say by a half, then, a significant increase in the resistance to flow increases (approximately a 16 fold increase). In addition to the reduction in the available space of the lumen, the underlying mucosa becomes oedematous, and flooded with a number of inflammatory cells (Dunnill et al 1969). Wide ranges of cells are present during the progression of the inflammatory mechanisms: mast cells, macrophages, leukocytes and predominantly eosinophils are distributed within both in the mucosa and the epithelial lining of the respiratory tract. A further morphological consequence post inhalation of an allergen is the denudation of the bronchial epithelium, which has been suggested and erstwhile described, as the primary barrier to allergens (Holgate 1999). In conjunction, the epithelium as well as being implicated as the principal target for the inflammatory response, is also a major source of inflammatory cytokines and mediators. These bio-chemicals express different patterns of adhesion proteins orchestrating airway remodeling and are the major target for the delivery of anti-inflammatory drugs. This highlights the importance of understanding the histological structure of the epithelium and its nature in the delivery of therapeutic aerosols.

1.3.4 Prevalence

Regrettably, there have been a number of deaths related to asthma, but the data accumulated from epidemiological studies dating from the 1960's have greatly advanced our understanding of the disease. Factors relating to the prevalence of asthma can be attributed to the following rather limited, but not exhaustive list of examples: air pollution, asprin intolerance, the use of beta adrenreceptor agonists, age and socioeconomic variables (damp housing, smoking, urban environment etc). The majority of cases are mild (Auerbach et al 1993) and it is estimated that approximately 14 million people are affected in the USA alone with the mild form of the disease. It is the most chronic disease of childhood (Newacheck et al 1986), and is a common disease of medical emergencies (Kerem et al 1990). The burden of asthma appears to be on the increase globally, particularly in areas undergoing rapid urbanization and asthma is now a global concern (Beasley et al 1992).

Recently the largest increase in world asthma has been in New Zealand (approximately a 34% increase, Wickens et al 1999). One possible cause behind such an increase can be related to the "hygiene theory". As the country has little pollution and good air quality, it is theorised that from the reduction in exposure to a variety of aeroallergens, subjects may result in hightened sensitivity, when exposed to such agents in the longer term.

1.4 Salbutamol and the Bronchodilator family

1.4.1 Pharmacology and Mechanism of action

Sympathomimetic agents are one of the most extensively prescribed classes of medication for the alleviation of asthma, the use of which dates back to pre-Christian times. The efficacy of these compounds stems from their molecular structure, which are similar in base architecture and functional group location to natural agents such, as ephedrine, which exerts its effect via an indirect release mechanism of catecholamines from storage granules, specifically adrenaline whose effects are mediated via direct action upon cell membrane receptors. Over the past few decades, developments in pharmacology have elucidated a range of membrane receptors that respond with specificity and receptivity to different families and classes of therapeutic compounds. Classification of alpha and beta-adrenergic receptors was originally proposed in the

1940's by Alquist, whereby the alpha forms were those blocked by ergot and beta by isoprenaline (Campbell and Soyka 1976).

1.4.2 Receptors and receptor subtypes

The biochemical mechanism of action of β_2 agonists is well established, and the smooth muscle tone responsible for airway lumen size within the respiratory bronchioles is ultimately regulated by intracellular calcium (Ca^{2+}) ion concentration. In essence, the cascade mechanisms that occur are complex and beyond the scope of this thesis, but in brief, contraction occurs when (Ca^{2+}) enters the smooth muscle cell or is released from intracellular stores, which firstly binds with calmodulin. The resulting complex activates a second kinase: myosin light chain kinase (MLCK), which in turn phosphorylates myosin light chains (MLC's). From this stage, promotion of the interaction of myosin ATPase and actin forms cross-bridge linkages and smooth muscle contraction occurs. However, when β_2 receptors are activated the enzyme adenylate cyclase initiates the conversion of cyclic AMP (cAMP) from ATP. The activation of cAMP protein kinase phosphorylates MLCK decreasing its activity, which finally results in a decreased affinity of (Ca^{2+})-calmodulin for MLC kinase and so results in bronchodilation

During the 1960's (Lands et al 1967), further sub-divided the beta adrenoreceptors into β1 and β 2 respectively, with cardiac responses (chronotropy and inotropy) mainly mediated through the β_1 receptor, while the receptors mediating the desired airway effect belonging to the β_2. The β_2 receptor is a ubiquitous moeity and can be found in other tissues: skeletal muscle, blood vessels and myocardium, which elicit systemic side effects (palpitations, tremors) even with the most selective of agents. The final structure of the β_2 receptor has not been fully described. A brief summary of the effects of adrenergic stimulation are provided in appendix A 1.2

1.4.3 Structure Activity Relationships

The efficacy of current synthetic adrenergic agonists results from their structure, which is based on the catecholamine sub-unit. They are inactivated in-vivo, swiftly, by one of two methods: type I uptake whereby storage vesicles reabsorb the compounds, or type II inactivation by the enzyme catecholamine-O-methyl transferase (COMT). The type II mechanism further proceeds, after methylation at the 3OH position of the benzene ring, via oxidation by monoamine oxidase, and to complement deactivation, both the gastrointestinal tract and hepatic functions further reduce activity by sulphonation again at the 3OH position (Reed 1978).

Subtle changes in chemical structure can markedly affect the associated activity of a molecule. For example, consider the catecholamine nucleus. Changing the ring positions of the hydroxyl substituents from the 3,4 to 3,5 positions significantly reduces the power of the COMT enzyme. As a trade off, this modification decreases the affinity for the β_2 receptor, but a longer duration of action ensues, giving rise to a class of compounds known as resorcinols. This class of compounds includes ephedrine, pirbuterol, metaproterenol, terbutaline and feneterol. Further adaptations to the basic structure leads to the development of compounds known as saligenins. A saligenin structure will result from the consequence of the transformation of the hydroxy ring substituents to that of a methoxy functional grouping, resulting in an orally more active form. Once modified, this gives rise to exemplary compounds such as salbutamol and pirbuterol respectively. In general, whenever synthetic modifications are made to active molecules two fundamental outcomes are sought:

(a) Firstly, in the reduction of systemic side effects, and
(b) Secondly, to facilitate the improvement in the duration of action.

Primarily, in this class of compounds addition or modification to the alpha carbon atom and/or the nitrogen atom on the molecule achieves this goal. In addition, to reduce the effects of MAO (monoamine oxidase, an enzyme) activity, further manipulation of the substituents on the terminal nitrogen moiety is required. An example of this is the molecule salmeterol, which is structurally similar to salbutamol with the exception of the long lipophillic nitrogen substituent, which it is postulated anchors the molecule to the β_2 receptor protein by intermolecular forces, increasing the contact time of the molecule with the receptor (D'Alzona et al 1994). This concomitantly increases the effect of duration for

up to 12 hours and shows an increased selectivity ratio 50,000:1 versus 650: 1 for salbutamol. The selectivity, however, has a critical size after which it diminishes with no gain (McFadden 1981). Other examples of where the alpha carbon is the choice for modification is evident in the alpha ethyl derivatives of isoproterenol and isoetharine (George 1981)

1.4.4 Enantiomers

It has been usual practice to deliver the majority of medicaments in the form of a racemate, even though it has been long established that stereochemistry and structural conformity are significant in physiological activity. Terbutaline, for instance, is approximately 3000 times more active in the laevorotatory form than the corresponding dextro form in relaxating guinea pig tracheal tissue with the said dextro form lacking any affinity for the β subtypes in general (Jepperson et al 1984), although even as a racemic mixture the overall efficacy is not apparently diminished.

However, considering salbutamol some studies have shown the + / dextro / (S) enatiomeric form of to illicit some constrictor functionality, but as illustrated by Ariens (Ariens 1984), to accurately evaluate the pharmacokinetics, enatiospecifc analytical methods must be employed to accurately compare effects of the individual enantiomers of each compound.

The use of single enantiomers confers other problems with the formulation, since individual densities, solubilities and melting points, of the eutomer, distomer and racemate, will all differ, which effectively necessitates the formulation of a "new" medicine. In this respect, and as an example, salt selection is crucial to ensure stability with laevo (R) salbutamol currently formulated as the tartrate salt in an MDI. Further, from a formulation perspective, peculiarities of single enantiomers have been observed in other pharmaceutical inhalation dosage forms, whereby mixtures of lactose and enantiomerically pure mandelic acid produced different respirable fractions (Nowaseb1998).

In the case of salbutamol, the racemate is composed of equimolar amounts of the (R) eutomeric active form, and the (S) distomeric inactive form. In terms of pharmacology, the (R) form exhibits the bronchodilator/bronchoprotective and anti-oedatous properties, with mast cell inhibitory effects; the (S) form has always been considered biologically inactive. However, recent studies have indicated that excessive use of the racemic mixture

induced negative reactions. The S-form induces pharmacological effects, which cannot be related to β_2 adrenoreceptor stimulation, and has been demonstrated to cause hypersensitivity of guinea pig airways, and in conjunction promotes the activation of human eosinophils *in-vitro* (Page and Morley 1999). From a mechanistic viewpoint, the distomer increases intracellular calcium ions, which negate the effects of the enzyme adenylcyclase by the eutomer. It has also been found that the distomer is metabolised more slowly and is retained preferentially within the respiratory tract.

The bronchoconstrictive effect of this enantiomer has been corroborated from its effects upon dissociated bovine smooth muscle cells (Mitra et al 1998), and has also been further postulated that the distomer binds with muscarinic receptors. It would therefore seem prudent to administer the pure laevo (R) form. However, a recent study has concluded in terms of cost and efficacy it is neither safer nor cost effective to do so. (Asthmus and Hendes, 2000).

1.4.5 Efficacy and Potency

When directly compared, *in-vitro* and *in-vivo* effects of bronchodilators do not correlate well. Isoproterenol for example, when assessed in an *in-vitro* situation exhibits a significant increase in potency when compared to salbutamol; but, when examined *in-vivo,* after aerosol administration, this significance is reduced and the clinical manifestation of the therapeutic action differs depending on the type of asthma. For example, the duration of action of these agents are reduced in exercise-induced asthma as compared to chronic stable asthma. This therefore necessitates that the comparison of such agents should be evaluated from a standardized method of measurement, such as illustrated by histamine or methacholine challenge protocols

1.5 Particle Deposition Mechanisms in Human Airways

1.5.1. Introduction

The main influences that dictate the deposition behaviour of inhaled aerosol particles incorporate the aerodynamic properties of the aerosol, the inspiratory manoeuvre of the patient and the geometry of the respiratory tract. The main deposition mechanisms of inhaled aerosol particles are through inertial impaction, gravitational sedimentation and the effects of diffusion. Other ancillary mechanisms are known to exist and include those of interception and electrostatic induced deposition. But, in the upper airways, large

particles deposit primarily due to inertial impaction, and in the conducting airways, both inertial impaction and sedimentation influence the deposition characteristics of the aerosol particles. By manipulating ventilatory parameters such as increasing the force of inspiratory airflow greater impaction in the upper airways may ensue. In contrast, increasing the breath holding manoeuvre increases the residence time of the aerosol dose within the lung thereby increasing deposition by sedimentation and diffusion in the respiratory zone. Selective or targeting deposition of inhaled pharmaceuticals to specific locations of the respiratory tract is preferred, as diseases are not distributed homogeneously throughout the lung. For example, cystic fibrosis may be distributed throughout the tracheobronchial tract. Asthma has been identified to localise within the large upper, central or smaller lower bronchial airways, whereas, at a specific regionalised locations carcinomas have a predilection for bifurcations (Martonen 1992). More recently, the respiratory tract has been identified as route for systemic drug delivery, and for this mode of therapy the particle size of the therapeutic agents should, ideally, be less than 1μm in MMAD. The peripheral regions of airways, the alveolar region, are separated from the systemic blood circulation via a very thin layer of epithelial cells (<0.2μm). As deposition is dominated by diffusion in this region of the lung, the small particle size, coupled with large residence time and the large cross-sectional area of the alveoli make this an ideal delivery vehicle for portal entry.

1.5.2. Inertial Impaction

Aerosol particles travelling along a gas stream have an inherent momentum (product of their mass and velocity). When the gas stream encounters a change of direction, the particles inertial force tends to resists this change, causing the particle to revert to its original path leading to impaction. If the particles momentum is such that it is not affected by the change it instantaneously relaxes into the direction of the flowing air (gas stream). This mainly occurs for low density and smaller particle size fraction of the aerosol cloud, and particles preferentially deposited by this mechanism end up proximal to the lung in the oropharynx. Only a small fraction of particles with aerodynamic particle diameters over 15 microns (mouth breathing) and 10 microns (nasal breathing) ever reach the pharynx due to the impaction within the nasal turbinates, and the complex laryngeal and pharyngeal geometries.

1.5.3 Sedimentation

Gravity affects particles when they have sufficient mass. The velocities at which these particles settle are related to Stokes Law, which is a solution to the generally insoluble Navier–Stokes equations, the governing differential equations describing fluid motion. These equations are difficult to solve, as they are non-linear partial differential equations, but solutions become available by making the following assumptions:

(a) Inertial forces are negligible as compared to viscous forces,
(b) The fluid is incompressible,
(c) There are no boundaries or other particles nearby,
(d) The motion of the particle is constant,
(e) The particle is a rigid sphere, and
(f) The fluid velocity at the particles surface is zero.

In still air the most important force acting on particles of the apprpriate size will be gravity; this force will be directly opposed by the buoyancy of particles due to the displaced air. As a result the net force F_n on the particles can then be written as,

$$Fn = g\pi Dp3(\rho p - \rho a)/6 \qquad \textit{Eqaution 1.1a}$$

Where g is the acceleration due to gravity and ρ_p and ρ_a are the densities of the particle and that of air respectively. However, inevitable interactions occur with air molecules, and create a force that resists gravity, when K_n is small. The total drag force F_D on a spherical particle moving with a velocity V through the fluid can be described by the following expression:

$$F_D = 3\pi\eta Vd \qquad \textbf{\textit{Equation 1.2}}$$

where η is the viscosity of the medium, V is the particle velocity and d is particle diameter. Thus, the particle accelerating under gravity will eventually reach a velocity at which the drag force balances the net downward force. The result is the terminal settling velocity V_{st}.

$$Vst = \frac{\rho_g d^2}{18\eta} \qquad \textbf{\textit{Equation 1.3}}$$

Where V_{st} is the terminal settling velocity ρ_g is the density of the medium with all other terms as per standard nomenclature.

1.5.4 Brownian motion

When the aerodynamic diameter of a cloud of aerosol particles approaches the mean free path of gaseous molecules, the continuous bombardment of the aerosol particles by the gas molecules may cause them to undergo random motion. The resultant force affects their direction. The particles therefore move from a high to a low concentration by diffusion, and, subsequently, the particles within the aerosol cloud (the bolus) diffuse from the lumen (centre) towards the walls of the respiratory tract. The rate of diffusion is inversely proportional to the particle size and is the dominant mechanism for particles smaller than 0.5 microns. The diffusion coefficient of a particle is given by,

$$D = \frac{\kappa T C_c}{3\pi\eta D_p} \qquad \textbf{Equation 1.4}$$

Where k is the Boltzman constant, C_c is the Cunningham slip factor, T is the Temperature in Kelvin, η is the viscosity of the medium and D_p is the particle diameter.

1.6 Aerosol Characteristics and Definitions

1.6.1 Definition

An aerosol is basically the dispersion of solid or liquid particles (typically smaller than 50 microns) in a gaseous environment (Gonda 1988).

1.6.2 Size Distribution

Ideally, it would be preferential to produce and deliver mono-disperse aerosol particles for targeting inhalation delivery. In reality, the aerosols delivered from such systems are poly-disperse and can be best described by a logarithmic normal probability function. The critical parameters that describe the aerosol are the geometric mean diameter, mass mean diameter, mass mean aerodynamic diameter and geometric standard deviations.

1.6.3 Geometric Mean Diameter (GMD)

The GMD is the i^{th} root of the product of particles which all have diameters *i.* Thus, if the aerosol generated contains say 6 particles 2 of which are 3 microns, 3 of which are 4 microns and 1 of 5 microns, the GMD is:

$$D_{GMD} = \sqrt[6]{3^2 x 4^3 x 5} \qquad \textbf{Equation 1.5}$$

$$D_{GMD} = 4.45\ \mu m$$

1.6.4 The Mass Median Diameter (MMD)

The mass median diameter, as suggested, divides the distribution of aerosol particles into two equal halves as a function of weight. Thus, by weight, 50% of particles will be below and 50% above this mass median value. If the logarithmic diameters fall in line with the normal probability function then the GMD equals the MMD.

1.6.5 Mass Mean Aerodynamic Diameter (MMAD)

The motion of aerosol particles travelling in a gas stream depends on the intrinsic variables of size, shape and density. The MMAD parameter combines these variables and is used to express the average cloud deposition within *in-vitro* and *in-vivo* models. This property is defined as:

'The diameter of a sphere of unit density, which has the same terminal settling velocity as the particle under assessment'.

and is related by the following equation:

$$MMAD = MMD\sqrt{\frac{\rho}{\rho_0}} \qquad \textbf{Equation1.6}$$

Where ρ is the density of the disperse phase and ρ_o is the unit density (1kg m^{-3})

1.6.7 *Geometric Standard Deviation (GSD, σ_g)*

The geometric standard deviation describes the poly-dispersity or spread of an aerosol particle distribution. An idealised monodisperse aerosol would have a $\sigma_{N=1}$ and ln $\sigma_g = 0$. It is practically impossible to produce totally monodisperse aerosols, and, so pragmatically monodisperse aerosols are quantified when they reach a value of approximately 1.2. For example, if an aerosol distribution has an MMAD of 5 microns and a GSD of 2 microns, 68% of the aerosol mass occupies the size range of ln 5 ± ln 2 and 95% of the mass occupies the size range ln 5± 2 ln 2.

1.7 Inhalation aerosol delivery devices

General Discussion

Several methods can be utilised in generating aerosols in the particle size range requisite for respiratory therapy. These are summarised in Table 1.1:

System	Reference
Jet Nebulisation,	(Fair et al 1984)
Ultrasonic nebuilsation	(Sollner, 1936)
Electrohydrodynamic techniques	(Rayleigh, 1882)
Dry powder inhalers (DPI's)	(Ganderton et al 1992)
Propellant driven metered dose inhalers (pMDI's)	(US Patent 1960)

Table 1.1 The major aerosol generation techniques used in respiratory therapy

Commercially, jet nebulisers, dry powder inhalers and propellant driven metered dose inhalers dominate the inhalation market. These systems are not, however, ideal delivery systems with each having inherent advantages and disadvantages. In achieving medicinal regulatory standards, they are usually simple in construction (with some exceptions), ergonomic, portable and relatively cheap to produce commercially. It has been widely accepted from a regulatory and, thus, a clinical viewpoint that the aerosol generated must be below 10 microns and ideally within a well-defined size range depending on therapeutic application (Usmani et al 2003). The dose delivered must be consistent and the respirable fraction suitable for the intended use. The packaging of the device and formulation is required to protect the physico-chemical integrity of the medicament and

excipients and not detrimentally interact with formulation. The system must be easily transportable and be 'patient friendly'.

1.8 Selection of a Delivery System

The selection of a system to deliver drugs to the respiratory tract depends not only on the active and the formulation, but also on the disease state, the patient and physicians preference. In theory, any medicament can be delivered by the major systems described, but some are specifically preferred to others. It could be argued that for peripheral delivery of large doses of active (e.g. an antiviral), pMDI's and DPI's are inefficient, whereas a baffled jet nebuliser e.g. the SPAG-2 (ICN Pharmaceuticals, Costa Mesa, CA) would be more efficient for such high dose delivery. Alternatively, DPI's and pMDI's may be preferred for delivery to the conducting airways in asthmatics, as these devices provide a bolus dose necessary for rapid bronchodilation. Biopharmaceuticals are generally formulated as an aqueous solution and stabilized with additives, therefore, these therapeutic agents currently lend themselves to a nebuliser delivery system.

1.8.1 Nebulisers

The principle of nebulisation has been known for over a century (Rayleigh 1882). With this type of delivery system, co-ordination of the inhalation breathing cycle, and the need to fluidise and disperse the aerosol cloud via an inspirational energy is not required. This makes nebulisers excellent for patient groups with poor coordination and poor pulmonary function: they have low peak expiratory flow (PEF), low forced expiratory volume curves (FEV_1), low ventilatory perfusion rates and have increased airway resistance and poor lung compliance. These advantages of this system are however negated by its size, as it requires a compressor and possibly an electrical supply and thus limits its portability. In conjunction, the nebuliser requires a respiratory solution or suspension and ancillary componentry making it a non-integrated system.

Air jet nebulisers operate on an external energy (air) supply. Compressed gas is forced through a restriction, which, results in an increase in velocity but a subsequent reduction in pressure (Bernoulli effect produced via a Venturi nozzle). With the help of capillary action, the solution or suspension of the drug is entrained by the negative pressure flow, and due to pressure gradients is sheared into a liquid film, which forms into aerosol droplets. Larger droplets become trapped by the internal baffle, coalesce and fall under

gravity to the recirculating solution. The particle size distribution and the density of the aerosol particles produced depend on the type of baffle used (Steventon and Wilson 1986). Smaller droplets escape the impaction experienced by larger particles, leave the nebuliser, and travel via the exit tubing to the patient. Because the patient generally uses a facemask or mouthpiece, minimal patient coordination is required with the patient undertaking a normal tidal breathing manouvere.

Problems can occur with nebulisers as the use of dry compressed air can aid evaporation of the drug solution/suspension and reduce its temperature, and changes in concentration have been reported that fundamentally change the rate of output and equilibrium particle size (Clay et al 1983). Further, the drug solution can concentrate and block the equipment. This in practice does not usually occur as the material is aerosolised quickly and the actives used usually have a high aqueous solubility. However, care is required with suspensions, particularly steroid formulations. The particle size of the aerosol produced depends as in other systems upon the formulation parameters: the density, surface tension, viscosity, added excipients, the design of system, operating conditions, and environmental conditions.

The majority of home use nebulisers are operated via small compressors that are very inflexible and the operational considerations are not well defined. Together with the ambient environmental conditions, patient usage is difficult to standardise.

1.8.2 Dry Powder Inhalers

Dry Powder inhalers store and deliver the medicament of choice in a granulated powder form, which is usually a blend of the active with a range of coarser excipients, although drug only formulations are known. The basic components of a dry powder inhaler consist of the following:

(a) A blister or capsule containing the formulation as a pre-metered system or a reservoir chamber with a metering mechanism,
(b) A de-aggregation system, which can either be active (the energy for dispersion is supplied externally); or passive which requires the patients inspirational energy to fluidise and disperse the powder formulation into an aerosol cloud,
(c) A suitable mouthpiece, which may contain the de-aggregation mechanism.

As previously indicated, the particle size range required for delivery to the conducting airways is approximately 2-7 micrometers in mass mean aerodynamic diameter (Newman and Clarke 1983). For most small non-biological entities, the active is usually in a micronised form. However, the particles may also be generated from spray drying or other particle engineering approaches utilised in producing particles with the desired shape and size. Gravitational effects on sub-10μm respirable sized particles, compete with several other significant particular forces: electrostatic, Van der Waals and capillary forces, respectively (Hickey et al. 1994). To reduce the influence of theses co-operative forces, large carrier are co-blended with the active to overcome the cohesive forces and aid the powder flow of the formulation during processing and fludisation upon device actuation. The de-aggregation and dispersion of the drug particles from the carrier particles are influenced by the size of carrier, which increases the drag force experienced by the drug particle adhering to the excipient (Ganderton 1992).

Thus, the removal of the drug particles from the excipient particles allows the delivery of the aerosol to the lower airways of the respiratory tract, whilst the excipients particles impact on the oropharynx due to their higher inertia. Successful delivery of aerosolised powders depends upon a closely related number of physico-chemical properties of the particles, which influence their fluidisation and dispersion behaviour. Crystallinity (including polymorphism (Wadke 1989)), particle size (Lalor and Hickey 1998), distribution, shape (Peitsch 1991), hygroscopic nature and moisture content, which may also be further modified during processing, affect the aforementioned properties of particle delivery from this system.

Fluidisation of the powder occurs either hydrodynamically or mechanically. Hydrodynamic (the motion of fluids and objects therein) fluidization utilizes a gas that passed through a permeable membrane then through the powder bed (gas assisted), or, by creating a low pressure field close to the surface of the powder, which causes a pressure differential of the air within the powder voids and the air flowing over the powder resulting in fluidization (capillary assisted). Finally, shear force fluidization or saltation can occur whereby a flow of gas passes over a powder contained in an open vessel fluidizes particles. Since particles on the surface have a smaller particle co-ordination number, separation by shear forces (pressure differentials) results in transfer of transitional and rotational energy over the powder bed. The impaction from momentum generated causes incipient fluidization. Mechanical fluidisation on the other hand, via vibration operates via the use of gravity when a powder falls through air e.g. the Spinhaler DPI device. Impaction fluidisation

occurs when a tangential force is applied to the powder such that the inter-particulate forces of the bulk are negated.

The internal geometry of the device is also important in generating the aerosol. The dose receptacle and the associated airflow conduits dictate the pressure drop across the device and the effort needed to generate the aerosol. Novel approaches have been taken to assist delivery. Active devices, where a complementary energy source is used in conjunction with inspiratory airflow, are now in use to help free the individual particles form the bulk. The materials of construction and geometry are also important since the formulation and the polymers may enhance electrostatic interactions (Staniforth 1994) and the subsequent accumulation of drug particles in the device.

1.9 Metered Dose Inhalers

1.9.1 Introduction

The development of pressurised systems can be traced back to the 1950's when Rexall laboratories developed the pressurized metered dose inhaler (pMDI) system. The development of the pressurized metered dose inhaler into the 21st century has been complicated due to their required reformulation facilitated by phasing-out of CFC's and the introduction of HFA propellants. The rationale for the phase out of CFC's outlined in the Montreal protocol, which dates back to the late 80's, basically describes the steps required by industry, to reduce the amount of ozone depleting substances (Ozone Secreteriat 1987). The pharmaceutical industry has been required to comply with the directive phase in new medications by substituting the compressed liquefied gase propellants. To complicate matters, the industry, naively, anticipated that the formulation change would be smooth and seamless. Active pharmaceutical ingredients however did not behave in a similar fashion and certain excipients were not as soluble as in the CFC free counterparts. Possible explanations for changes in formulation behaviour will be discussed later, but, essentially, industry is still struggling with the imposed change.

The systems are complex and deficient in a number of areas, due to the high exit velocity of the aerosol, poor patient co-ordination of the inhalation manoeuvre, and incorrect actuation of the device, all of which probably relates to only a relatively small dose of the active ever reaching the patients lung. (Newman et al 1981)

The main components of a pMDI have evolved very little since its inception. The basic components of a pMDI consist of the following:

(a) A container (extruded aluminum canister with the inner surface either coated and/or uncoated or a glass bottle)

(b) A metering valve (one of several variants containing multiple polymers and coatings)

(c) An actuator to generate the aerosol and or a spacer device

(d) The medicament (as either a solution or suspension) and ancillary excipients (co-solvents and propellant(s))

A schematic representation of a pressurized metered dose inhaler is shown in figure 1.1

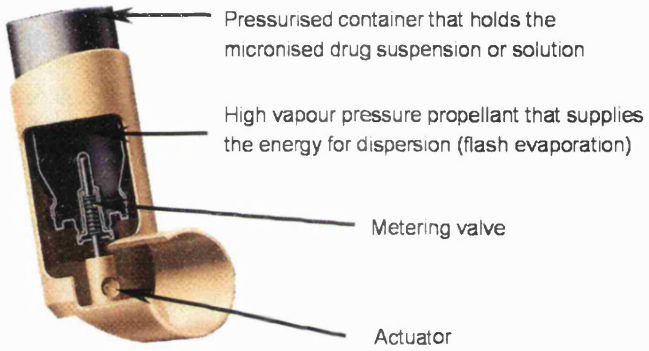

Figure 1.1: ***A representation illustrating a working pMDI***

1.9.1 (a) Basic Operation

The energy supplied via a pMDI system lies in the vapour pressure of the compressed liquefied gas(es), which are held under pressure in the container. Prior to operation the metering valve holds a dose of medicament and excipients suspended or dissolved in the compressed liquefied gas (CLG). Once the valve stem is depressed, it retreats into the body of the valve and the metered dose (MD), emitted as a bolus cloud, travels into the actuator sump. The vapour pressure of the formulation exiting the actuator orifice, termed the emitted dose, (ED), then equilibrates with that of the surrounding environment resulting in a fine spray, with initial velocities approximating 15 ms^{-1} (Dhand et al 1988). The formation of droplets and the underlying factors of spray formation will be considered in some depth later.

1.9.1 (b) Disadvantages of Pressurised systems

Although pMDI's are small, portable, robust and the formulation substantially unaffected from the surrounding environment there are a number of other considerations regarding their efficiency:

(i) Patient Coordination.

Effective lung deposition necessitates co-coordinated delivery from the device and the inspiratory cycle of the patient (Crompton 1982). To compensate for this, breath coordinated devices (BCD) and breath-activated devices (BAD) have been developed. In BCD systems, mechanisms are in place whereby the dose is actuated by depression of the canister but airflow is restricted and timed to coincide with generation of the aerosol cloud. In BAD systems, the canister is generally spring-loaded and is balanced on top of a flapped valve. As the patient inhales, the flap co-ordinates the depression of the valve stem delivering the drug at the start of the inspiratory cycle.

(ii) Incorrect Inhalation Manouvre

Patient information leaflets illustrate the correct procedure for administration of an inhaled medicament. A slow continuous breath followed by a long breath hold (10s or so) is advisory, which can reduce impaction in the ororpharynx (Newman et al 1980). However, in practice, this is almost never complied with and breathing conditions and characteristics of inhaled air have been shown to impact on particle deposition mechanisms, (Martonen and Yang 1996; and Martonen and Katz 1996).

(iii) Atmospheric Relative Humidity

High humidity and the ingress of moisture into pMDI's via diffusion can be problematic in both solution and suspension systems (Miller 1990), and requires careful selection of components e.g. the metering valve (Williams et al 1997). Indeed, HFA propellants have a greater affinity (water solubility) than their CFC counterparts. (Pischtiak 1999).

(iv) Dose Delivery Consistency

Suspension based systems, due to their thermodynamic instability, can deliver inconsistent doses of drug. Density differences between the active and propellant mixture, insufficient dispersion and distribution of the active, shearing forces by shaking, and delay between shaking and inhalation all affect dose delivery and clinical efficacy (Dalby 1992). Solution systems, which are easier to manufacture, and exhibit superior drug dose uniformity, do have several negative points. Due to molecular segregation of the drug reduced stability can occur. Drug can be absorbed into the elastomers and at low temperatures can precipitate and crystallize out of solution (via unstable supersaturated states), and can lead to a decrease in dose delivery per actuation (Atkins 1991). During operation through the life of an inhaler, after each actuation there is a liquid volume loss, resulting in a possible a 10-20 % increase in dose towards the use of a 200-dose pMDI system (Howlett 1996). Lewis et al. corroborated this finding (Lewis et al 2000).

(v) Particle Size Distributions.

The particle size distributions emitted from solution based HFA pMDI systems have in general smaller mass mean aerodynamic sizes particle (MMAD ≈ 1.2 microns) when compared to their CFC counterparts (MMAD 3.5 - 4 microns), (Leach 1998) and possess a different distribution pattern when measured *in-vitro*. From a regulatory viewpoint, this has been negatively received, as a seamless transition between CFC and HFA driven systems is the ultimate goal of the medicinal formulator. *In-vitro* correlation, at ambient temperatures, via Andersen cascade impaction is a standard analytical test. But, it does not take into account *in-vivo* conditions of temperature and humidity and therefore may be misleading in the interpretation of results. *In-vivo* correlation of solutions and suspension inhalers has indicated major differences. Leach (Leach 1998) demonstrated that 51-56% of the dose was distributed through the lungs uniformly, with little oropharyngeal deposition (28-30%) for a BDP solution inhaler. In contrast, the suspension CFC counterpart deposited mainly in the oropharynx (94%). Possible reasons for the differences in deposition can be postulated from the nature of the aerosolised cloud. Even though the vapour pressure and therefore the exit velocity of the HFA clouds are greater, particles should experience increased impaction. However, the formulations are different (namely solution versus suspension), and the solution produces a smaller overall particle size distribution. This may be in part due to the nature of the active form: molecular versus micron size active ingredients. With solution aerosols the particles are generated

in a "nascent" fashion. Suspensions inherently are predetermined to a large extent by the particle size of the micronised active.

1.10 Pressurised metered Dose Inhalers: The Current Situation

1.10.1 General Discussion

As introduced, the transfer from CFC to HFA propellant systems was perceived, by the industry, to be a 'like for like' transition with one propellant directly, interchangeable with the other. However, the chemistry of the HFA propellants is somewhat different to that of the CFC's, and consequently the conventional surfactants utilised were not soluble to any appreciable extent in HFA propellants. However, HFA propellants are good solvents when compared to CFC's and some drugs e.g. steroids are partially soluble necessitating the formulation of solution-based systems. Safety issues here have been identified here as the respirable fraction and deposition patterns of solution formulations when compared to CFC products, e.g. QVAR (3M Pharmaceuticals) may enhance systemic delivery, which for a steroid over a long period of time may have clinical significances.

The alternative chemistry of the HFA propellants has led to the conventional toxilogically acceptable surfactants, Span's, Tween's and Oleic acid to become effectively redundant, on grounds of reduced solubility. This has therefore forced pharmaceutical companies to take one of three reformulation routes: firstly, the use of ethanol to replace the low volatile CFC-11 component. Secondly, direct suspension of micronised active material in propellant 134(a) with attempts to reduce particle container reaction by coating the inside of the can with a fluorocarbon coating; finally, the synthesis of novel surfactants compatible with the propellants. -, e.g. polyoligolactic acids (3M pharmaceuticals Minnesota, US)

1.11 Solutions versus Suspensions (Pros and Cons)

1.11.1 General Discussion

The majority of pressurized metered dose systems are formulated as suspensions in preference to solutions. Of the common marketed pMDIs only tornalate and QVAR to date are solutions (Smyth 2003), and these products are formulated with an ethanol co-solvent to aid dissolution of the active compound. Other solution-based systems are indicated in

the literature in which the MMAD of the aerosol cloud can be directly modulated by the addition of non-volatile excipients: glycerol and PEG 400 (Brambilla et al 1999). Suspensions, which are unstable thermodynamic systems, are susceptible to several problematic areas. Depending on the formulation and metering valve, dose variations have been observed (Byron 1994; Cyr et al 1997). Coupled with canister orientation and environmental conditions crystal growth via Ostwald ripening can occur, which can lead to the dissolution of smaller suspended particles and the subsequent growth of larger crystals during storage. This may concomitantly lead to an increase in mean particle size of the delivered drug, increasing potential variations in deposition of the aerosol, and this may also result in either drug over or under-dosing (Phillips 1993). Other problems related with suspension based formulations, particularly with high drug loading, is the potential build up of drug on the actuator, which may block the spray orifice. As the drug in suspension systems are in a solid form, problems with polymorphism is a major concern. Polymorphism affects many intrinsic physico-chemical properties, and can increase solubility in the propellant/propellant systems enhancing the aforementioned problems.

Solution based pMDI systems would seem initially to be the preferred dosage form. However, there are difficulties formulating soluble ionic forms of drugs in organic solvent systems. Indeed it has been found that the solubility of salt forms is generally lower in aprotic solvents than that of free bases or acids. This is affirmed from the ethanol level in tornalate (Bitolterol Mesylate), presently at 38%w/w (Tzou et al 1997). Whereas non-ionic, lipophillic. compounds, particularly steroids, are suited to solution inhalers due to their solubility levels in both propellants and ethanol. This is borne out by the fact that an organic salbutamol ester could be solubilised directly into propellant 134(a) (Seville et al 2000), and both butyric acid and Tetrahydocannabinol are soluble in HFA propellants Solution systems are obviously prone to chemical degradation as the drug is at the molecular level, but with appropriate use of theory and practice, soluble and stable salt solutions are possible. In addition to the in-situ, chemical, drawbacks experienced with solution-based systems data exists, which indicates that aerosol particles of this type of pressurised system is prone to greater changes in particle size than suspension-based counterparts (Hiller et al 1979). This is routinely considered to be a disadvantage with solutions, as the particle size distribution shifts, and exhibits a greater non-respirable fraction; but this has not been fully investigated in the solution setting. Changes in particle size ranges may, here, provide pharmaceutical benefits.

1.12 Aims of the study

1.12.1 Discussion

The main objective of this thesis was to investigate the effects of hygroscopicity on the delivery of salbutamol salts to the lung, and to facilitate investigations an holistic approach was undertaken.

1.12.2 Experimental Rationale

To achieve such objectives, the following work will be performed:

1.12.3 Salbutamol Derivatives: Synthsesis, practical solubility evaluation and predictive solubility theory of novel bronchodilators.

To progress the study, it will be necessary to synthesise novel drug derivatives with the capability of being formulated as solution based pressure systems, as no salbutamol derivatives, to date have this fumndamental capacity. Initially, theoretical principles will apply to salt formation in order to predetermine which candidates would be most suitable for subsequent evaluation. Solubility in pure organic media and media blends will also require evaluation, in order to formulate thermodynamic and kinetically stable solutions. From a practical standpoint, the data generated should allow the application of theory to predict solubility as support to current empirical, visual methods.

1.12.4 Pre-formulation Studies: Characterisation of Novel Derivatives

Post-derivative synthesis, the molecules will require physico-chemical investigation. Fundamental data relating to structural confirmation, which will assist in describing the potential reasons for solubility, allow accurate assay, and cxritically discuss the rationale for data generated regarding the nature of the aerosol cloud formation, will be performed in conjunction with standard techniques.

1.12.5 Formulation Variables: The effect of temperature, co-solvent level and drug structure on cloud formation and the semi-empirical prediction of particulate aerosol cloud size.

To date in-vitro aerosol measurements have been performed under standard laboratory and therefore standard product testing conditions. Being solution systems the nature of the integral components (drug, co-solvent and anti-solvent) may be affected by temperature and thus pressure. By systematically evaluating the effects on stable systems and the resulting cloud dynamics, it may be possible to theoretically predict in conjunction with fundamental physicochemical constants and componentry hardware the MMAD and GSD of the resulting cloud blous.

1.12.6 Environmental Variables: The effect of temperature, humidity, drug structure and formulation on cloud formation.

Studies have indicated that substantial changes may occur in particle size distribution when considering simulated physiological conditions when compared to those of conventional, standard, ambient *in-vitro* environments (Hickey and Martonen 1993). Some of these studies have conditioned the aerosol cloud formed for tens of seconds at elevated humidity and temperature prior to *in-vitro* testing. In the majority of practical cases, such exposure does not occur *in-vivo,* even with good patience compliance and breath holding. Due to the complexity of the dosage form both evaporation and condensation processes occur and compete to produce the final particle size distributions. In this thesis both temperature and humidity will be varied in a controlled manner, in a matrix approach study to observe the effects at ambient and "respiratory like" conditions on the novel systems formulated.

2 METHODS AND MATERIALS

2.1 Materials

The salbutamol base used throughout was supplied in a micronised form (Batch number E 19081) and kindly donated by CCL pharmaceuticals (Runcorn, Cheshire, UK). All acids utilised in synthesis were of ultrapure grade from Sigma Aldrich chemicals (Poole, Dorset, UK), as were all solvents: absolute ethanol (99.5%), acetone and diethyl ether (methanol dried). All other reagents utilised were of the appropriate standard for the specific analytical technique: far UV-HPLC grade acetonitrile, HPLC grade methanol and associated mobile phase additives. Ultra pure water was produced by reverse osmosis (MilliQ, Millipore, Molsheim, France).

2.2 Salbutamol Salts: Selection criteria and synthesis.

2.2.1 Rational Drug Salt Selection.

At present there is no single rational approach to drug salt selection for the use in pressurised solution based systems; such an approach would assist greatly in inhalation therapy. An appreciation of the stability and integrity of the solid material, the solubility profiles of the molecular species in the dosage form, and the manipulation of the resultant aerosol cloud would assist in clinical applications. Rapid screening processes and methodologies for solid compounds have been documented (Morris et al 1994 and Wells 1988), but for pressurized systems, however, this approach is limited, and there is paucity of research in the literature. One study describing salt derivatives and aerosol dosage forms has, however, been documented (Sciarra et al 1972). Sciarra et al. produced a series of epinephrine (adrenaline) salts and determined the solubility, partition coefficient and finally the product stability in a variety of propellant systems. Four salts were synthesized: the bitartrate, maleate, malate and the fumarate, respectively. The salts were initially prepared according to a previously documented literature sourced method (Remington 1970), but it was found necessary to add small quantities of ether to inaugurate precipitation due to the unanticipated, elevated solubility of the salts in ethanol. Ether was utilised as a non-solvent or antisolvent (precipitating agent) in the study, and its use is described later. Interestingly, in the study performed by Sciarra (Sciarra et al 1972) the maleate salt was the most soluble in the propellant systems investigated, and the solubility of the maleate salt increased as the hydrogen atoms on the propellant molecule

investigated were replaced with fluorine atoms. The greatest solubilities in the study described were for salts within propellant 152(a) difluoroethane, which contained the highest fluorine content. The solubility of epinephrine maleate the most soluble salt in the remaining propellants, utilised in the study, are shown in table 2.0

	Propellant	Solubility % w/w
12	dichlordifluoromethane	0.009
114	dichlorotetrafluoroethane	0.013
142(b)	monochlorodifluoroethane	0.152
152(a)	tetrafluoroethane	0.272

Table 2.0: ***The solubility of epinephrine maleate in various propellants (taken form Sciarra et al 1972).***

As background to this study, investigations into the bronchodilator, salbutamol, revealed the synthesis of several salts to date. For reference, table 2.1 indicates the salt form and associated reference.

Salt	Reference
Hydrochloride (Single Enantiomers)	Hawkins et al 1973
Stearate	Jashnani et al 1993
Adipate	Jashnani et al 1993
Acetate	Brown et al 1994 (1)
Benzoate	Brown et al 1994 (1)
Tosylate	Brown et al 1994 (2)
Formate (Methanolate)	Brown et al 1994 (2)
R / S Tartaric	Ferrayoli et al 2000
R / S Mandelic	Ferrayoli et al 2000
R / S Dibenzoyl-D-tartaric	Ferrayoli et al 2000
+ di-p – toluoyl-D-tartaric	Ferrayoli et al 2000

Table 2.1 ***A comprehensive list of salbutamol salts synthesised to date.***

2.2.2 Salt Characteristics

Salt forms of pharmaceutical actives do little to change the inherent pharmacology of the active; they only serve to alter the physical properties of the parent compound (Corrigan 1997). The changes that occur from the formation of different salts mainly affect the

solubility, bioavailability and stability of the solid e.g. hygroscopicity. It is imperative, therefore, that each candidate must be screened as part of a pre-formulation program to study its potential as a candidate drug. The salt form selected may not only have an effect on solubility and dissolution rate as described, but may also influence polymorphism, melting point and wettability. Salt selection is therefore crucial to a dosage form. And fundamentally, to change the attributes of a salt form, manipulations of the counter anion are necessary. Increasing the melting point usually reduces solubility, which can be readily achieved by using small counter ions (Wells 1988), or by using hydroxy acids and, therefore, increasing hydrogen bonding. The properties of salts in pharmaceutical formulations are primarily related to aqueous based systems as drug formulations are typically formulated or tested within aqueous media. For pressurised aerosols, however, the binary solvent system, in which the salt has to remain in solution with, prior to dissolution in physiological fluids, is predominantly ethanol and (HFA 134(a)). HFA 134(a) is a particularly poor solvent for pharmaceutical actives as charcaterised by its chemical parameters, and as solubility and dissolution are dependent on thermodynamics properties, kinetics, and the nature of the components, salts were chosen to be readily soluble in ethanol. Theoretically, the salt formed had to possess a low lattice energy, a high positive solvation energy, preferably be charged, and possess a high dielectric constant. Physiologically acceptable acids for use in salt formation (and their percent usage) are adapted from Wells (Wells 1988) and are given in table 2.2

Anion	pKa	% Usage
Hydrochloride	-6.10	43
Sulphate	-3.00, 1.96	7.5
Tosylate	- 1.34	0.1
Mesylate	- 1.20	2.0
Napsylate	0.17	0.3
Besylate	0.70	0.3
Maleate	1.92, 6.23	3.0
Phosphate	2.15, 7.2, 12.38	3.2
Salicylate	3.00	0.9
Tartrate	3.00	3.5
Lactate	3.10	0.8
Citrate	3.13; 4.76; 6.40	3.0
Benzoate	4.20	0.5
Succinate	4.21; 5.64	0.4
Acetate	4.76	1.3
Remainder		30.2

Table 2.2: ***Commonly used physiological acids.***

Table 2.2 introduces the pKa term. The pKa value of a compound can be equated to the pH (potential of hydrogen) when 50% of the parent molecule is ionised. If an acid or base is "strong", it will possess a K_a value > 10^{-2} and will have a corresponding pKa value in the region of <2 ; as such it will be fully ionised in solution, with the dissociation constant (K_a for acid and K_b for base) indicating the relevant ionic equilibria. This can be represented by the following equations:

Acid $HA + H_2O = H_3O^+ + A^-$ then $K_a = \frac{[H_3O^+][A^-]}{[HA]}$ ***Equation 2.0***

Base $B + H_20 = BH^+ + OH^-$ then $K_b = \frac{[BH^+][OH^-]}{[B]}$ ***Equation 2.1***

In essence for a successful reaction to occur, in this case a salt adduct to form, the "rule of three" is usually applied: there should be a difference of 3 pKa units between acid and base. Small inorganic acids tend to predominate as primary the salt formers, probably because of their low pKa's readily forming salts with the majority of bases and can be made readily available in liquid form either as an aqueous or organic solution.

2.2.3 Counter Anion and its effects on Salt Character.

The properties of salt adducts prepared from physiologic acids can be partially predicted in advance. The counter ions that can be used (as indicated in table 2.2) fall broadly into inorganic and organic acid categories. The common acids along with their counter ion attributes are shown in table 2.3 Melting points, where applicable, are taken from the Merck Index Ninth edition 1976.

Counterion	T_m°C		Salt Characteristic
Inorganic Acids		----	Small ion increase mp
Hydriodic		----	increase lattice energy
	----		increase solid state stabilty
Hydrobromic			
Hydrochloric	----		for processing and handling
Sulphuric	----		increase (aq) solubility low pKa
Nitric	----		
Phosphoric	----		
Sulphonic acids			
Methane	20		
Ethane	----		
Benzene	43		May reduce solubility,
Toluene	70		destroy crystal symmetry
Carboxylic acids			
Maleic	131		increase solubility(aq) >pKa < M.P.
Benzoic	122		Hydrogen bonding acids
Acetate	16.6		increases solubility(freeOH/CO_2H)
Salicylic	158		
Succinic	185		
lactic	17		
Tartaric	205		
Stearic	69		Hygroscopicity reduced
Oleic	4		inc stability, inc wettability

Table 2.3: ***Physiological acceptable salt formers and integral their influence on resulting salt structures.***

Due to the low solvency power of the HFA propellant substitutes, it was envisaged the addition of an ethanol co-solvent would be required, and depending on thermodynamic and kinetic conditions the amount of co-solvent would need to be manipulated for stability reasons. As pKa differences, which are required for salt formation, are not solely responsible for predicting solubility, other important factors in predicting solubility need to be considered. These include lattice and solvation energy, dielectric constant and solubility parameters. It is evident that the overall characteristics of the drug are therefore highly dependent on anion selection.

2.2.4 Acid Selection: Solubility Considerations

As described, the solubility of the salt derivative can be theoretically modeled by careful selection of the counter ion. The following characteristics should be considered:

(i) A centre for inducing a polarisable charge (unsaturation, to induce dipoles)

(ii) A potential for hydrogen- carbon dipole bonding with hydroxyl or preferably carboxylic acid groups. Coupled with data from table

(iii) Low melting point,

(iv) The ability to destroy crystal symmetries, and for purposes of this study,

(v) Be highly hydrophilic (water soluble, for this study),

(vi) Be highly hydrophobic (water insoluble, for this study).

Carboxylic acids fulfilled the above criteria particularly the unsaturated moieties: maleic acid z butenedioic acid and the Oleic acid z octadecenoic acid. In addition, oleic acid is normally used as a pharmaceutical lubricating aid, so it was therefore hypothesized that use of this species would lubricate the valve, and may aid in potential long-term valve function.

2.2.5 Synthesis of Salt Derivatives

2.2.5.1 Introduction

The method employed for the synthesis of salt derivatives of salbutamol utilised a combination of techniques encompassing evaporative, thermal gradient, chemical reaction and vapour/liquid diffusion, and where necessary adjustment of the temperature and the use of anti-solvents. The difference in pKa values between salbutamol base and all the acids in table 2.2 indicated a sufficient difference theoretically to produce salt adducts (pKa's Salbutamol base pKa_1 9.1, and pKa_2 10.4 (Martindale 2002)). The major solvent chosen for these studies was ethanol, for several reasons: it is toxicologically acceptable, both the base and free acids are soluble in the solvent and it is easily removed post synthesis by conventional methods. Acetone was chosen for oleic acid due to its high solubility and ease with which crystallisation could be achieved.

2.2.5.2 Synthesis of Salbutamol cis-butenedioate (Maleate)

Approximately 0.5g (0.004 moles) of maleic acid was dissolved in approximately 4ml (3.2g) of absolute ethanol and 3.2 g of diethyl ether by gentle warming and agitating for several minutes until complete dissolution had occurred. Approximately 1.0g (0.004 moles) of salbutamol base were subsequently added to the acid solution. The vessel was sealed and then warmed with agitation until the base had completely dissolved. The

vessel was chilled for 24 hours at approx 2-8ºC to induce precipitation. The supernatant was removed and a further 5 ml of diethyl ether was added. The resultant oil was triturated until a white solid appeared. The solid was then vacuum filtered and air-dried. Further investigation indicated that by careful manipulation of the reagents the salt could be crystallised directly in the flask. Alternatively, crash precipitation could also be achieved by rapid addition of HFA directly to a concentrated solution of the salt in ethanol. The rapid method of crystallisation was briefly investigated, and it was discovered, from visual obserbvations, that the final particle size of medicament could be manipulated, from this *in-situ* method. This it was postulated may present an alternative method for manufacture of suspension aerosols rather than pre-micronising drug to a particle size specification.

2.2.5.3 Synthesis of Salbutamol cis-octadecenoate (Oleate)

Approximately 0.33g (0.001 moles) of oleic acid were dissolved in 10ml of acetone with warming. To this solution was added approximately 0.25g (0.001 moles) of salbutamol base, which formed a milky suspension formed. The vessel was sealed and the suspension heated with serial venting until complete dissolution of the base. The solution was then chilled and a white oil formed, which was re-dissolved by agitation at room temperature, and a white precipitate formed after several minutes. As with the previous example, careful manipulation of the reagents resulted in direct precipitation from the flask. Large crystals were observed via this method Again the *in-situ* crash precipitation method could be utilised for this salt. Depending on salt derivative, co-solvent concentration, temperature of reagents and rate of addition particle sizes of the final product could be tailored.

2.2.6 Final Salt Selection

The major discriminating parameter in salt selection for potential use in the study was primarily, solubility, in ethanol. Only four salts prepared, although others may exist, fulfilled the aforementioned criteria, and required the use of an anti-solvent to induce precipitation The remaining organic and inorganic salt derivatives synthesised readily precipitated from ethanol, and, as such, therefore would be formulated as suspension-based products, and were rejected from any subsequent study. During screening, several organic and inorganic derivates were synthesised and subjected to infrared and differential scanning calorimetric methods of characterisation. A full table of salts synthesised and their melting points is illustrated in appendix A 2. 1. This was the only

pre-formulation characterization performed, as they were not utilized in any further work. Two salts, the adipate and stearate, had been previously synthesised and were prepared as a control. These gave similar spectra but different melting points, and the rationale for this difference will be discussed in detail later.

Even though the majority of the salts are not suitable as solution based pMDI's, investigation into their intrinsic physicochemical properties, both as crystalline solids and aerosolized medicaments, do warrant further study. This point is illustrated from the development and production of an enantiomerically pure form of salbutamol i.e. laevo salbutamol Xoponex® (i.e the Tartrate was requisite to enable a stable formulation. Sepracor, Inc, Marlborough, USA.)

From the salts described in the table in appendix A 2. 1, the maleate and oleate were selected for further investigation on the following grounds:

(a) They were freely soluble in ethanol. Visual experiments were performed initially before accurate quantitative analysis by HPLC. These indicated short-term stability at low levels of the co-solvent. Interestingly, 10-20% w/w ethanol/134(a) propellant combinations do not adversely lower the vapour pressure of the system; in fact, the reverse occurs and the vapour pressure increases (Smyth et al 2002). The stearate salt although freely soluble in ethanol alone required a 50:50 ethanol:134(a) mixture to remain in solution. It was decided to terminate further study of this salt due to the high level of co-solvent required to maintain stability.

(b) Both salt derivatives had different water solubilities and therefore, it was inferred, may exhibit varying hydrophobic and hydrophilic properties. This would be useful in aerosolisation studies under differing environmental conditions, as hygroscopicity has been observed for a number of water-soluble entities (Martonen 1982).

(c) They could be synthesised in suitable quantities with good recoveries.

2.3 *In-Vitro* Particle Size Analysis

2.3.1 Particle Size Distribution Analysis

There are several methods that can be utilised in the evaluation of aerosolised particle size distributions; effectively they can be broadly categorised into the following techniques, although others exist: mechanical, electrical and optical, and irrespective of the technique all are susceptible to errors. Two types of sampling are utilised to evaluate

particle sizes of aerosol droplets: spatial and temporal. Spatial sampling describes the observation and/or measurement of droplets contained in a cloud volume that the contents do not change during observation or measurement. This includes optical techniques such as photography and holography. Temporal sampling describes the measurement of droplets that transverse a fixed area during regular time intervals. Inherent within pressurised drop generation techniques smaller droplets decelerate quicker than the larger drops leading to increased concentrations of smaller drops downstream during measurement.

For this study the cascade impactor was chosen. The cascade impactor operates via a temporal mode. The method is based on the principle that particles in an aerosol cloud will have a range of mass distributions move with a range of velocity profiles resulting in particles with specific momenta. Basically, if a travelling particle has a specific momentum in an entrained airflow it will impact on a collection plate. If a particle has insufficient momentum it travels to the next collection plate and this "cascade" mechanism of particles transferrance continues until impaction occurs. And, it is this impaction that dictates its mass mean aerodynamic diameter. The technique has the advantage of being able to be sampled isokinetically, as it avoids discrimination at extremes of droplet sizes within the spray.

Collection of drug deposited on each stage allowed the calculation of both the total mass balance, the recovered drug, and a non-linear least-squares fit of the cumulative distribution data (calculated from stage deposition) determined the respective MMAD and GSD of the outputs. The total mass deposited in the impactor is a simulation of what would be expected from a normal inhalation manoeuvre. In this study data generated from the least squares analysis approximated to log normality and was calculated over the probability range of –1.5 to +1.5. All results gave a R^2 values greater than 0.95 and a standard error value of Y less than 0.25 respectively.

2.3.2 The Andersen Cascade Impactor

The choice of particle sizing technique is primarily dependent on the application, the environment and particle size distribution under investigation. In this study, the Andersen Cascade impactor was chosen, primarily as it is routinely used in bio-aerosol assay, is a robust analytical item being able withstand changes in temperature and humidity. Functionally, It is designed to measure the mass weighted size distribution of aerosol

particles in the aerodynamic diameter particle size range from 0.4 to 10 microns (Andersen 1979). An impactor is a multistage, multi-jet device that fractionates particles into various class sizes according to their inherent inertia. A schematic representation of an impactor jet is shown in figure 2.0.

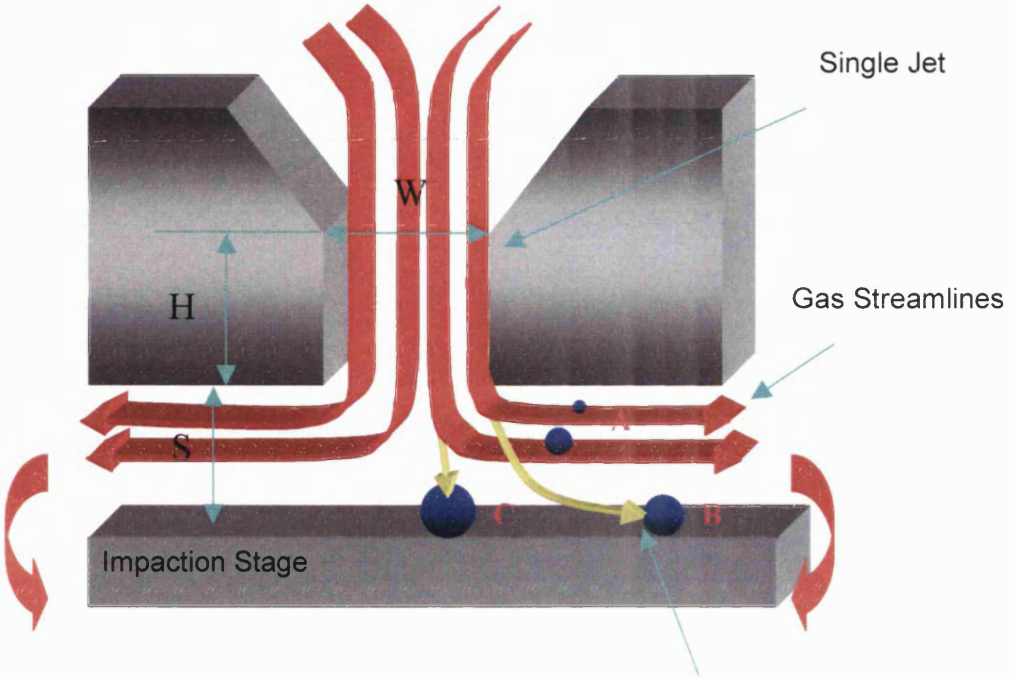

Figure 2.0: ***A schematic representation of a single jet of an impactor stage and the trajectories of particles of various sizes.***

Each stage consists of a series of jets, beneath which is located a collection of plates usually manufactured from a variety of metals (aluminium, stainless steel, titanium). For correct operation to occur certain dimensions are critical as indicated by the nomenclature in the schematic: where w is the diameter of the jet, h is the distance from the base of the aperture to the angle of the jet chamfer and s is the distance from the base of the jet orifice to the impaction plate for that stage. As the aerosol bolus travels through the equipment, the inertial properties of aerosol particles are increased upon passing through each jet. If a particle has gained sufficient inertia, as a function of its mass, it will be unable to follow the air stream around the plate and will impact on the plate, indicated by particles B and C. Particles with insufficient inertia will quickly relax and follow the air stream, thereby missing the collection plate and continuing through to the next stage, indicated by path A, where the inertia of the particles is further increased.

The collection efficiency of the system is defined as the number of particles that enter a stage and are collected by the associated specific impaction plate, and ideally, collection will be stepped: collection occurs, whereby particles greater than the critical size will be collected and those smaller will not. In reality, the efficiency follows a sigmoidal shape and a proportion of large particles will be missed by the stage; and, conversely a proportion of undersized particles will be collected. An impactor consists of several stages and the collection efficiency increase with decreasing jet size.

A robust impactor should have approximately the same number of undersized as oversized particles, and. the aerodynamic diameter can be related mathematically to the density, shape, and slip factors by:

$$d_{ae} = d_v \left[\frac{d_\rho}{\chi d \rho_o} C \frac{d_v}{d_{ae}} \right]^{1/2} \qquad \textbf{Equation 2.2}$$

Where d_{ae} is the aerodynamic diameter, d_v is the volume equivalent diameter, d_ρ is the particle density, $d_{\rho o}$ is the reference density, X is the shape factor and, C is the Cunningham slip factor for particles with a diameter of 0.1 microns or less.

2.3.3 Impactor Calibration and In Study Use

The impactor used in this study was calibrated by the manufacturer, and so the stage cut offs utilised were those described by theory. The same impactor was used throughout the study so systematic error was effectively reduced. During calibration, impactor plates are coated with a suitable solvent, leak tested and calibrated with monodisperse krypton irradiated polymer latex or methylene blue particles. Perhaps the most difficult and arguably the major difference from standard *in-vitro* testing and *in-vivo* manoeuvres is equilibration with a krypton irradiation source. Irradiation endeavours to put a uniform Boltzman charge on the aerosol particles, effectively giving a residual or minimum charge distribution on particles after exposure to a bipolar ion field; this then eliminates a source of deposition error. Aerosol particles electrostatically charged, may interact differently with each other and effect subsequent deposition patterns. (Griffiths et al 1998). In reality, particle charging and thermophoresis occur, and, so, it can be argued that although this practice is possibly acceptable for calibration is not totally practical for actual analysis.

To obtain accurate and precise measurements the study focused on controlling and monitoring the following parameters. During analysis the active compounds were removed from the impactor with methanol, a universal solvent for both the drug salts and co-solvent. Assembly was checked to ensure correct operation and functioning of the stage seals as the cut off diameters are related to flow rate, which was checked by use of a calibrated flow meter, and as flow rate is related to actual volumetric flow rate by temperature and pressure factors, the flow meter was left in thermal equilibrium with the equipment, and the flow checked between studies, in the environment of test. This removed a source of systematic bias, as it can be shown that at 25°C there is approximately a 5% difference in flow rate and at 40°C there is about a 12% difference with 100% water saturation. The difference in pressure at 0°C is only about 0.6%, but this increases to 3% at 25°C and 6% at 38°C. Post quantitative washing of the impactor plates, the apparatus (as chemical analysis of the drug on each impactor stage was conducted) was left to air dry in the laboratory at the test condition for a minimum of one hour to reach thermal equilibrium with its surroundings, as the importance of thermal influences on aanalysis have been highlighted previously (Finlay and Stapleton 1999).

2.4 Statistical Analysis

Statistics is based on probability; and distributions of data sets are mathematical functions, which assign probabilities for domain outcomes. Modern theories of statistics are based on normally distributed data while the majority of sample means from all probability functions tend towards normality for large sample sizes. In this study, data generated relating the effects of temperature equilibration on particle size distribution chapter 4, and also the effects of temperature and humidity controlled environmental testing conditions on particle size distributions on individual salt formulations, intra-formulation correlation, was performed by one–way analysis of variance (ANOVA) using the Minitab® statistics package version 12.1. ANOVA is a standardised statistical tool, for analysing series of data sets. Inter-formulation comparisons were compared using a two tailed heteroscedastic student's t-test with confidence limits set at p 0.05. Basically a stage-by-stage comparison of cascade results generated for each salt formulation over all testing criteria were compared at a confidence level of $p<0.05$, after these data had been percentage normalised in terms of deposition. Where differences did occur at an inter-group level, a Tukey's significant difference test was performed on the data again at the 95% confidence level in order to identify the were the differences occured.

2.5 Differential Scanning Calorimetry. (DSC)

2.5.1 Materials and Methods

Differential scanning calorimetry was performed on approximately 5 mg of material (4.384 mg Maleate and 3.918 mg Oleate) using a TA 2910 11R, (Thermal Analysis instruments Crawley, West Sussex, UK), (University of Bath, Dept of Materials Science). The heating rate was set at 10°C per minute and samples were run from ambient 30°C to 150°C. No liquid nitrogen cooling was applied; however, the sample and reference materials were tested in a dry, inert atmosphere via a positive flow of nitrogen gas, which was perfused within the instrument at a rate of 25 ml per minute.

2.5.2 Results and Discussion

The onset temperatures, enthalpy changes and instruments used in determining these parameters of the synthesised salts, (with comparisons selected salts in the literature donated by onset temperatures with an asterisk), are given in table 2.4. The thermograms for each salt are given in figures 2.1 and 2.2 respectively.

Salt Derivative			DSC data	
Maleate	ΔH_f J/g		72.63	
Onset Temp/°C	(mass mg)		127.5	(4.384)
Oleate	ΔH_f J/g		85.70	
Onset Temp/°C			76.7	(3.918)
Adipate	ΔH_f J/g		37.32	
Onset Temp/°C		182*	190.3	(1.460)
Stearate	ΔH_f J/g		93.00	
Onset Temp/°C		116*	110.9	(5.794)

Table 2.4 ***A table illustrating heats of fusion and melting points (onset temperatures) or several salbutamol salts cross-referenced where applicable to those quoted in the literature. Data marked with asterisk indicates published data.***

The major differences between the onset temperatures of that quoted by Jashnani et al (Jashnani et al 1997) and this thesis are the solvents utilised in the synthesis. Jashnani utilised a crystallizing solution methanolic solution followed by a re-crystallisation step

from aqueous ethanol for the adipate; the stearate, on the other hand, was precipitated by evaporation from a methanolic solution in a 1:1 molar ratio. In this thesis the adipate was precipitated from an ethanolic solution and the stearate from an acetone solution.

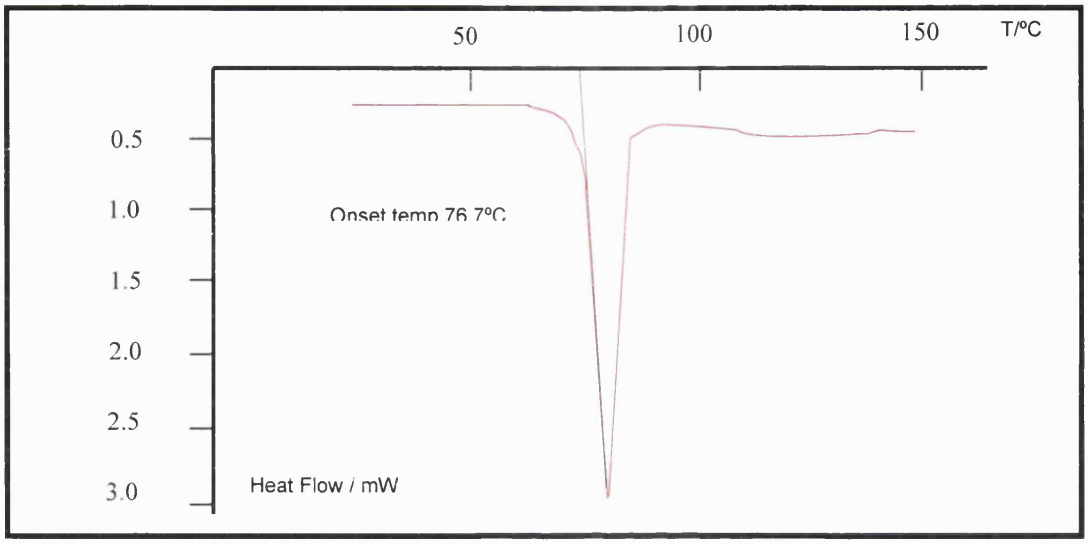

Figure 2.1: ***A DSC thermogram of salbutamol oleate***

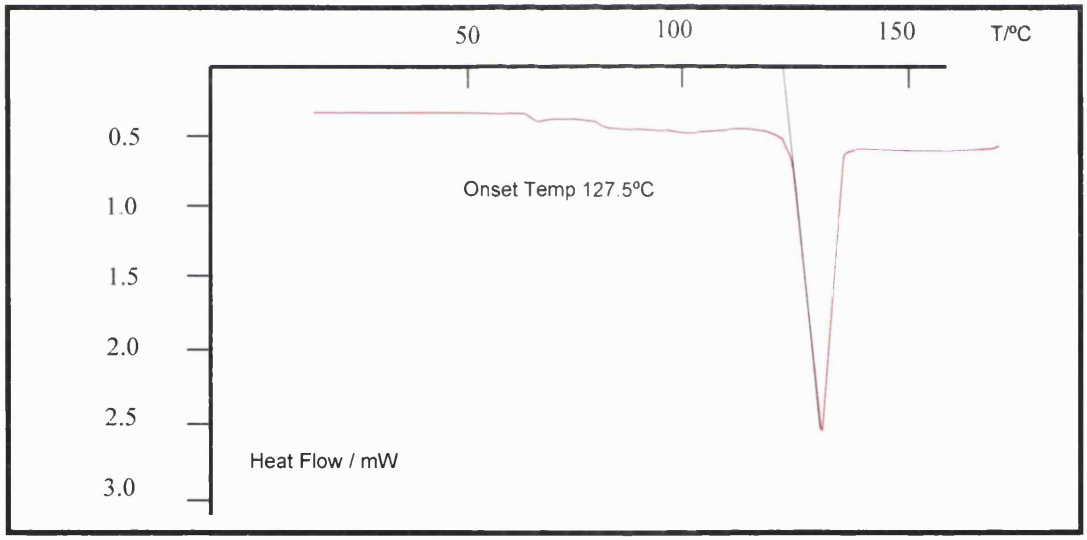

Figure 2.2: ***A DSC thermogram of salbutamol maleate***

The use of different solvents can give rise to pseudo polymorphism: hydrates, solvates and clathrates. Solvates and hydrates occur due to the molecular arrangement of the solvent its polarity and dielectric constant. When the salt starts to nucleate and then precipitate, the molecules physically undergo physical adsorption onto specific crystal faces. When analysed by DSC the solvent will boil off at a temperature close to its specific

boiling point. Clathrates on the other hand again formed due solvent crystal interactions actually become trapped within a cage of the crystal, and therefore boil off at a higher temperature. In fact as the molecular size of the solvent molecule increases say from methanol, ethanol, diethyl ether towards highly substituted ketones e.g.MEK, this effectively gives rise to a new crystal structure by differential spatial arrangement of the constituents. Other confirmatory techniques would be required to determine number and amount of polymorphs present.

The adipate synthsised by Jashnani formed a diethanolate, and although not fully investigated this author postulates the stearate formed a methanolate structure. Such solvates may account for the differences observed.

2.6 Infrared Spectroscopy

2.6.1 Methods and Materials

Samples of material were analysed using both a Nicolet AVATAR 360 FTIR (direct powder loading performed at CCL Pharmaceuticals) and a Perkin Elmer post preparation in KBr discs by direct compression to 15 tones. Samples were scanned from 500 to 4000 cm^{-1} respectively (University of Bath Dept of Pharmacology).

2.6.2 Results and Discussion

Infra red spectroscopic measurements of both compounds further indicated salt formation as confirmed by shifts in the absorption bands when compared to the freebase and acid. Salbutamol base is a secondary aliphatic amine and as such exhibits a bending stretch at 3300 cm^{-1} and a bending motion at 1650-1550 cm^{-1}. Conversely, free carboxylic acids examined as KBr discs will exist as a dimer and a confirmatory stretching band (C=O group) appears at 1725-1700 cm^{-1} when saturated or acyclic. However, when conjugated or unsaturated the stretching vibrations are reduced by 20-30 cm^{-1}. This is evident in the maleate salt, which has two carboxylic acid groups with only one of which is ionised. Evidence of a carboxylate anion is indicated by dual absorptions between 1300 and 1420 cm^{-1}, both of which are present in the spectrograms.

For clarity, the free acid and salt traces are overlaid on the same spectrogram. Finally, amine salts absorbed around 1500-1550 cm^{-1} and both these stretching vibrations are present.

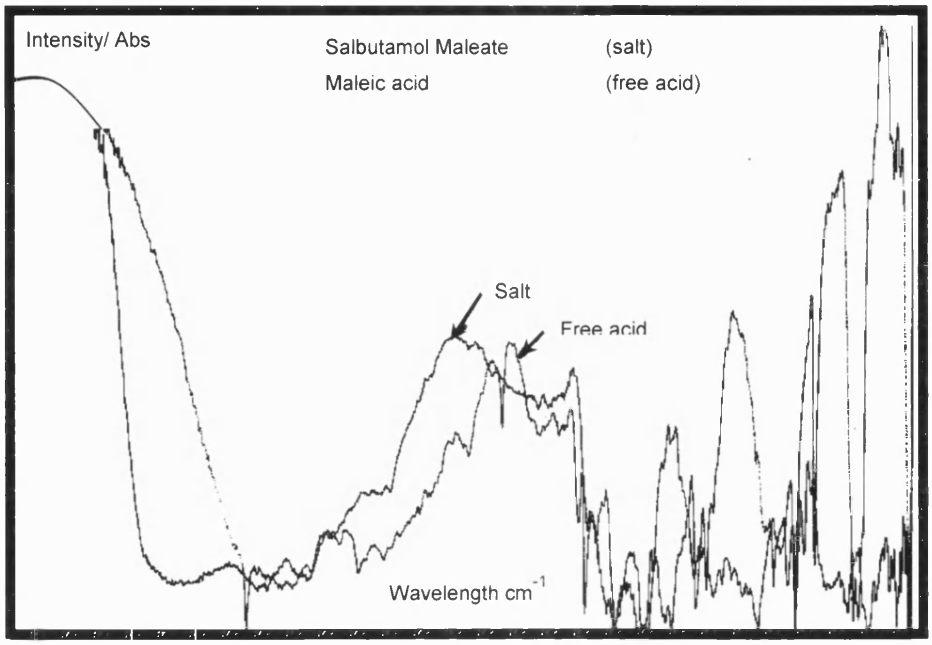

Figure2.3: An infrared spectrogram of salbutamol maleate illustrating the differences in absorbance from the free acid.

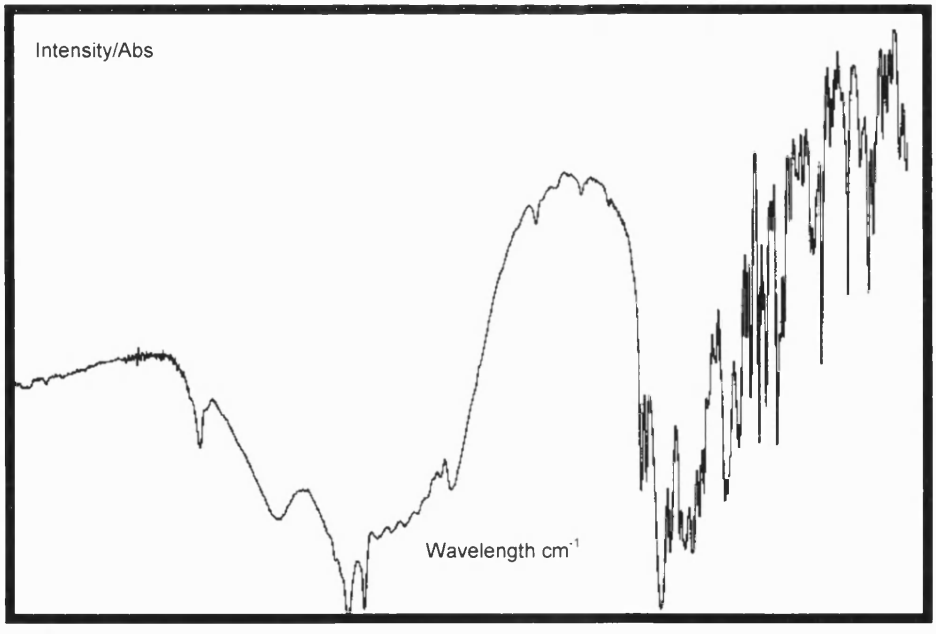

Figure 2.4: An infrared spectrogram of salbutamol oleate. (Free acid not overlaid)

2.7 X-Ray Crystallography

2.7.1 Materials and Methods

The crystal structure of salbutamol base has been previously identified and documented by Beale and Stephenson (Beale and Stephenson 1972). Crystals of size applicable for X-ray crystallography were produced for both compounds. The data was collected (University of Liverpool X-Ray crystallography dept) using a Stoe IPDS image plate diffractometer, using a Molybdenum (Mo K alpha 0.71073Å angstroms) radiation source at a temperature of 100 Kelvin. The diffractograms of salbutamol maleate and oleate are depicted in figs 2.5 and 2.6 and atomic and thermal parameters in appendices A 2.3, A2.4 A 2.5 and A 2.6 respectively.

2.7.2 Results and Discussion

The definitive structure of salbutamol (z) butenediaote is shown in Figure 2.5.

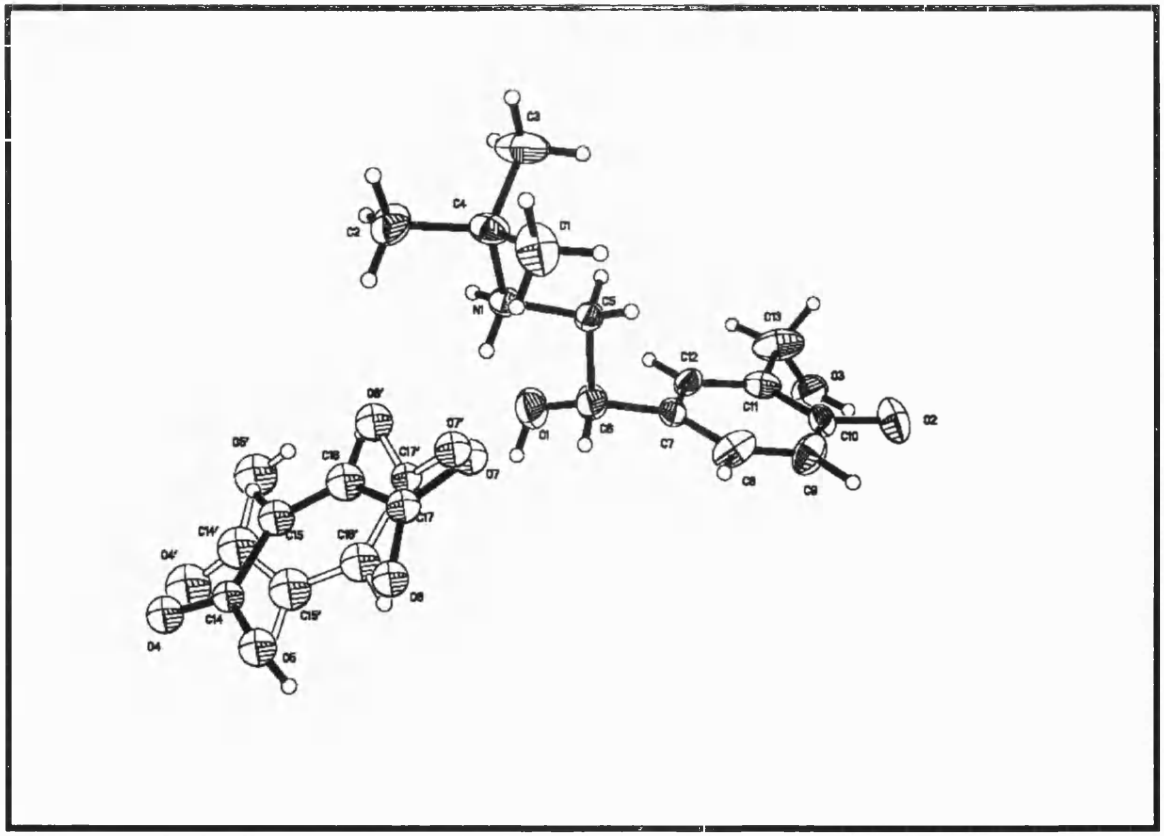

Figure 2.5: The spatial arrangement of salbutamol maleate by elucidated from XRC

The space group for salbutamol base has been evaluated as Pbca where a= 2.1654 (10), b = 0.8798(4), c = 1.4565(7) nm Z=8, with an observed density of 1.15gcm^{-3}. For salbutamol maleate, data determined that the molecule had an orthorhombic structure, unit cell parameters of a=8.4487(8), b=15.4327 (15), c= 13.8712 (13), a volume of 1808.6 Å^3, were established. Other important parameters indicated an absorbance of 0.101 mm^1 and an observed density of 1.305gcm^{-3}; the space group was determined to be Pna21. The salbutamol base structure has been altered substantially form its original structure with the addition of Z butenedioic acid. The molecule from the parent base has effectively been 'bent' into a W shape via rotations at the C5, 6, and 7 positions, and the amino and hydroxyl groups are in a cis orientation with respect to a plane running through C4, C5 and C7. Both the cis orientated protons on the amino and hydroxyl groups N1 and O1 are orientated towards the O7 of the maleate ion. One interesting effect to note was the 80:20 crystal disorder in the Z butenedioate molecule. In figure the molecule is shown on bold lines and grey lines. The bold lines indicate the 80 ratios. In the 20, the molecule has 'flipped' 180 degrees.

The definitive structure of salbutamol (z) octadecenoate (Salbutamol Oleate) is shown in figure 2.6.

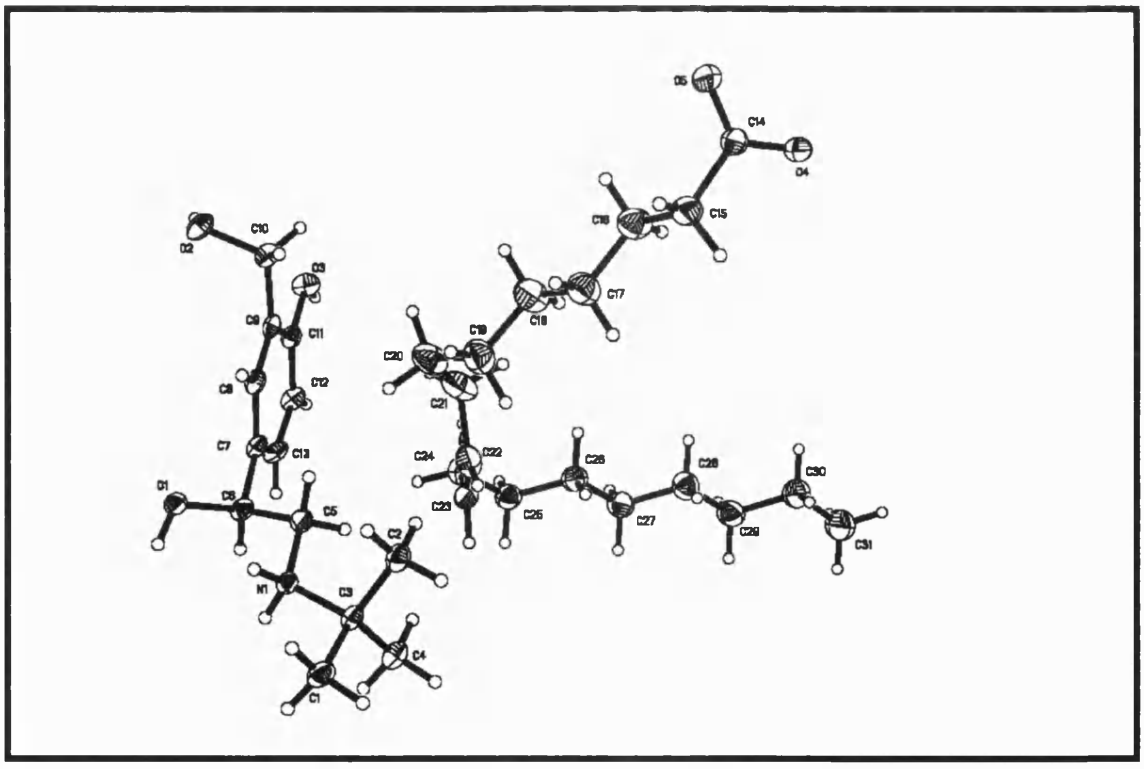

Figure 2.6: ***A spatial arrangement of salbutamol oleate elucidated from XRC***

Crystallographic data generated for salbutamol oleate gave substantially different lattice and group parameters: the crystal structure was determined to be monoclinic, the unit cell parameters were, a=14.9781(8), b=18.3004(14), c=11.5501(9), the volume of the crystal was 3106.8$Å^3$, the absorbance was evaluated at 0.073mm^{-1} it had a density of 1.096 gcm^{-3} and the space group was P21/c.The structure of the Oleate derivative was different again from that of the base and maleate, being monoclinic, with rotations at positions C3, C5 and C6. Rotation at C6 had orientated the plane of the benzene ring so it is virtually parallel with the double bond at positions C21 and C22 of the oleate molecule. Again the amino and hydroxyl were in a cis orientation, and protons on these atoms were juxtaposed to the carboxylate group of the oleate molecule.

2.8 Fluorescence Spectroscopy

2.8.1 Materials and Methods

Prior to analysis, the emission and excitation wavelengths of synthesised salts were scanned over 220 to 800nm to ascertain the maxima for analytical determinations. Previously, salbutamol sulphate had been determined and gave an excitation value of 275 and an emission value of 410nm. In order to determine the respective emission (em) and excitation (ex) wavelengths of the salts, a Hitachi F200 fluorimeter was set on to auto scan mode and samples were prepared in methanol at concentrations ranging from 25 to 0.05mcg/ml. Traces analysed exhibited identical maxima for excitation and emission spectra. An example of an excitation spectrum is shown in figure 2.8. Prior to analysis, acting as a calibration check, standard recoveries on duplicate solutions were performed. Calibration checks ensuring system accuracy precision and linearity were also carried out before quantitative analysis. Acceptance limits were set at 98.0-102.0%, for duplicate solutions as per pharmacoepia for HPLC assay. To ensure linearity, a five-point linear regression analysis covering 10-200% of nominal drug mass concentrations were routinely performed, and was suitable in terms of quantitation limit and adequate in detection terms at 50 ng/ml an order of magnitude less than the lowest drug concentrations routinely collected.

2.8.2 *Results and Discussion*

The wavelengths scan of a mid range linear regression solution is shown in figure 2.8. As an operational check, the instruments ''wavelength accuracy' was calibrated according to manufacturers instructions. Essentially, a new xenon lamp was installed and the signal to noise ratio measurements were routinely performed with ultra-pure water. The system conformed to manufacturers specifications, and the output is shown in figure 2.9.

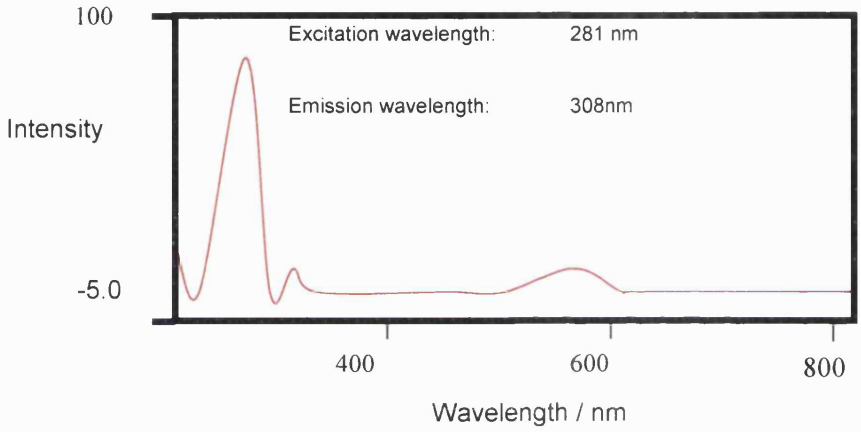

Figure 2.8: ***A fluorescence spectrogram indicating excitation and emission maxima for use in analytical determinations.***

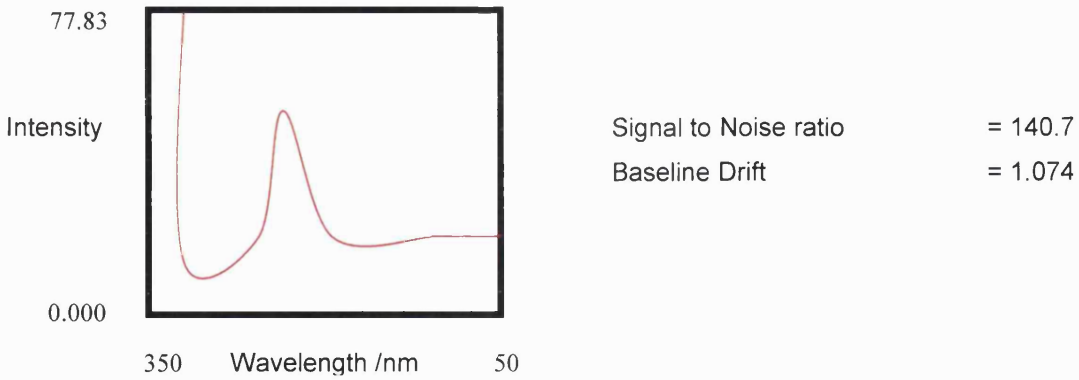

Figure 2.9: ***Fluorimeter calibration data***

2.9 High Performance Liquid chromatography

2.9.1 Materials and Methods

High performance liquid chromatography was performed using a Jasco HPLC system (Great Dunnow, UK) with UV detection. A UV detection wavelength of 276 nm was used for salbutamol upon scanning both salts. The co-anion had no effect on the wavelength maxima for salbutamol. Standard recovery on duplicate solutions and five point linear regression was performed before analysis. Limits for these variables were set at a recovery percentage and regression coefficient of 98.0-102.0% and 0.995 respectively. Standards were stored at 4°C and kept for no longer than one month. Working standards were also kept at this temperature, but discarded after a week.

2.9.2 Results and Discussion.

An ion-suppressed isocratic method was developed for the salbutamol assay, utilising the conditions described in appendix A 2.9. An example chromatogram is illustrated in figure 2.10.

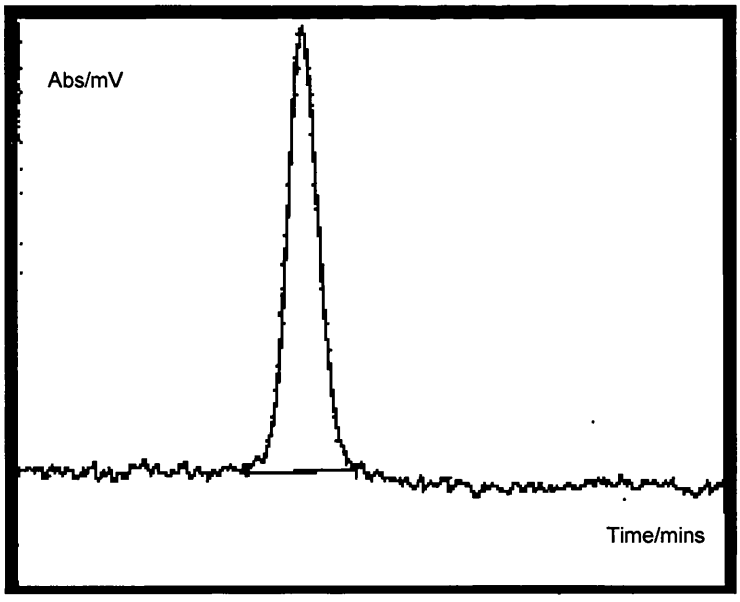

Figure 2.10: ***A typical HPLC chromatogram of salbutamol maleate (NB. Salbutamol oleate gave an identical retention time for an equivalent concentration.***

3 THE EFFECTIVE SOLUBILITY OF SALBUTAMOL SALT DERIVATIVES IN pMDI MEDIA

3.1 General Overview

The first step in the characterisation of a compound for its potential use in a pharmaceutical dosage form is the determination of its pKa and intrinsic solubility, or the solubility in its unionised form (Wells 1981). For solution-based pressurised systems, the solubility should be evaluated in a number of solvents and anti-solvents. An anti-solvent being the terminology used for a liquid phase of widely dissimilar dielectric constant or substantially different physicochemical character to the solute in question. Solubility evaluation is necessary since propellant systems and associated co-solvent blends, if in certain proportions, may induce instability, which may lead to destabilisation of the formulation and crystallisation of the drug from solution upon storage. The use of co-solvents to fully dissolve partially soluble drugs such as beclomethasone dipropionate, which have a limited solubility in propellants to prevent precipitation from solution, have become industrially acceptable (Leach et al 1998). The effects of solubility, dissolution and crystallisation have been observed in suspension systems (Voorhees 1985).

The stability of this dosage form has historically been based on empiricism and visual methods. While adequate, this has not made any links, connections or discussed the complex interplay between the intrinsic components, and, as such, poses a fundamental question: Can solution stability be predicted from theory based upon thermochemical data and practical solubility measurements on individual formulation components?

It is theorized that solubility may increase with temperature, but, at present, this has not been substantiated.

3.2 Initial solubility and stability investigations via visual assessment

Physical stability assessment.

Solubility and consequently stability of solution aerosols, as intimated, has largely been based on empirical visual methods (Brambilla et al 1999). As such, formulations are usually manufactured in a visually suitable medium, either glass or plastic and drug

loaded at the required concentration per actuation in order to appropriate a therapeutic dose. To emulate long-term moisture ingress by passive diffusion, they may be spiked with water. To investigate solution stability, formulations are conventionally stored at low temperature or alternating temperature regimens (4°C or cycling conditions –5°C to 40°C over a defined period of temperature fluctuation) and assessed at specified intervals. Later in this chapter, an alternative approach will be introduced and utilised to assess solubility and stability of solution based pMDIs. However, in the first instance, visual assessments were utilised in primary evaluation as a control to verify later experimental findings. Solubility using this method was performed on the following formulation compositions:

(i) In order to assess final co-solvent levels for stability, salbutamol maleate and oleate formulations (at a drug mass of 100µg per actuation equivalent to the freebase, based on equivalent relative molecular masses) were prepared over a range of ethanol and 134(a) concentrations, and stored under the standard regulatory pharmaceutical temperatures.

(ii) In order to simulate long term solution stability by moisture ingress from increased humidity storage, formulations of salbutamol maleate in Ethanol / HFA 134(a) / Spiked water systems were prepared. It should be noted that only the maleate salt was utilised in the water spiking study, since the oleate salt is water insoluble and was in short supply. The spiked mass of water was charged from 5000ppm, which was equivalent to 0.5% w/w of the final formulation, to 50000 ppm or 5.0% w/w of the final formulation. This was performed in order to ascertain a crude level of stability upon ingression of water. In the final phase, maleate formulations were prepared at the optimal co-solvent level, the minimum level necessary for stability, and again spiked with water ranging from 5000 to 30,000 ppm and stored at low temperature for prolonged periods.

Chemical stability assessment.

Chemical stability of the salt derivatives within pressurised systems is also an integral part of product performance. This was also investigated. Briefly, formulations of exact composition (ranging from 10-30% w/w ethanol for each derivative) were stored at 25ºC and 100% RH and assessed after 3 and 6 months respectively; Initial testing (T0) was omitted due to the limited number produced. Assay data widely ranged for both salts and is note quoted here primarily due to inadequate optimization of the analytical method:

Upon opening of the units large proportions of active were lost from violent propellant evaporation.

3.2.1 Methods and Materials

Plastic coated glass pMDI bottles (St Gobain, France) were weighed on a validated balance (Sartorius UK) and tared after first undergoing a rinse with clean and dry compressed air. Drug was weighed accurately by difference in order to give an equivalent of 100mcg freebase per actuation related to molecular mass of the salt and the formulation density. The same procedure was repeated for absolute ethanol (Fisher scientific Poole, UK). A continuous spray valve was then crimped on (Bespak, Kings Lynn, UK), according to manufacturers specifications and the bottle then sonicated (Decon FS 3006) for several minutes to induce complete dissolution of the drug. The bottle was then dried and once again tared on the balance. HFA 134(a) was subsequently charged through the valve using a Pamasol 2002 hand gasser crimper (DH Industries, Laindon, Essex, UK). The final formulation preparation was sonicated for a further several minutes to ensure complete dissolution. Formulations were then stored at specified temperatures and assessed periodically. All solutions were prepared in duplicate.

3.2.2 Results and Discussion

Figures 3.1 A to D depict solution stability profiles for maleate formulations prepared at the following co-solvent levels: 10, 12.5, 15 and 20% w/w after storage at the following temperatures ambient 25°C, 0°C and –23.5°C. The co-solvent level (% w/w ethanol) of the formulations are indicated in figure 3.1 A. The order/sequence of the bottles were identical for figures 3.1 B-D inclusive thus indicating the relative formulation. The side elevations indicated, in Fig 3.1 A and C and, for clarity, recumbent plan views B and D system, destabilisation, highlighted by drug precipitation. (View respective arrows on the 10 and 12.5% w/w co-solvent level photographs for the maleate derivative). No indications of crystallisation at co-solvent levels above 15% w/w were observed. For further descriptions of visual observations see Appendix 3 table A 3.1(c). Finally, figures 3.1A and B indicate the results for the formulations when stored at ambient 25°C, and 3.1C and D for those stored at low temperature –23.5 .5°C.

The oleate salt formulations depicted in figures 3.2 A to D, indicated that a minimum of 30%w/w co-solvent was required for stability. It should be noted that for the maleate

system, crystals aggregated at the base of the vessel, whereas those of the maleate formed at the liquid vapour interface possibly due to the density of the solids in the medium and the fact that the oleate derivative being a surfactant would preferentially align at this boundary. The size of the crystals were also different. The maleate salt crystals tended to be large and aggregated while the oleate crystals were small and discrete. For a further description of the visual observations made see appendix 3 table A 3.1 (d).

Figure 3.3 illustrated the results for the moisture spiking study, indicating that at the optimal co-solvent level (15% w/w for the maleate) solution stability could be acheived (shown by a single phase) when moisture levels, up to levels of 30,000 ppm or 3% w/w were incorporated into the final formulation. After this, at low temperature storage, the 30,000 p.p.m solution formed a "cloudy" two phase system. This re-dispersed into a single phase with equilibration to room temperature. Documented observations relating to these systems can be found in appendix A 3.2, tables 3.1(c-e).

3.2.3 Conclusion

In general, using the visual method, the maleate salt required only a 15% w/w co-solvent level (1.5g per 10g formulation) to remain as a stable single-phase solution exhibiting no observable crystal growth, equating to about 0.25% w/w drug concentration with respect to the final formulation (see Figures 3.1A-D).

The oleate, however, required approximately 30% w/w co-solvent levels (3.0g per 10g formulation) to remain stable, crystal free and as a single phase. In this case, the drug concentration equated to approximately 0.37%w/w. However, instability did not manifest itself instantaneously. Even for the 10% w/w co-solvent level the solution remained stable for approximately 3 days before de-stabilisation by thermodynamic and kinetic factors. Other possible factors for solution stability may have been the container surface roughness or the presence of extraneous fibers, which may instigate heterogenous nucleation.

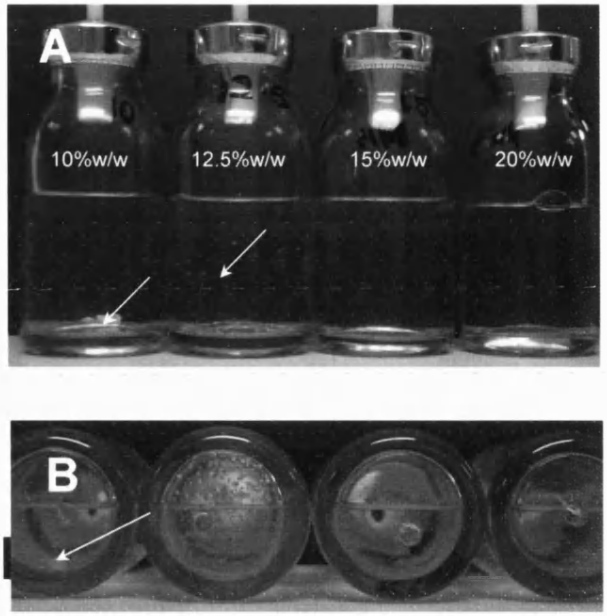

Figures 3.1 A and B: Photographic images of salbutamol maleate formulations after prolonged storage at ambient temperature (25°C) equilibration (A = side elevation and B = plan view). Co-solvent concentrations (ethanol) as a %w/w of the final formulation are depicted in ,A and the sequence is refelected in B.C and D respectively.

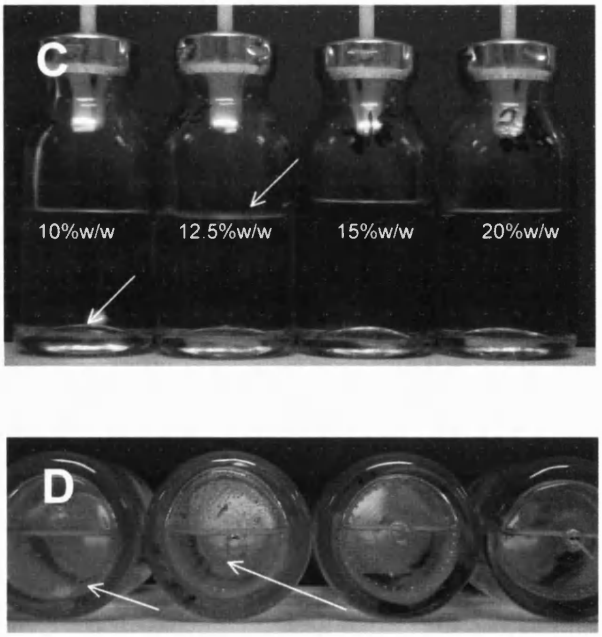

Figures 3.1 C and D: Photographic images of salbutamol maleate formulations after prolonged storage at low temperature (0 and –23.5°C) equilibration (C = side elevation and D = plan view)

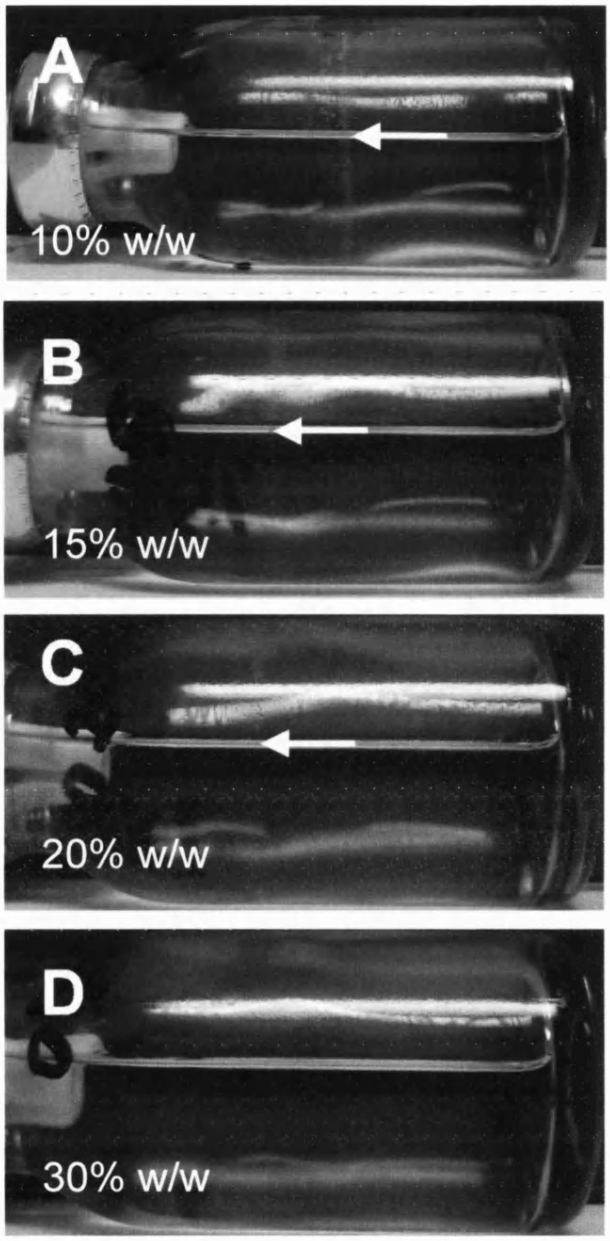

Figure 3.2 A to D: Visual solubility of salbutamol oleate solutions. Arrows indicate instability due to precipitation. Small salt crystals can be seen at the liquid gas interface. This indicated that 30% w/e co-solvent was necessary for dissolution. The respective level of co-solvent is indicated at the botton left hand of the figure.

Figure 3.3: ***A photographic image illustrating the effect of water spiking on physical stability of Salbutamol maleate solutions. Visual stability indicates single-phase systems up to 30,000ppm (3% w/w water by mass of the final formulation)***

3.3 Theoretical Evaluation of derivative solubility as a function of the Co-solvent.

3.3.1 General Discussion

Prior to practical determination of solute solubility in the co-solvent, theoretical predictions of solubility for both synthetic derivatives were determined primarily as an initial step in facilitating any possible links between theory and experimentation. Ideal behaviour assumes there is a complete absence of attractive or repulsive intra and inter-molecular forces and solubility *per se* is effectively independent of the solvent present. In this case, the solubility depends upon the temperature, molar heat of fusion (ΔH_f), where the heat of solution is equivalent to this value. During the mixing process heat exchang occurs adiabatically and the ideal solubility is given by the following relationship:

$$\log Xi = \frac{\Delta H_f}{2.303R} \times \frac{To - T}{To \times T} \times \left(+ \Delta Cp \frac{[Tm - T]}{T} - \log \frac{Tm}{T} \right) \qquad \textit{Equation 3.0}$$

Where X_i is the ideal mole fraction of dissolved solid, To is the melting point of the solute, Tm is the melting point of the pure solute, T is the ambient temperature, R is the universal gas constant and ΔCp is the change in specific heat capacity. However, the second term of the equation may be omitted as the specific heat capacity changes very little with

temperature. Real solutions approximate to Raoult's law (for the solvent component) and Henry's law (or the solid component) particularly well when dilute and chemically similar.

When a solid is left in contact with a solvent, over a period, it will dissolve depending on thermodynamics and kinetics until a saturated solution is generated. At this point, the chemical potential of the pure material is equivalent to the chemical potential of the solute in the solution, which it saturated, and when saturation occurs the following relationship applies:

$$i^*(solid) = i(liquid) = i^*(liquid) + RT \ln x\beta \qquad \textit{Equation 3.1}$$

Where i* (liquid) is the chemical potential of the pure liquid solute, i* (solid) is the chemical potential of the pure solid, R is the gas constant T is the temperature in Kelvin and xß is the mole fraction of the solid in solution. Since we can determine the heat of fusion and melting point from DSC experiments, an approximate measurement of the molality at the melting point of the pure solid compound when ΔGf = 0 and intuitively when $\frac{\Delta Gf(T^*)}{RT} = 0$ can be determined. The chemical potential of the solid can be related to the Gibbs free energy of fusion, via:

$$\ln x\beta = -\left[\frac{i^*(liquid - i^* solid)}{RT}\right] = \frac{\Delta G_f(T)}{RT} \qquad \textit{Equation 3.2}$$

it also follows that:

$$\ln x\beta = -\left(\frac{\Delta Hf}{R}\right)\left(\frac{1}{T} - \frac{1}{T^*}\right) \qquad \textit{Equation 3.3}$$

Over the temperature range of interest it can be assumed that ΔS and ΔH change very little and so the fraction of solid that will dissolve can be calculated from equations 3.3. Close to the melting temperature T≈T* and so the following relationship may be used

$$x\beta = \exp\left[-\left(\frac{\Delta Hf}{R}\right)\left(\frac{1}{T} - \frac{1}{T^*}\right)\right] \qquad \textit{Equation 3.4}$$

3.3.2 *Theoretical Determination of Solubility*

It is common practice to calculate the molality of the solid in said solvent, which is the amount of solid per 1000g of solvent. The theoretical mole fractions and molalities of several salts are summarized in table 3.0.

Salbutamol Salt	Thermal	Data
	$\Delta Hf/Jg^{-1}$	$T_m°K$
Salbutamol maleate	78.47	403.20
$x\beta$ (mole fraction)	0.055	
$n\beta$ (molality mol Kg^{-1})	1.259	
Salbutamol Stearate	93.00	384.07
$x\beta$ (mole fraction)	0.0123	
$n\beta$ (molality mol Kg^{-1})	0.270	
Salbutamol Oleate	85.7	349.85
$x\beta$ (mole fraction)	0.0696	
$n\beta$ (molality mol Kg^{-1})	1.624	

Table 3.0: Theoretically calculated molality values for salbutamol salts in ethanol from experimentally determined enthalpy values.

From the data in Table 3.0, the following table 3.1 was constructed to indicate the theoretical solubility as a percent weight / weight over common pharmaceutically encountered temperatures.

	Theoretical Solubility % w/w			
Salt Derivative	0°C	4°C	25°C	37°C
Maleate	13.231	15.797	37.047	57.251
Stearate	1.417	1.931	8.559	18.307
Oleate	9.261	12.305	48.280	97.033

Table 3.1: Theoretical solubilities of salbutamol salts based on enthalpy of fusion and melting temperatures in ethanol.

3.2.3. Conclusion

Thermodynamical calculations predicted that solutes with high melting points and high heats of fusion would have low solubilities. Based on such calculations, the maleate should have be slightly more soluble at lower temperatures and the oleate at higher temperatures; with the stearate having a lower solubility overall. Overall, the data indicated that all of the synthetic derivatives would be suitable for formulation in pMDI solution systems.

3.4 Experimentally Determined Solubility of Salt Derivatives as a Function of Co-solvent.

3.4.1 Introduction

Solubility, as formerly described, is routinely evaluated by forming a saturated solution of the compound of interest, agitating for a prolonged period to ensure equilibrium followed by filtration of the saturated solution and chemical assay. In this case, a preliminary visual assessment (active was sequentially added in small increments quantitatively to a volume of approximately 3 ml of ethanol) indicated this approach was not wholly acceptable. All salts were found to be freely soluble in ethanol, and, in relative terms, large quantities of solid was required to form a saturated solution. However, as the oleate salt was in limited supply and was observed to be particularly soluble, compared to the other derivatives, and formed a colloidal gel at very high concentrations, the stearate was substituted for the oleate, based on the fact that it was a C18 fatty saturated acid and structurally comparable. From the preliminary assessment, the standard approach for solubility in all solvent and propellant combinations was taken.

3.4.2 Methods and Materials

The salbutamol salt (maleate approximately 0.123g and stearate 0.126g) was quantitatively added to separate 25ml volumetric flasks. Before addition, the maleate material was triturated in a pestle and mortar in order to de-aggregate the material and ensure a fine free flowing powder was produced. Absolute ethanol was then added in small aliquots and the flask agitated between each addition until the level of the ethanol in the flask covered the salt, forming a saturated solution. Approximately 5g of ethanol were required for this purpose. The flask was then agitated and transferred to a water bath,

which was set at a prescribed temperature. The water bath had an integrated agitation function to keep the solute in constant movement with the solvent. To confirm the actual temperature of the bath, the thermostat reading was checked against standardised mercury in a glass thermometer.

3.4.3 Results and Discussion

Theoretical and experimental solubility determinations of salbutamol maleate, and the theoretical solubility of salbutamol oleate in ethanol are illustrated in figure 3.4. The theoretical and corresponding experimental solubilities of salbutamol stearate in ethanol are depicted in figure 3.5.

Theoretically, the predicted and practical determinations of the solubility of salbutamol maleate correlated well. Experimental solubility of salbutamol maleate showed, however, a slightly higher propensity than predicted from theory particularly at extremes of high and low temperature. Theoretical predictions of the solubility of salbutamol oleate corroborated the difficulty in appropriating a saturated solution of the unsaturated fatty acid (oleate) derivative, as the solubility was approximately 99% w/w, compared to that of the maleate, 58% w/w at 40ºC in ethanol. This trend was reflected at other temperatures, with a predicted solubility of 48% w/w for the oleate and 37% for the maleate at 29.5ºC; while at 4°C the solubility the maleate salt was predicted to have a slightly higher solubility than the oleate.

The stearate salt had been abandoned early in the initial solubility study due to the level of co-solvent required for solution stability. Approximately a 50%w/w ethanol/134(a) solution was required to stabilise this salt at 4ºC, and vapour pressure of solutions at very high co-solvent levels would not be expected to produce a viable aerosol. The solubility determination of the stearate salt was in excess of the theoretical prediction.

Differences in the experimental results versus the theoretically calculated solubilities for salbutamol sterarate were 13.99%, 15.75%, 9.02%, and 24.39% at 4, 25, 30 and 37ºC, respectively. No experimental error could account for the large deviation in the results observed.

3.4.4 Conclusion

All the physiologically acceptable acids, described in chapter two, were capable of forming salt derivatives, given their respective pKa's. Theoretical considerations indicated that the chosen acid would benefit from having a centre for inducing a polarized charge, thus, enhancing the potential to form hydrogen and carbon-dipole bonding; both free carboxylic acid groups and un-saturated moieties perform these functions well. Both the novel carboxylic acid derivatives fulfilled these criteria, and in conjunction had the added water miscible (maleate) and immiscible (oleate) characteristics, required for the necessary future aerosol studies.

Theoretical predictions of solubility assuming an ideal behaviour, derived from Raoult's law, dictated that the maleate and oleate salts were preferred for use in solutions rather than the stearate. This was subsequently corroborated by the experimental measurements, with the solubility of the oleate predicted to be higher than that of the maleate. This rationale is in agreement with theoretical predictions, since at a given temperature solutes with high melting points and large enthalpies of solution relate to a low solubility (Atkins 1982). However, at lower temperatures, this trend reversed in favour of the maleate. Solubility depends upon specific surface energy, molecular mass and shape factors. At lower temperatures, compounds will have greater crystal symmetries, leading towards lower chemical potentials and lower solubilities.

The actual solubility of the oleate could not be fully determined due to a paucity of raw material, but the correlation between theoretical prediction and experimental data generated for maleate and stearate derivatives (See figures 3.4 and 3.5) predicted a practical solubility to be in the same magnitude and suitable for use in the study.

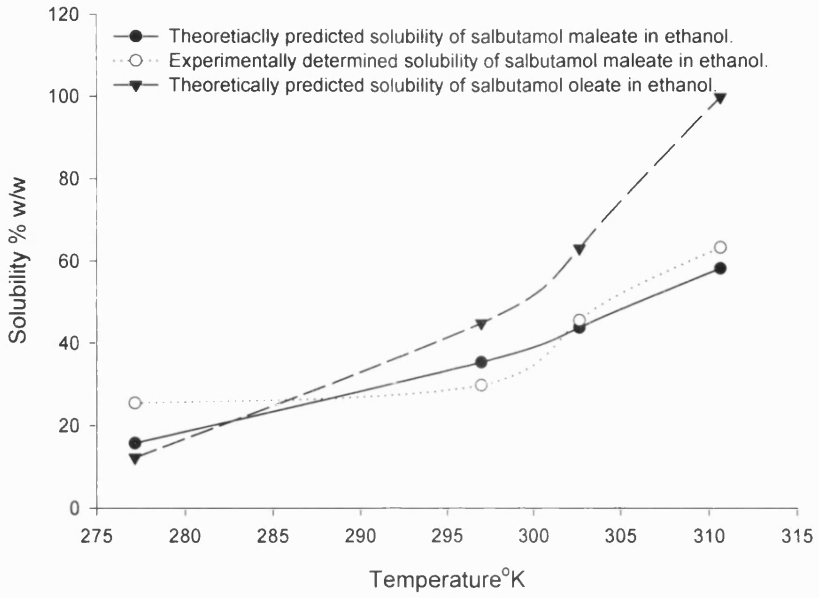

Figure 3.4: ***A graphical representation of the theoretical and experimental solubilities of salbutamol maleate and the theoretically predicted solubility of salbutamol oleate.***

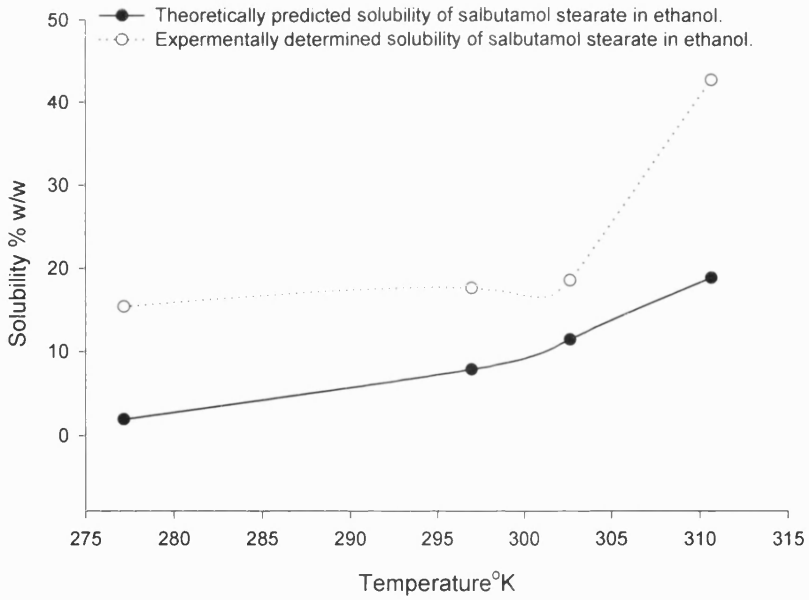

Figure 3.5: ***A graphical representation of the theoretical and experimental solubility of salbutamol stearate.***

3.5 Experimentally Determined Solubility of Salt Derivatives as a Function of 134(a) the Anti-solvent.

3.5.1 Introduction.

The measurement of solute solubility in liquefied propellant systems naturally imparts difficulties in quantitative determination. An experimental apparatus has been previously utilised for pressurized systems (Dalby et al 1991). The equipment comprised two piastic coated glass bottles communicated together via a suitable filter housing. In one was the parent suspension of micronised drug with varying levels of a CFC propellant: mixtures of P11 and P12. The receiving container, the second glass bottle, which had been pre-purged and was connected to the first via a 0.22µm filter. Once the valve containing the suspension was depressed the soluble portion of the drug in propellant passed through the filter into the receiving flask. The procedure was validated using different concentrations of suspended material with investigation of equilibration times, followed by replicate sample manufacture and blank determinations. The equipment cited formed the basis for the development of a novel propellant solubility-measuring device.

3.5.2 Methods and materials

3.5.2 (a) A novel drug solubility apparatus: Design and manufacture

Figure 3.6 illustrates a schematic representation of the designed solubility device. The device was manufactured and used experimentally throughout the study, and differed considerably from the previous system.

The body (2) was constructed from stainless steel and the base (5) from aluminium. This was intentionally designed into the apparatus to allow a gas tight seal to form from the connection between the two dissimilar metals. The base was machine turned so that a recessed shoulder and a well were formed. The well itself formed the powdered drug receptacle. The shoulder formed on the rim of the well acted as the connection to the body allowed a circular metal frit (4) with a pore size of 0.2µm which when assembled formed a seal, effectively allowing only dissolved solute to pass through. Particle size determination of bulk-synthesised drug, by laser diffraction indicated a particle size distribution was in excess of this cut-off diameter. The filter frit was held in place and sealed to prevent leakage of propellant/co-solvent mixture via 2 "O" rings (3) that sat

above and below the filter. A suitable valve (1) was crimped on to the stainless-steel body of the device.

A continuous spray valve was chosen as the shorter ferrule provided a superior crimp to the neck profile.

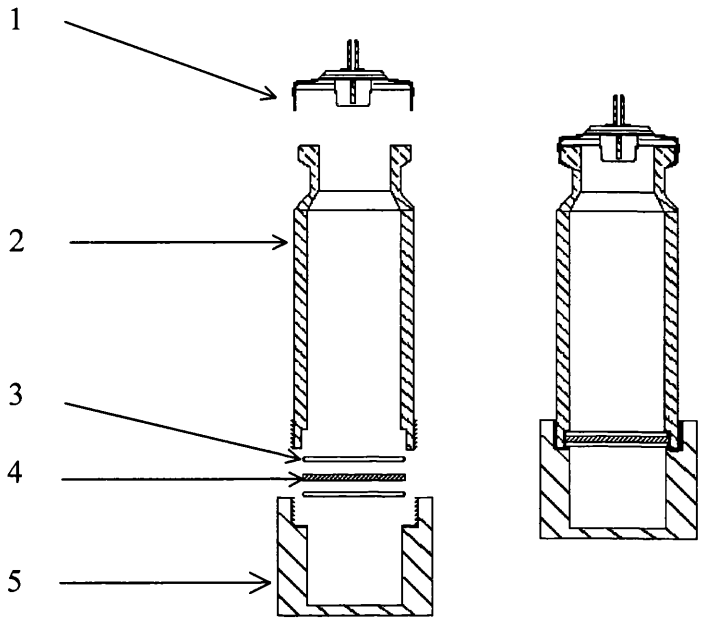

Figure 3.6: A front / side elevation of the novel solubility apparatus (NSA).

The main advantages of the NSA were:

(a) It was constructed of metal and is intrinsically safer than plastic coated glass bottles. Glass is not routinely utilised in inhalers given the transition from CFC's to HFA's.

(b) The device was reusable and allows consistency within determinations as the same can/valve assembly is used.

(c) The device could be made from any metallic/metallic polymer coated material, which would simulate the conditions encountered by the formulation.

(d) The material could be recovered after contact with the metal and analysed for any physicochemical changes i.e. polymrophic induction for example.

(e) There was a low potential for drug losses between transfer of solution from bottles, as may be encountered with the standard equipment.

(f) With an appropriate metering valve the influence of temperature/moisture ingress could be undertaken with a single device.

3.5.2 (b) Sample preparation and analysis

Salbutamol salts were synthesized as described earlier. The salts were accurately weighed into the receptacle (base station (5)) of the device and an accurate mass of 134(a) was charged into the solubility apparatus. The device was equilibrated at a known temperature with constant agitation for 24 hours per time-point to ensure thermodynamic equilibration. Samples were then prepared for analysis by preparing a solution of the solubilised salt. The solution was prepared by placing a small stainless steel tripod in a 50 ml beaker charged with 25ml of HPLC grade methanol. The tripod was constructed with an aperture to accommodate the valve stem, and allow travel into the valve body so that a dose actuation was accomplished. The apparatus was accurately weighed by mass difference before and actuation so an accurate determination of solubility, expressed as drug mass, per mass of 134(a), could be established. Prepared samples were analysed by X-ray fluorescence using a standardised and calibrated fluorimeter. System suitability was determined by standard recovery and five point linearity curves. (see section 2.8)

3.5.3 Results and Discussion

For solubility measurements, it was essential to ensure that drug was in an equilibrated, saturated state within the solvent system. To assess the optimal dissolution time, multiple solubility determinations were performed on the 10%w/w co-solvent system at 4°C, after equilibration at three specific timepoints: 2, 3 and 72 hours in order to assess if there were any statistical differences with equilibration time. The same experimental set-up was utilised in order to reduce the number of variables. Comparisons of inter group means were performed using a one-way ANOVA with a Tukey's significant difference test. The statistical analysis of the raw solubility data at 4°C as a function of equilibration time (for salbutamol maleate in a 10% w/w ethanol/HFA 134a solution) is illustrated in appendix A3.1. The low P value (>0.05) indicated that the null hypothesis should be accepted and no significant difference existed between the means of the assay results as a function of equilibration time. Thus, a 2 hour equilibration period was acceptable to use as a dissolution time as compared to a 72 hour equilibration time. For further validation, the Tukey's honestly significant difference test also indicated no significant difference. (The probability of achieving an F (Fisher ratio) of 0.98 from variances of 2 and 14 degrees of freedom is 0.4). The graphical illustrations for individual salt solubility profiles in pure propellant over equilibrated temperature ranges are depicted in figures 3.7 and 3.8. Both curves followed a similar trend. Each indicated an increase in solubility when the temperaure was increased. The solubility in 134(a) was not taken above a temperature of

40°C for two reasons. A temperature of 40° C was close to body temperature of 37°C and exposure to higher temperatures may have compromised the seal integrity of the valves on the body and the neck of the device. Both salts had an increased solubility over the sulphate and base, which are routinely used. The relative changes in solubility with temperature profile are highlighted in table 3.2

Temperature Range° C	Change in Solubility %	
	Maleate	Oleate
4-15	5.98	6.80
15-25	59.99	66.45
25-30	26.69	ND
25-37	ND	19.39
30-37	5.03	ND

Table 3.2: ***Changes in salbutamol salt solubility as a function of temperature range.***

The observed changes in solubility were smaller at the extremes of temperature (4-15°C) and exhibited the greatest rate of change within the mid-range (15-25°C). The greatest increase in solubility of maleate and oleate salts were found between 15 and 25°C with a solubility of 60 and 66%, respectively. Although some ranges were not determined (ND), it was predicted that intermediate unknown temperature ranges would have revealed greater changes for the oleate salt. It was inferred that solubility in pure propellant could be attributed to the structure of the salt modified by the counter-ion and from the pH of the solution produced as this may have affected the rate of ionization and inter molecular attraction. To account for such observed changes, both salts have an unsaturated double bond and at least one carboxylic acid group. Indeed solvation at the atomic level has been theoretically based on interactions within aqueous systems (Lynden–Bell 2000). However the approach can be intuitively correlated to organic based counterparts. In these cases, it is hypothesised that the interaction of the solute with the solvent causes a cavity of the correct shape and size to form to accommodate the solute molecule. The medium is effectively polarized by the electric field of the solute, and can be expressed mathematically with the Born model of free energy.

$$A_{sol} = -\frac{q^2}{8\pi e_o r_{cav}(1-e^{-1})} \qquad \textit{Equation 3.5}$$

Where A_{sol} is the energy of solvation, q is the charge on the ion, ε_o is the dielectric constant of the medium and r_{cav} is a cavity formed within the solvent the salts with their

centers of unsaturation may form strong dipole interactions, particularly being in a cis configuration. The dipole of the anion may cause a repulsive effect to occur and inagurate and help synergise the formation of a solvent cavity. In conjunction, free carboxylic acid groups could form intermolecular hydrogen bonds, and the resonance stabilised carboxylate anion may form a bond with the hydrogens present on the propellant. Crystal shape may also be important, since the oleate is more soluble in 134(a) and is monoclinic in nature, compared to the maleate, which is orthorhombic.

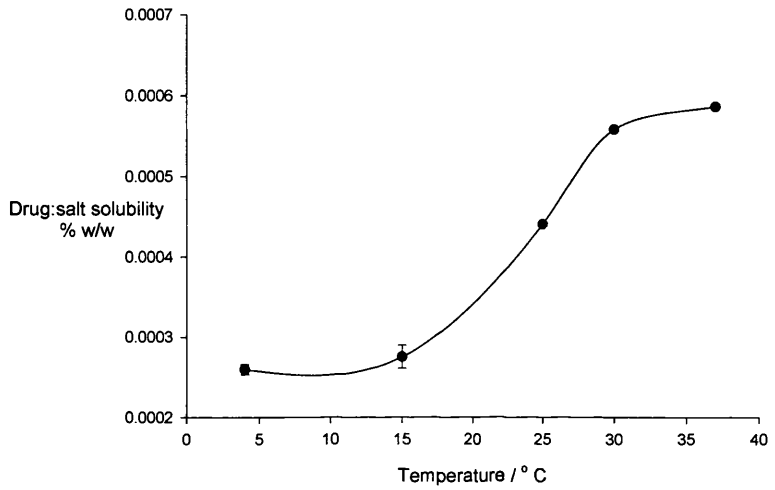

Figure 3.7: ***A graphical illustration of the solubility of salbutamol maleate in pure 134(a).***

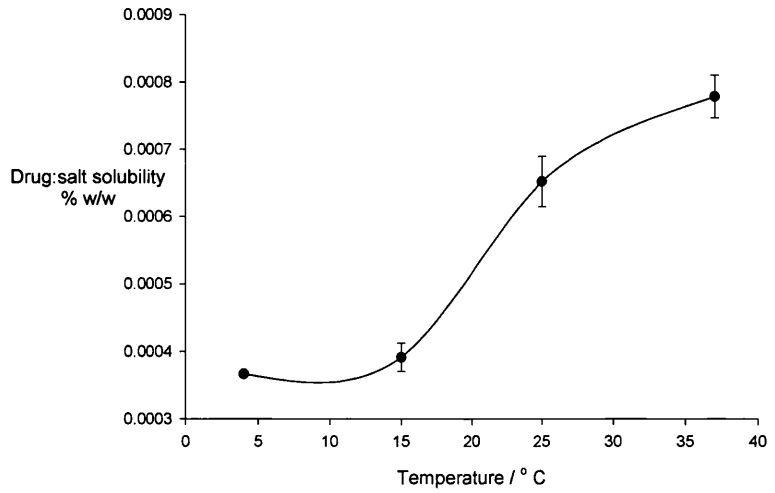

Figure 3.8: ***A graphical illustration of the solubility of salbutamol oleate in pure 134(a).***

3.6 Experimentally Determined Solubility of Salt Derivatives as a Function of Ethanol and 134(a) Mixtures.

3.6.1 Methods and Materials

The same solubility apparatus was utilised for this phase of the study as the previous. As ethanol 134(a) mixtures cannot be purchased commercially, mixtures were generated according to the following method. The drug was prepared and dried as described previously in chapter 2.2.5. It was then quantitatively weighed into the well of the solubility apparatus and an aliquot of absolute ethanol dispensed on top of the drug. The apparatus was quickly assembled and the apparatus re-weighed. Propellant was charged into the device and the mass calculated from gravimeteric measurements to give the appropriate concentration of co-solvent. This was repeated for the oleate salt, however due to lack of material, and its superior solubility profile, a 5% w/w co-solvent mixture only was prepared for this salt.

Figures 3.9 and 3.10 illustrate the experimentally determined solubility profiles of salbutamol maleate in varying co-solvent/propellant concentrations over a specific range of temperatures: 4ºC to cover pharmaceutical stability, 25ºC to encompass ambient temperature, and 37ºC to simulate physiological 'body temperature'. Included for completeness on these graphs are two supporting data sets namely: the solubility in 100% "pure" propellant (the anti-solvent) and the drug concentration in the ethanolic component (the drug concentrate component), and as solubility was different by several orders of magnitude for all systems, it should be noted that graphically log scaling was required. The second parameter (the concentrate phase) is included graphically, to introduce, and assist in the explanation and description of the novel solubility concept.

The results and accompanying discussions are considered within section 3.7. One caveat is placed upon the method of determination: sources of errors between solubility as a function of both single and dual stage propellant combinations are assumed equal. To clarify, solubility from the addition of ethanol followed by 134(a) to the requisite final blend is assumed equal to the addition of a pre-prepared blend in a single stage fill.

3.7 Introduction to a novel model for Predicting Solubility in pMDI systems: A Theoretical Approach.

From the solubility data generated, and the individual compositions of the corresponding formulations, it has been possible to theoretically predict formulation stability rather than use purely solitary empirical methods alone, which can be corroborated by visual stability assessments. The concept is simple, but powerful. Fundamentally, the data generated indicated that when the solubility of the active (expressed as a percent w/w, in the formulation namely co-solvent, and HFA 134(a)), exceeded that of the drug co-solvent concentrate alone, then solution stability was highly probable; viewed graphically indicated by figures 3.9 and 3.10 summarised in 3.11, and is intuitively correct. By plotting the data on a standard solubility versus temperature graph, then the drug concentrate phase appeared as a horizontal line parallel to the x-axis. Finally, plotting the active solubility in the final formulation, on the same graph resulted in a data plot that lay below (10% w/w co-solvent) or above (20% w/w) the drug concentrate line. If it lies below the drug concentrate plot (as per the 10% co-solvent level) then the solution was predicted to be an unstable system. Conversely, if it lies (as for the 20% co-solvent level) above the drug concentrate plot then the system was predicted to be stable.

The graphical representations, figures 3.9-3.10, illustrate the outcomes of the predicted theory, described above incorporating the experimental results. Also, for completeness, the data for solubility in propellant (anti-solvent) alone are plotted on the same graphs and due to the significant reduction in solubility expressed as percent w/w then the Y scale is log normalised (relative increase in solubility over the largest change in dielectric constant: 134(a) 9.5 to ethanol 24.3). As the dielectric constant changes substantially from pure 134(a) to pure ethanol and in conjunction the active concentration within the co-solvent changes accordingly these combined factors become important solubility indicators. The drug concentrate factor is calculated simply as follows and in practice actual and not idealized values would be used.

Example Calculation:

Convert the drug mass to the relevant unit:	0.25	%w/w	= 0.025g,
Repeat (i) for the co-solvent:	10.0	%w/w	= 1.00g
Calculate the drug concentration	0.025/1.00 X 100		= 2.5 % w/w

3.8 Solubility Data: Comparison of intra-formulation solubility profiles.

Data in table 3.3 depicts the experimentally determined solubility of salbutamol maleate in the relevant pMDI media at specific temperatures. Table 3.4 illustrates the relative intra-formulation percentage change in respective solubility.

Temperature°C	Experimentally determined solubilities of salbutamol maleate at 10 and 20% w/w Co-solvent levels at specificed temperatures.	
	10 % w/w	20% w/w
4	0.104	1.079
25	0.196	3.042
37	0.606	3.849

Table 3.3: ***The solubility of salbutamol salts (expressed as % w/w) at varying levels of co-solvent and HFA 134 (a)***

Temp Range °C	Change in solubility %	
	10% w/w co-solvent	20% w/w co-solvent
4-25	88.46	181.92
25-37	209.18	26.52
4-37	482.69	256.72

Table 3.4: ***The relative percentage change in solubility for salbutamol aerosol formulations.***

3.8.1 Intra-formulation evaluation: Data Discussion

The greatest change, for both formulations, was an increase of approximately 483%, which was exhibited by the 10% w/w co-solvent formulation over the full operating (4-37° C) temperature range, equating to about 1.88 times greater than the change for the corresponding 20% w/w formulation. The 10% co-solvent formulation also indicated a progressive increase in solubility whereas the 20% w/w co-solvent formultion exhibited minima over the 25-37°C-temperature range. The change in solubility over the low range 4-25°C was deemed important, as crystallisation had a greater propensity to occur over this range. As a result, the 20% w/w formulation was superior to that of the 10% approximately two fold. Data indicated that the change in solubility when the co-solvent

levels were increased from 10-20% w/w at 4 and 25°C were in the region of 0.98 and 1.55 orders of magnitude.

3.9 Application of the novel solubility concept: Theoretical vs. visual stability correlation

Principally, the new solubility theory centered on the fundamental concept that, when the solubility of the drug expressed as a %w/w within the overall formulation/media was greater than that of the drug concentrate alone (again expressed in % w/w terms) solubility would be highly probable at any temperature. The new theory predicted that an unstable system should result in a formulation containing a co-solvent level of 10%w/w and salbutamol maleate at a concentrate level of 2.5% w/w (Ultimately, an overall concentration drug of 0.025% w/w with respect to the final formulation). This indeed occured over the temperature range studied, and empirical visual data, depicted in figures 3.1A to 3.1D, (observe the arrows on the 10 and 12.5%w/w formulations) confirmed the prediction.

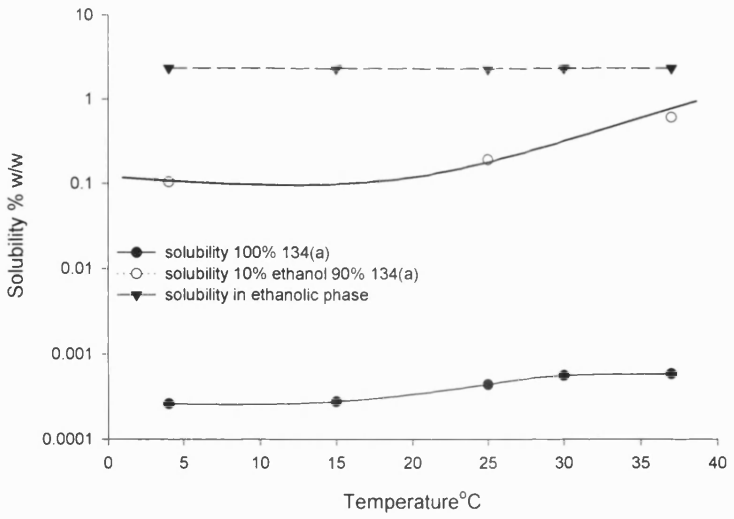

Figure 3.9: ***A graphical illustration indicating the solubility of salbutamol maleate in a pMDI formulation containing 10%w/w ethanol.***

The theory predicted that for 20% w/w co-solvent level, see figure 3.10, a stable system should result at all temperatures, as the solubility of the active in the overall media exceeded that of the drug concentrate. Again, this was confirmed visually from the glass bottle studies.

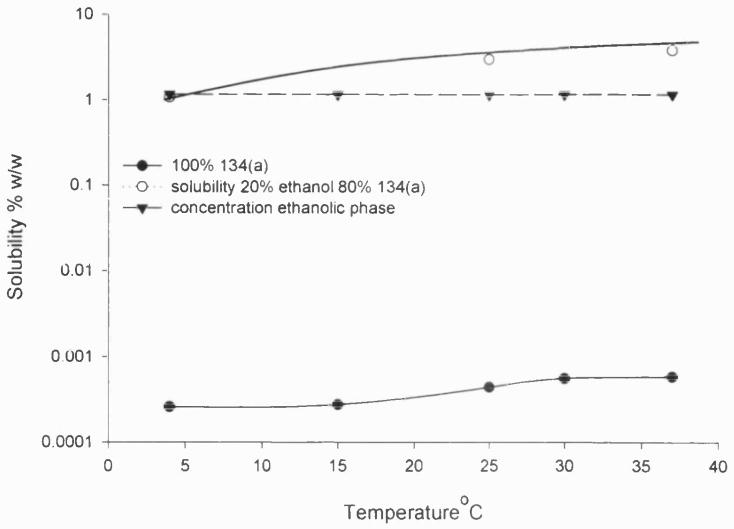

Figure 3.10: ***A graphical illustration indicating the solubility of salbutamol maleate in a pMDI formulation containing 20%w/w ethanol.***

The data in figure 3.11 is a composite graphical representation of the solubilities relating the 10% w/w co-solvent formulation, the 15% w/w co-solvent formulation and the solubility of the drug in pure ethanol (ideal infinite dilution). The horizontal lines, drug concentrates values, are for ideal formulations but serve to ilustrate the rationale. The theory predicted that the solubility of a 15% w/w co-solvent formulation at 4ºC should have an idealized solubility of approximately 1.6% w/w (visual solubility observations confirmed stability is achieved). Deviations in solubility may occur, but it is reasonable to assume that the solubility of a 15% w/w co-solvent formulation when experimentally determined and plotted on the graph in 3.11 would lie below the drug concentrate line, as it was unlikely to be greater than the 20% w/w system. It was assumed in section 3.6.1 that the two stage manufacturing process (ethanol added to excess drug followed by addition of 134(a)) would produce similar solubility profiles to that of a single stage process (ethanol and 134(a) added to excess drug). If the material was initially dissolved in a solvent and stabilized it may be thermodynamically and kinetically less favourabe to disrupt the solvated components, than solvate them initially in a solvent of reduced dielectric constant and 'liquid structure'. Irrespective of the erstwhile hypothesis it is likely from a kinetic viewpoint that at a level between 12.5 and 15% w/w co-solvent, a metastable region is likely to exist.

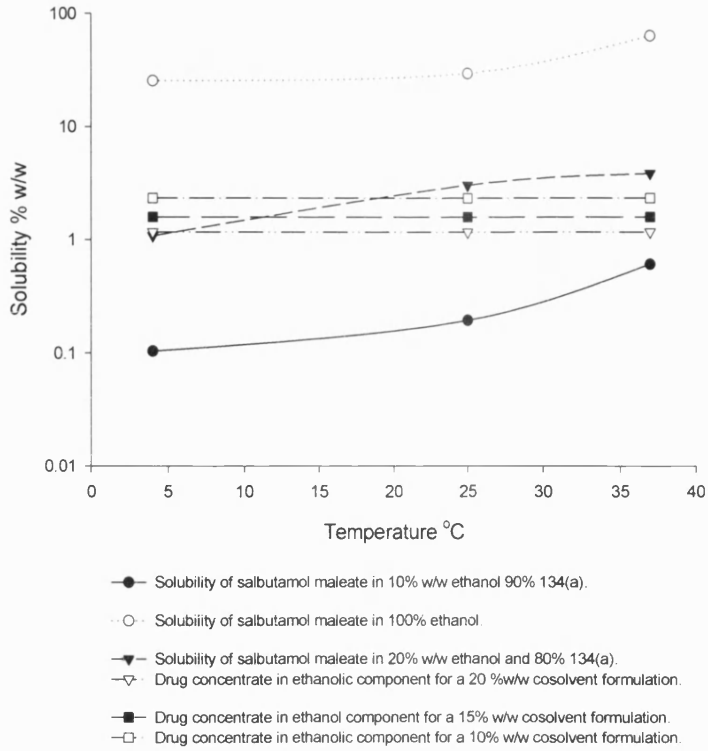

Figure 3.11: A graphical illustration indicating salt solubility and ethanol phase concentrationfor use in solution stability theory.

3.9.1 Conclusion

From visual observations, a 15% w/w co-solvent level was required to stabilise a 0.25% w/w drug loading of salbutamol maleate, which effectively equated to a drug/ethanol concentrate of approximately 1.64 %w/w. In the final formulation, and for the salbutamol oleate, a 30% w/w co-solvent level was required to stabilise a drug loading of approximately 0.37% w/w, which effectively equated to a drug ethanol concentrate of approximately 1.22% w/w in the final formulation. Due to several factors, the solubility theory could not be directly applied to the oleate salt, as the solubility in ethanol and propellant blends were not established. Future practical work would be required for this derivative to substantiate the theory. In addition, the situation with the oleate salt would be further complicated by the fact that it has low water solubility, and stability of this derivative in formulations would have to contend with effectively a second anti-solvent. The novel theory predicted that the 15% w/w co-solvent system should destabilise below 25ºC. Practically this did occur. Such a deviation may stem from several possible sources: the existence of metastable states, changes in media dielectrics, morphology, crystal

structure and enthalpies of solution i.e. the regions were the rate of formation of crystal nuclei is negligible in a supersaturated state.

Considering metastability, nucleation and eventual destabilisation in the systems illustrated previously resulting in crystallisation centres upon the critical nucleus size of the drug aggregate or the number of molecules congregated around a nucleation site. The 15% w/w system due to the stability exhibited indicated its probable existance in the metastable state. (Graphical illustrations of these zones are given in figure 3.13). Under equilibrium conditions, the rate of aggregation of active molecules and de-aggregation via solvation and dissoloution are equal. If the aggregates are smaller than the critical size they will re-dissolve, if they are larger than the critical size, they will form stable nuclei for crystal growth. The activation energy or barrier to aggregation and growth is largely dependent on the purity of the solution and the amount of solid phase and extraneous material present. From the methodology utilised in both the synthesis and in the preparation of the formulations, the metastable hypothesis is highly probable. This was confirmed from visual stability measurements from storage at low temperatures. The reader is directed to tables A 3.1 (a) –(c) appendix A 3.2 in relation to the these observations. Electronic effects may also be of significance. The rationale behind the effects of dielectric properties of formulation blends and their effects are discussed extensively in appendix A 3.2. Disruption of the crystal structure and the increase of intermolecular distances cement the link between melting point and solubility, and thermodynamically is the latent heat of fusion. Quantitatively, the data collected from DSC determinations intuitively explained that the low melting points and heats of fusion corroborate the high solubilities in ethanolic solutions, as indicated in equation 3.4. The nature of the counter-ion has been elaborated previously, however, further investigations into the structure of unsaturated carboxylic acid derivatives may help to explain the potential differences. The size and orientation of the anion helps to disrupt the crystal lattice, and, further, stereochemistry (geometric isomerism) also seems to have a degree of importance. For example, cis butenedioate (maleate) is soluble whereas trans butenedioate (fumarate) is not. As size and shape affects polarisability (Apell et al 2002) the spatial shape of the electron clouds and the orientation of the functional groups, may account for increases in solubility in ethanol. *Cis* isomeric acids from steric considerations may form stronger hydrogen and dipole-proton bonds with the solvent. *Trans* acids may lack some of these properties. Indeed *cis-trans* isomerism is evident in the solubilities of the parent acids as maleic is freely soluble in most common solvents whereas fumaric is not (Merck Index 9th Edition).

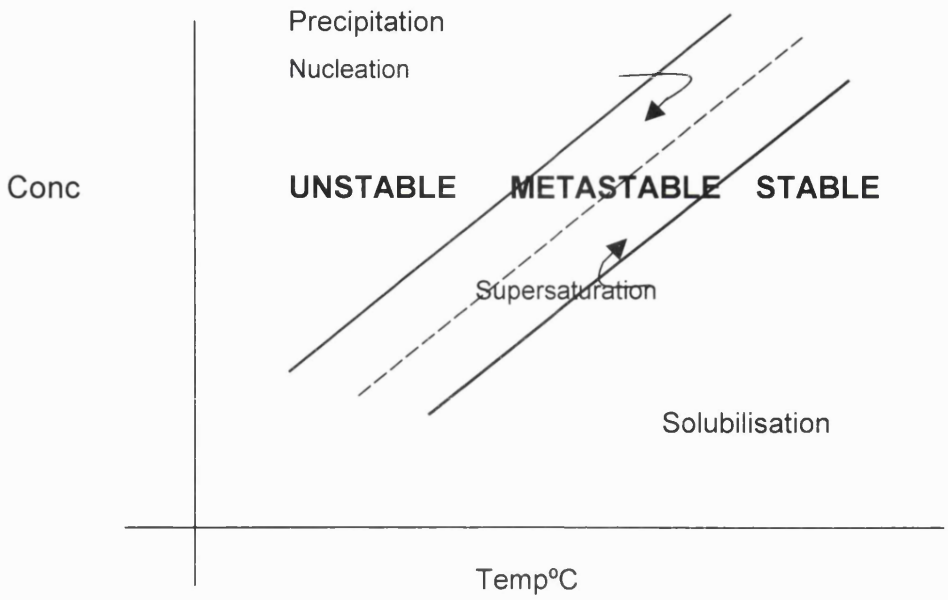

Figure 3.13 : ***An illustration indicating stable, metastable and unstable solution zones for a two component system with a positive temperature coefficient.***

Following the discussions on stereochemistry and solubility, the majority of derivatives synthesized were insoluble in ethanol and precipitated from bulk solution. Although other ethanol soluble derivatives were not structurally determined, DSC measurements were used to calculate the theoretical solubility to verify, where possible to confirm predictions. See appendix A.2 table A 2.1. All derivatives in table 3.5 indicated substantially lower solubilities than the organic carboxylate anions and did precipitate from the reaction vessel. Theoretically calculated solubility measurements for a selection of inorganic derivatives are shown in table 3.5.

Salt	Sulphate	Phosphate	Nitrate	Hydrochloride
Solubility %w/w	0.590	2.021	36.579	3.016

Table 3.5: ***Calculated solubility for a selection of inorganic salbutamol salt derivatives***

The solubility data generated on the derivatives in pure solvent indicated the oleate was the superior form. Figures 3.7 and 3.8 depict the only direct comparison between the salts, as the solubility of the oleate was not performed in identical co-solvent formulations to the maleate for reasons previously discussed. The main differences between derivatives outlined from crystallographic data were: Bravais lattice structures, space groupings, molecular volumes and densities. Shape here may also be an important factor.

The monoclinic structure (electric field of the solute) of the oleate may polarise the continuum/discrete structure of the medium (propellant 134(a) creating a cavity of the correct size to accommodate the respective ions (Lynden-Bell 2000). This would seem logical. Moreover, the volume of the oleate is approximately twice that of the maleate. Again the volume of the cavity, depending upon the solvent, may be important. If more than one molecule fits into the cavity inter-molecular attraction may reduce overall solubility.

Considering the fundamental question posed at the start of the chapter. It has been possible to theoretically model the stability of pMDI solutions by appropriate use of theory and experimental data, but deviations occurred. Due to the complex nature of pMDI formulations it may be possible to predict deviations, but extensive consideration of inherent physical chemistries would be required.

4.0 *IN-VITRO* EVALUATION OF NOVEL SOLUTION FORMULATIONS UNDER NON-STANDARD LABORATORY TESTING CONDITIONS

4.1 Aerosols: An Introduction

The primary deposition mechanisms of aerosols have been discussed in detail in chapter I, section 1.5. However, these mechanisms do not describe those inherent within spray generation (aerosolisation) and the associated droplet phenomena.

A spray is a type of two-phase flow (Sirignano 1999), involving a liquid as the dispersed or discrete phase primarily in the form of droplets or ligaments, and a gas as the continuous phase. (A solid can also be the dispersed phase and when this occurs, this is termed dusty flow). The second type of flow is 'bubbly flow' whereby the gas is the discrete phase and is conversely dispersed within a liquid, and during motion, the relative movement between the droplets and ambient the gas instigate boundary layers leading to the formation of wakes. The fluid dynamics that occur on an individual droplet level, involve complex mass and heat transport phenomena, which can also affect motion (Sirignano 1993), including shear-driven internal circulation of the liquid inside the droplet, Stefan flow resulting from vaporisation and condensation, droplet-droplet interactions, interfacial flow instabilities, droplet shape distortion and interactions within internal gas flow vortices. Importantly, the problem is exacerbated by temperature and concentration gradients and coupled particle-particle interactions. In addition, the constant changing gas conditions and multi-component liquids compound the problem, and clearly, an interdisciplinary approach is prerequisite to provide a full physical description of the complex and interlinked processes that occur. A good overview of the science is detailed by Lefebvre (Lefebvre 1989).

4.2 Overview of Droplet Formation Mechanisms.

Droplet sizes within an aerosol cloud are a key parameter in influencing the resulting particles behaviour. Depending on the composition of the liquid, the surface tension will tend towards reducing the surface of the droplet and produce a spherical shape; and the presence of surfactants and co-solvents that alter the surface tension highly influence the particle sizes during droplet formation (Seaver et al 1992). Moreover, during atomisation, temporal variations occur in droplet sizes, and as a result smaller droplets decelerate and accelerate faster than larger droplets, and ultimately, smaller droplets will heat and vaporise faster. Injection of liquid streams (pressurised in the case of this study) into a gas obviates the initial instability, and can be empirically described in terms of the Weber number.where inn turbulent flow fields the net velocity between gas and drop are similar and can expressed via the following expression:

$$We = \frac{\rho \Delta U^2 L}{\sigma} \qquad \textit{Equation 4.0}$$

Where ρ is the density of the gas, ΔU^2 the relative gas-liquid velocity, L is a characteristic dimension of the stream and σ is the surface tension of the liquid.

In basic terms, this expression relates the aerodynamic forces (pressure dependent) to the surface tensional force, and below the critical Weber number surface tension dominates and the stream of liquid is undistorted. (These criteria would become important in later experiments where pressure was the driving force for aerosolisation). Higher Weber numbers indicate that the aerodynamic forces dominate over those that restore droplet integrity. Here atomisation proceeds typically via the formation of liquid ligaments with a characteristic length dimension, and during the atomisation process, these continually reduce from their original length scale of the stream. This cascade effect continues until the decreased length scale drops and brings the Weber number below the critical value. It is not easy to describe the atomisation process overall for a simple plain orifice atomiser, but Haenlein has described three other distinct regions of droplet break-up (Haenlein 1932). These are illustrated as follows:

(1) The first is termed varicose and is independent of air and occurs from jet velocity. If the wavelength of the disturbances in the jet are greater than the minimum required for stability then disintegration would proceed.

(2) The second mechanism occurs with the influence of air and here the aerodynamic forces are no longer negligible, accentuating the waves formed in (1).

(3) Wave-like break-up can occur caused by air friction and the influence of aerodynamic forces and the reduced influence of surface tension. This region is usually termed "sinous".

(4) Complete and irregular disintegration of the jet.

The most common descriptions of jet disintegration were thosed proposed by Ohnesorge who introduced the importance of gravitational, inertial, surface tension and viscous effects. From dimensional analysis, it was concluded that the mechanisms of jet break up could be generalised into three regions by plotting the Ohnesorge number (obtained from dimensional analysis) versus the Reynolds number. This description details four regimes of breakup: Rayleigh, first and second wind and finally atomisation

It is postulated that on depression of an MDI metering valve stem, the aerosol cloud formed follows the above description, although demarcation around regions is difficult to quantitate. This is partially corroborated by dark field photography, as large droplets are formed at the front of the stream, and are effectively non-therapeutic being larger than 10 microns in MMAD. A snapshot of this atomisation process is illustrated in figure 4.0

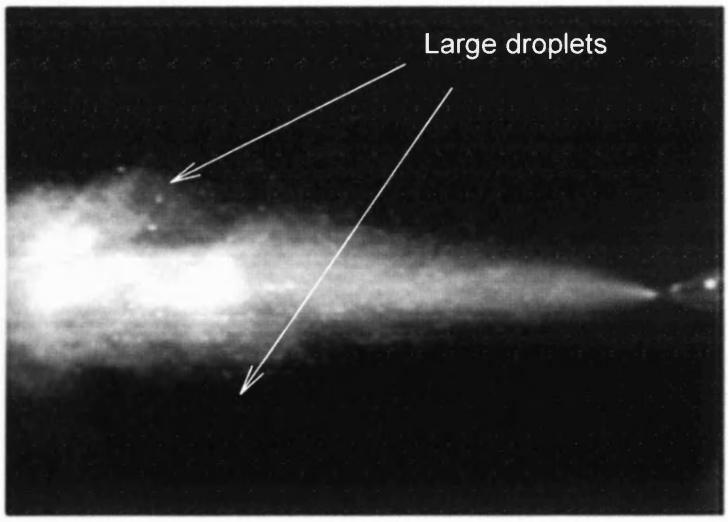

Figure 4.0 A typical photograph of the aerosol cloud emitted from a pMDI

4.3 Practical Evaluation of Droplet Formation: Previous Studies

The study of droplet formation has been studied for over a century covering many applications (Lefebvre 1989). For therapeutic applications, aqueous solutions have been the primary focus (Stapleton and Finlay 1995, Phipps and Gonda 1990), and although very different in composition to pMDI's the same general principles can be applied. The complexity of such non-aqueous systems has highlighted that no one theoretical model can predict the final particle size output from a metered dose inhaler. The individual components affecting particle size output will be considered in detail later, but, for now, there are three basic methods of predicting droplet sizes:

(a) The use of empirical methods (the most widely used)
(b) The solution of the Navier-Stokes equations in their inviscid or limiting form, the Euler equations to predict liquid break-up, and,
(c) The approach, which satisfies maximum entropy in addition to mass and energy conservation.

Clark (Clark 1996) took the empirical theory approach and applied Rosin – Rammler distributions to his experimental data in order to predict the initial median droplet diameter for a suspension-based system with varying levels of surfactants. The relationship correlated from the data is given in equation 4.1.

$$D_{[0.5]} = \frac{8.02}{q_{ec}^{0.56}} \left[\frac{(pec - pa)}{pa} \right]^{0.46} \qquad \textit{Equation 4.1}$$

Where $D_{[0.5]}$ is the initial median MMD, q_{ec} is the mass fraction of vapour in the expansion chamber, p_a is the ambient pressure p_{ec} is the pressure in the expansion chamber and integers are constants relating to quality of flow, droplet size and pressure to droplet size.

His work considered discharging the aerosol into a stagnant gaseous environment. The results approximated to the classical inverse d^2 law, as vaporisation occured in a quasi-stationary fashion. It is important to recognise that droplet behaviour is different when

aerosols are discharged into stagnant or turbulent flow fields (Hinze 1972). Although different propellant mixtures were utilised (CFC's) the valve was not metered and the determinations were made at one temperature, which was not specified, and assumed to be ambient.

In the aforementioned study, both droplet velocities and particle diameters were considered. As the volume of a droplet has an associated mass and also experienced a drag force in terms of particle size changes and velocities, the results generally agree with theory (Particle acceleration is inversely proportional to a positive power of the diameter, and particle size, to a certain extent is related to the d^2 principle, whereby the square of the diameter decreases linearly with time).

The fundamental work by Clark highlighted the importance of formulation on spray velocity and on oral deposition. Oral deposition has led to a concomitant reduction in therapeutic drug delivery to the respiratory tract and has been shown to induce side effects, particularly with corticosteroids (Konig 1988). In fact, reduction of throat deposition would be advantageous as it had been shown, historically, that only about 10% of the dose was delivered to the lungs via MDI systems (Davies 1975). However, with the advent of HFA solution systems deposition has shown to be up to 60% (Wildhaber 1998). The relationship has illustrated the importance of vapour pressure and aerosol formation and has been shown to correlate well with HFA systems (Dunbar et al. 1997).

4.4 Multi-component Aerosol Systems

A number of complications have been shown to arise in multicomponent liquid systems utilised for aerosolisation (Landis and Mills 1974). Each component will vaporise at different rates, which, in turn, will cause concentration gradients in the liquid phase affecting mass diffusion (mass diffusion is slower than heat diffusion in both liquid and gas phases), and also solid materials namely the drug substance(s), which also exist within the droplets will again affect both the mass and heat transfer rates. The consequence of formulation variables within solution systems has been previously illustrated by Gupta, whereby the MMAD of a BDP solution formulation increased with increasing solid concentration (Gupta et al 2003). The MMAD was shown not to be significantly affected by co-solvent level; however, important temperature, and associated vapour pressure considerations were not taken into account. Subsequently, Lewis and co-workers have generated several data sets comparing a number of variables: co-solvent level, actuator

orifice size and sump expansion volumes. They concluded that the MMAD was independent of both actuator orifice size and HFA 134(a) content over the particular range studied. However, although, co-solvent level and actuator orifice produced no statistically significant changes in MMAD, the spread or GSD of particles was shown to be greater for increased co-solvent level, and MMAD was found to be dependent upon the cube root of the mass of non-volatile component added, glycerol in this case. For 134(a) and 227ea, the MMAD was also dependent upon a constant which was peculiar to the propellant in relation to their physiochemical characters. These constants of proportionality were determined for HFA 134a and 227ea as 2.31 and 3.26, respectively (Lewis et al 2004). The equations proposed by Lewis are depicted in equations 4.2(a) and 4.2(b).

$$MMAD_{134(a)} = 2.31\ (\%w/w\ NVC)^{1/3} \qquad \textit{Equation 4.2 (a)}$$

$$MMAD_{227(ea)} = 3.26\ (\%w/w\ NVC)^{1/3} \qquad \textit{Equation 4.2 (b)}$$

4.5 Aerosol Device performance

As previously discussed, It is well known that formulation parameters and the device hardware influence the aerosol behaviour of a propellant driven MDI (Polli et al 1969). The seminal work systematically investigated the effects of changing formulation and actuator parameters. By doing so, the resulting MMAD for a suspension-based inhaler could be controllably manipulated. The aforementioned criteria have some credence when solution systems are considered, but, inevitably, several deviations occur. The main problem with solution systems are the 'finer' particle size distributions produced and the resulting implications that follow related to the therapeutic index (June 1997). In conjunction, aerosol devices are currently tested under *in-vitro* laboratory environments by a variety of sizing methods (see methods and materials section Chapter 2, section 2.3), which measure the aerosol particle size fractions *in situ* or by fractionating into particle size ranges. This allows the calculation of the average particle size, the total drug recovered, and the residual drug deposited on the device (actuator). There are, however, two major problems with the testing of aerosols by current pharmacopeial methods: firstly, when aerosols are measured by different methods results may differ (Hickey and Jones 2000), and, secondly, all measurements are made at ambient conditions of temperature and relative humidity, even though the human body and respiratory tract essentially operates at 37°C and 99.5 % relative humidity, and temperature and humidity gradients are known to exist, (Swift and Proctor 1977).

4.6 Aerosol Device Optimisation

Low systemic related effects with an amelioration of clinical symptoms have been deemed a measure of success when evaluating device optimisation. Delivery of a therapeutic, heterogeneous aerosolised cloud dispersion to elicit a therapeutic effect, for asthma type symptoms, should ideally deliver an areosol cloud with an MMAD in the region of 1.8 to 2.8 microns (Zanen et al 1994 and Clay et al 1986). The range of particle sizes illustrated may be due to receptor location as Clay utilised a β_2 agonist and Zanen an anticholinergic. The particle size distributions of different compounds that maximise the therapeutic ratio may be different for varying compounds (Lovtall 2001), so it would be beneficial, therefore, to manipulate formulation and environmental conditions to optimise the dose, such that the overall conditions dictating aerosol generation and deposition are better understood. These will be considered in this chapter and extended in the final chapter.

Ultimately, the ideal device would consist of a system, which would deliver optimal drug while reducing throat and device deposition, and be relatively independent of patient in inspiratory parameters.

4.7 In-vitro determination of PSD's emitted from a novel solution pMDI

4.7.1 Introduction

The following experimental sections describe the systematic investigations into the combined effects of temperature and co-solvent levels on the salient particle characteristics emitted from solution based metered dose inhalers. The actuator spray orifice diameter was kept constant, and, for comparison, to illustrate the differences with a suspension-based aerosol of similar co-solvent concentration composition and hydrophilic salbutamol salt, a commercially available inhaler (Airomir, 3M, Loughborough, UK B/No 8E103N) was tested at ambient lab conditions. The suspension-based inhaler was not subjected to the temperature equilibration as the solution systems such as temperature, as it has been shown to have little effect on particle size distribution within suspension dosage forms (Stein and Stefely 2003). Ultimately, the data generated would be used to

formulate an empirical equation to predict the MMAD of solution systems from their inherent composition.

4.7.2 Methods and Materials

Formulations were prepared according to the methodology in chapter 3, section 3.2.1 and stored for a minimum of 3 hours to temperature equilibrate, (indicated within the optimal time frame from solubility experiments), via a temperature controlled water bath (Grant LTDGG, Cambridge, UK). The components utilised for all succeeding formulations produced comprised of an aluminium canister (C128, 18ml Presspart, Blackburn, Lancs), a 50 µl metering valve (Bespak, Kings Lynn, Norfolk) and these subsequently dischared through a salamol Pk 0284 modified actuator (Baker Norton, Waterford, Ireland). For a further description of the variables altered in the study the reader is directed to appendix A 4.2 in its entirety. Three canisters were equilibrated and were weighed before and after ten consecutive actuations into an Andersen cascade impactor, in order to give a precise mass balance on recovery based on the formulation composition on an actual weight-by-weight basis. The units were primed by actuating 2 shots to waste prior to daily experimentation. As solutions, they did not require shaking between shots. In order to prevent the canisters equilibrating to room temperature, prior to transfer from storage to analysis, they were housed in a specially constructed polystyrene block to insulate the canister and prevent heat transfer. In order to assess the effect of temperature on the subsequent vapour pressure of ethanol co-solvent mixtures, which may be of significance in defining particle size equations, vapour pressure measurements of placebo formulations, covering a range necessary to ensure salt solubility (15 and 20% w/w) were performed (n=3) and the data is presented in table 4.0 (standard deviations are in brackets).

Co-solvent level (%w/w)	Temperature °C		
	4	25	37
		Pressure (psi)	
15	-	4.0 (± 0.28)	6.9 (± 0.14)
20	-	3.5 (± 0.14)	6.7 (± 0.14)
30	1.2 (±0)	-	6.9 (± 0.12)

Table 4.0: ***The effect of temperature and co-solvent level on the vapour pressure of placebo pMDI solutions.***

4.7.2 (a) Device Functionality: Dose Delivery and Performance

As the study was essentially in the development phase, no definitive specifications could be established for either delivered or emitted doses in relation to current pharmacopeial standards. In addition, temperature equilibration of the units further complicated dosing issues as valves and associated formulations are rarely if ever utilised clinically or pharmaceutically tested at temperature extremes. Recovered shot weight data calculated for both formulations over the equilibration temperatures ranged from 84-117% of theory, based on individual thermochemical data of the formulation components. Delivered dose data was calculated from said measured shot weights and individual results ranged from 69.5-90%, mean delivered dose results for each permutation ranged between 76.6-88.3% and emitted dose data ranged between 69 and 81%. All results conformed to current EP specifications for metered dose inhalers. (For clarity, the delivered dose was the total drug recovered from the metering chamber and the emitted that emitted from the actuor).

The actual mean delivered doses (micrograms) recovered from the replicate experiments (with the standard deviations in brackets), for each formulation and temperature combination of the following sequence, 15%/4ºC, 20%/4ºC, 15%/37ºC, and 20%/37ºC, were 111.35 (201.18), 114.17 (62.26) 127.76 (65.02) and 112.77 (27.34), respectively.

Table 4.1 summarises the major particle characteristics for formulations analysed post temperature equilibration, with standard deviations in brackets. Relevant data from the summary table is compounded with the appropriate particle size deposition data where applicable for completeness.

Formulation	MMAD	GSD	%FPF	% Delivered Dose	% Emitted Dose
15% : 4ºC	2.08 (0.06)	2.47 (0.06)	39.07 (0.02)	88.33 (2.39)	79.85 (1.90)
20% : 4ºC	2.30 (0.19)	2.74 (0.03)	31.20 (0.01)	84.10 (1.55)	81.47 (7.35)
15% :37ºC	1.67 (0.19)	2.20 (0.03)	49.98 (0.06)	77.41 (6.86)	68.87 (6.11)
20% :37ºC	1.96 (0.005)	2.54 (0.001)	37.16 (0.61)	76.59 (0.87)	67.66 (0.88)

Table 4.1: ***Data summary of the major particle parameters generated for salbutamol maleate solutions over a range of co-solvent levels and equilibration temperatures (FPF based on 10 consecutive shots).***

4.7.3 Results and Discussion

4.7.3 (a) *Intra-formulation particle size distributions 15% w/w co-solvent* (salbutamol maleate: hydrophilic salt)

Figure 4.1 graphically illustrates the differences in the delivered particle deposition patterns for 15 and 20% w/w solution formulations post equilibration at 4 and 37ºC. The graph also includes the data generated for a commercially available suspension formulation of a hydrophillic salt for comparison to highlight deposition profiles. Data statically evaluated by ANOVA with a Tukeys LSD at a p value of 0.95 indicated differences on stages 1, 6 and 7. The fine particle fraction increased by about 10% when the temperature was increased, but the delivered dose was reduced by about 11% as was the emitted. The reduction in emitted dose was about the same when compared to the delivered dose irrespective of the equilibration temperature, approximately 9%.

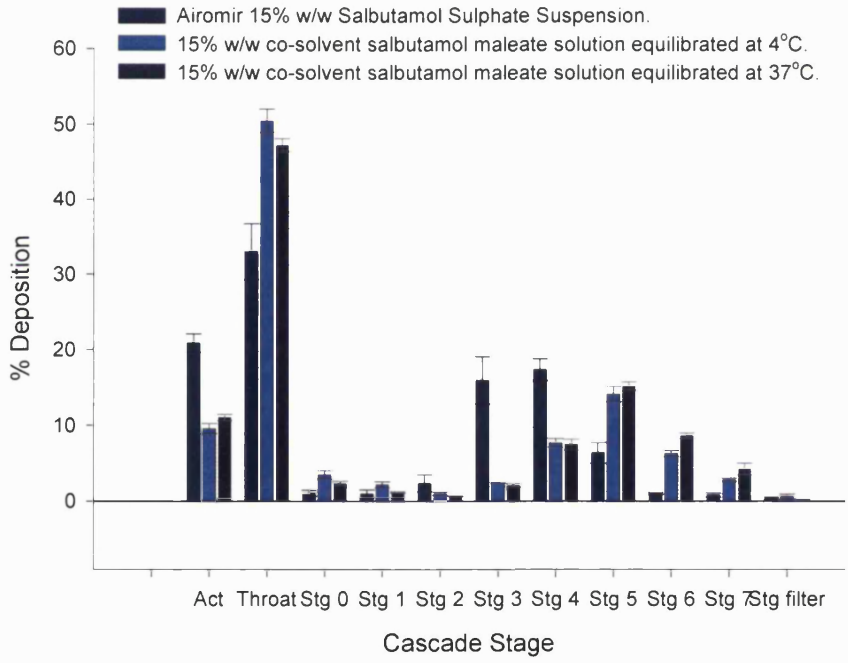

Formulation	MMAD	GSD	%FPF	% Delivered Dose	% Emitted Dose
15% : 4ºC	2.08 (0.06)	2.47 (0.06)	39.07 (0.02)	88.33 (2.39)	79.85 (1.90)
15% :37ºC	1.67 (0.19)	2.20 (0.03)	49.98 (0.06)	77.41 (6.86)	68.87 (6.11)

Figure 4.1: ***The effect of extremes of temperature on particle size distributions emitted from a 15% w/w co-solvent salbutamol maleate solution pMDI.***

4.7.3 (b) *Intra-formulation particle size distributions 20% w/w co-solvent*

A similar trend in particle deposition profiles was observed for the 20 % w/w co-solvent level of ethanol, see figure 4.2 when compared to that of the 15%w/w (Figure 4.1). The data indicated that the solution system produced a finer overall particle size distribution over the secondary aerosolisation mechanism stages: a smaller MMAD as compared to the suspension counterpart. When evaluated statistically, a similar difference pattern was observed as for the 15% solution. Significant differences were observed on the actuator, stage 1 and stage 6. The fine particle fraction data indicated an increase of about 6% when the temperature was increased, but the delivered dose decreased by about 8%. Emitted doses for both formulations also decreaed but this was only 3% when equilibrated at 4°C compared to approximately 9% when equilibrated at 37°C.

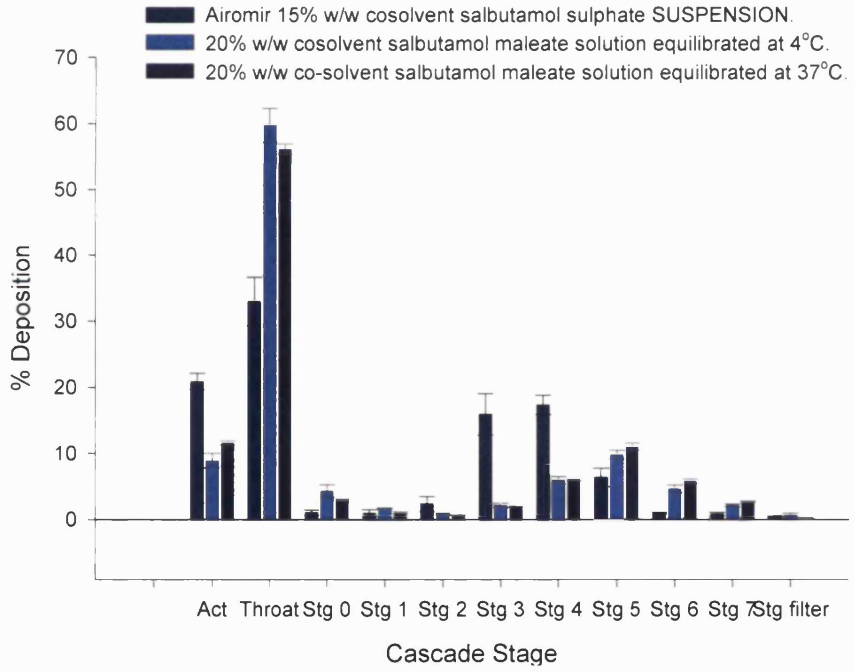

Formulation	MMAD	GSD	%FPF	% Delivered Dose	% Emitted Dose
20% : 4°C	2.30 (0.19)	2.74 (0.03)	31.20 (0.01)	84.10 (1.55)	81.47 (7.35)
20% :37°C	1.96 (0.005)	2.54 (0.001)	37.16 (0.61)	76.59 (0.87)	67.66 (0.88)

Figure 4.2: ***The effect of extremes of temperature on particle size distribution on a 20% w/w co-solvent salbutamol maleate solution pMDI formulation.***

4.7.3 (c) *Inter-formulation particle size distributions at low temperature*

Figure 4.3 depicts the deposition profiles for 15 and 20% w/w co-solvents equilibrated at 4ºC. Formualtions containing a 15 and 20% levels of co-solvents, when measured, indicated that there was only 0.5 bar pressure difference (see table 4.0), This can be related to the similar trend in fine particle fractions, delivered and emitted dose data. Data generated indicated an increase of approximately 8% for the lower co-solvent level formulation, with a corresponding increase of about 4% for the delivered dose data. Emitted doses differed by only 2%. Statistical analysis (as per previous sections) of the data generated indicated significant differences on the actuator and the following cascade stages: the throat, 1, 4 and 5.

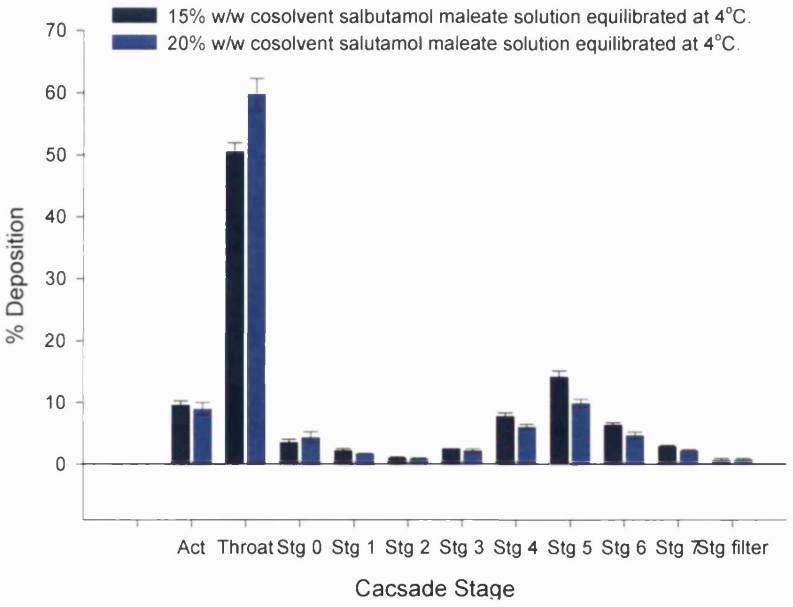

Formulation	MMAD	GSD	%FPF	% Delivered Dose	% Emitted Dose
15% : 4ºC	2.08 (0.06)	2.47 (0.06)	39.07 (0.02)	88.33 (2.39)	79.85 (1.90)
20% : 4ºC	2.30 (0.19)	2.74 (0.03)	31.20 (0.01)	84.10 (1.55)	81.47 (7.35)

Figure 4.3: ***An inter-formulation comparison of the effect of low temperature equilibration on particle size distribution.***

4.7.3 (d) ***Inter-formulation particle size distributions at high temperature***

Figure 4.4 graphically represents the data generatd when 15 and 20%w/w co-solvent levels were equilibrated at 37°C. Again the deposition profiles follow the same trend for all stages. Significant differences in particle size deposition data between these formulations were observed on the throat and cascade stages 4, 5, 6 and 7 resepctively.

It should also be noted, that at this temperature very little pressure difference occurred; only about 0.2 bar when formulations were comapared. Both the delivered and emitted dose data for formulations equilibrated at the higher temperature of 37°C were approximately equal.

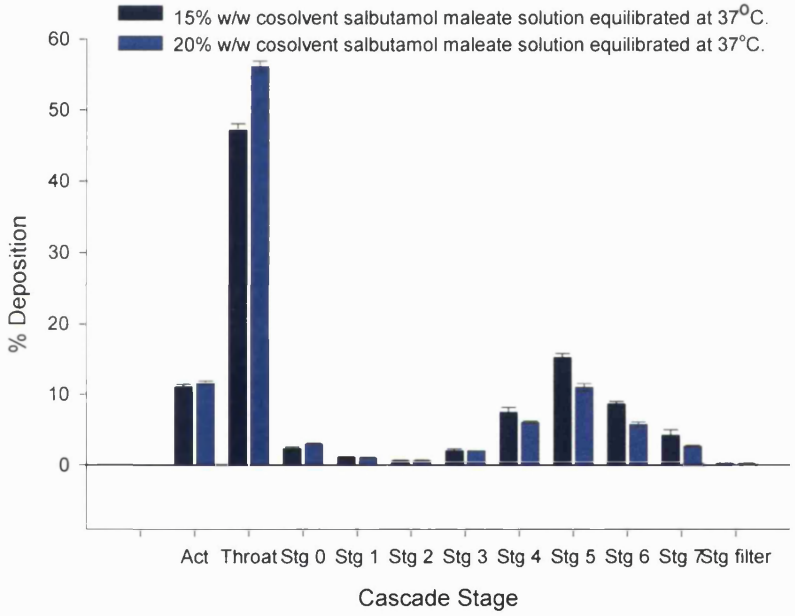

Formulation	MMAD	GSD	%FPF	% Delivered Dose	% Emitted Dose
15% :37°C	1.67 (0.19)	2.20 (0.03)	49.98 (0.06)	77.41 (6.86)	68.87 (6.11)
20% :37°C	1.96 (0.005)	2.54 (0.001)	37.16 (0.61)	76.59 (0.87)	67.66 (0.88)

Figure 4.4: ***An inter-formulation comparison of the effect of high temperature equilibration on particle size distribution.***

4.7.3 (e) *Effect of co-solvent level and temperature on MMAD.*

Figure 4.5 illustrates the data generated for MMAD distributions when both temperature and co-solvent levels were varied. Interpretation of the data indicated that temperature, vapour pressure, and co-solvent level had a significant effect on MMAD. The MMAD of the aerosol cloud tended to increase for higher co-solvent levels and lower temperatures, with the novel hydrophilic drug, when inter and intra formulation modes were evaluated under test conditions. Statistical significances in MMAD were not observed for the 15 and 20% formulations at 4°C, but were when permutations of the remaining combinations were considered resulting in a value of p=0.001. For the 15% co-solvent level formulation (intra-formulation/high temperature) a decrease of 19.7 % in MMAD was observed and for the 20% co-solvent level a decrease of 14.5% was calculated. At 4°C, an increase from 15 to 20% (inter-formulation) in co-solvent levels resulted in a 10.6% increase in MMAD, and at 37°C an increase in 17.4% was observed. In general, increasing the co-solvent level and decreasing the temperature increased MMAD.

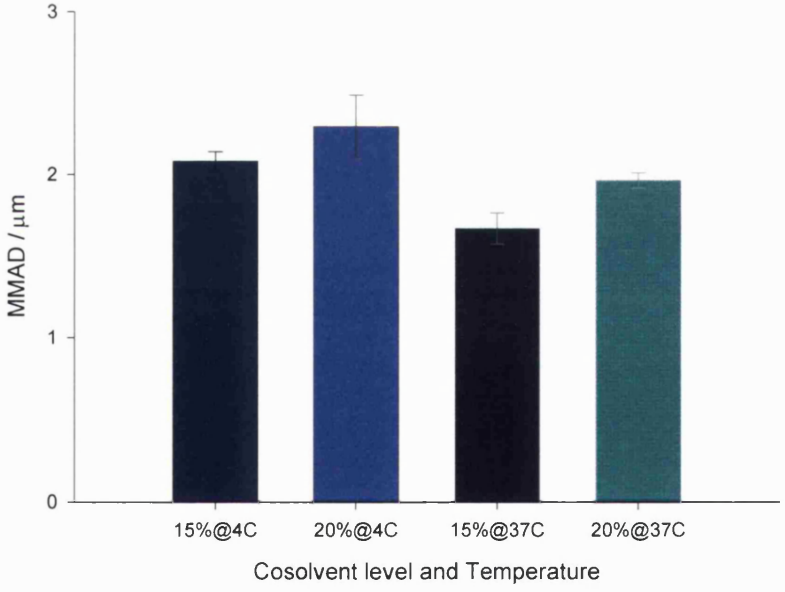

Component	15% co-solvent	20% co-solvent	15% co-solvent	20% co-solvent
Equilibration Temp / °C	4	4	37	37
MMAD	2.08 (0.06)	2.30 (0.19)	1.67 (0.19)	1.96 (0.001)

Figure 4.5: ***The effect of co-solvent level and temperature on the resulting MMAD of aerosol clouds generated form a salbutamol maleate solution pMDI.***

4.7.3 (f) ***The effect of co-solvent level and temperature on GSD.***

A similar pattern was observed in the amount of polydispersity of the aerosol cloud, when the GSD was compared with the MMAD, as depicted by the data in figure 4.6. Polydispersity increased with increasing co-solvent level and decreased with increasing temperature (the decrease of GSD with increasing temperature occurred when considered only for intra formulation comparisons). Statistical evaluation of the data via ANOVA at P=0.95 indicated the only conditions that were not significantly different from one another were the 15% formulation equilibrated at 4°C and the 20% formulation at 37°C. When significance was achieved this was at a level of $p<0.001$ Considering intra formulation effects, when the 15% co-solvent level formulation experienced an increase in temperature the result was a reduction in cloud polydispersity by about 10.9%; when the 20% co-solvent formulation was considered the drop was less, with a 7.3% reduction. Inter formulation comparisons indicated a similar but reverse trend: an increase in polydispersity as both co-solvent level and temperature were increased: an increase of about 10.7% at 4°C and an increase of about 15.5% at 37°C.

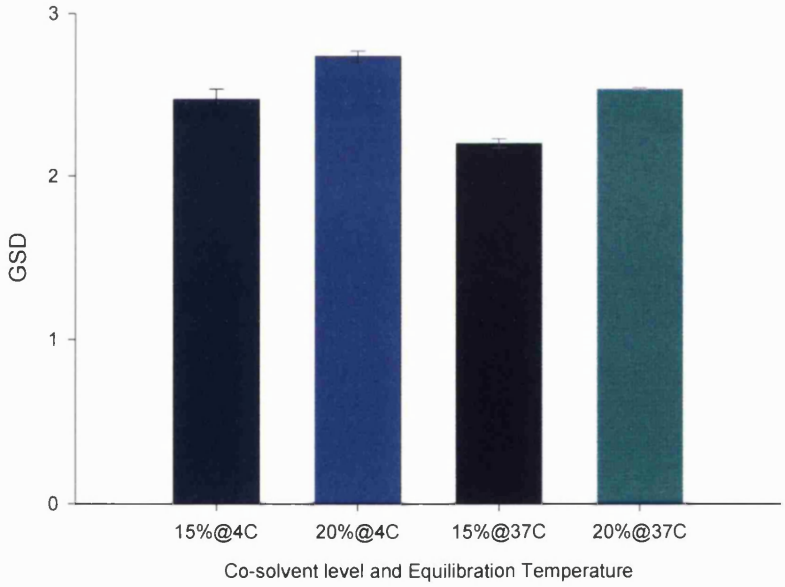

Component	15% co-solvent	20% co-solvent	15% co-solvent	20% co-solvent
Equilibration Temp / °C	4	4	37	37
GSD	2.47 (0.06)	2.74 (0.03)	2.20 (0.03)	2.54 (0.001)

Figure 4.6: ***The effect of co-solvent level and temperature on the resulting GSD of aerosol clouds generated form a salbutamol maleate solution pMDI***

4.7.3 (g) Effect of co-solvent level and temperature on FPF.

Figure 4.7 illustrated the data generated for the respective fine particle fraction of the aerosol cloud when formulations were equilibrated at varying temperatures. When analysed statistically, a significant difference between the data sets was established for all respective combinations, bar one: the 15% co-solvent level equilibrated at 4ºC compared with the 20% co-solvent level equilibrated at 37ºC, as elucidated by Tukeys LSD. The fine particle fraction increased when the temperature was increased for formulations compared on an intra-co-solvent level. The greatest fine particle fraction was exhibited by the 15% co-solvent formulation equilibrated at 37ºC. The change in fine particle fractions, for each of the formulations and equilibration conditions, can be directly related to the data in the table beneath the graphical representation.

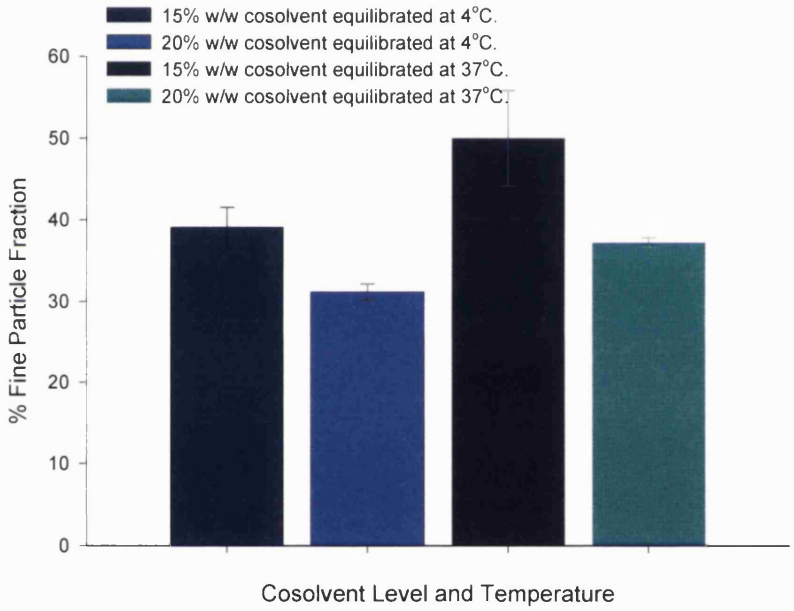

Component	15% co-solvent	20% co-solvent	15% co-solvent	20% co-solvent
Equilibration Temp / ºC	4	4	37	37
% FPF	39.07 (0.02)	31.20 (0.01)	49.98 (0.06)	37.16 (0.61)

Figure 4.7: ***The effect of co-solvent level and temperature on the resulting fine particle dose of aerosol clouds generated form a salbutamol maleate solution pMDI.***

4.7.3 (h) ***The effect of co-solvent level and equilibration temperature on the Large Particle Fraction (LPF).***

Figure 4.8 illustrated the change in the large particle fractions of the formulations. In general, a trend occurred for identical co-solvent levels: the actuator deposition increased with temperature, (about 1.5%) but the throat deposition decreased (about 3%). When compared on an inter formulation and temperature equilibration mode throat deposition increased with cosolvent level increase (about 9%) at 4°C and 37°C, but there was no discernable trend in actuator deposition. Significant differences were detected in deposition for the following combinations: 15% w/w 4°C and 20% w/w 37°C; 20% w/w 4°C and 15%w/w 37°C; and 10%w/w 4°C and 20% w/w 4°C and 20% w/w 37°C at alevel of p= 0.005. For throat depositions, significance at a level of p=0.001 was achieved for all combinations bar those of 15% w/w 4°C and 15% w/w 37°C and 20%w/w 4°C and 15% w/w 37°C

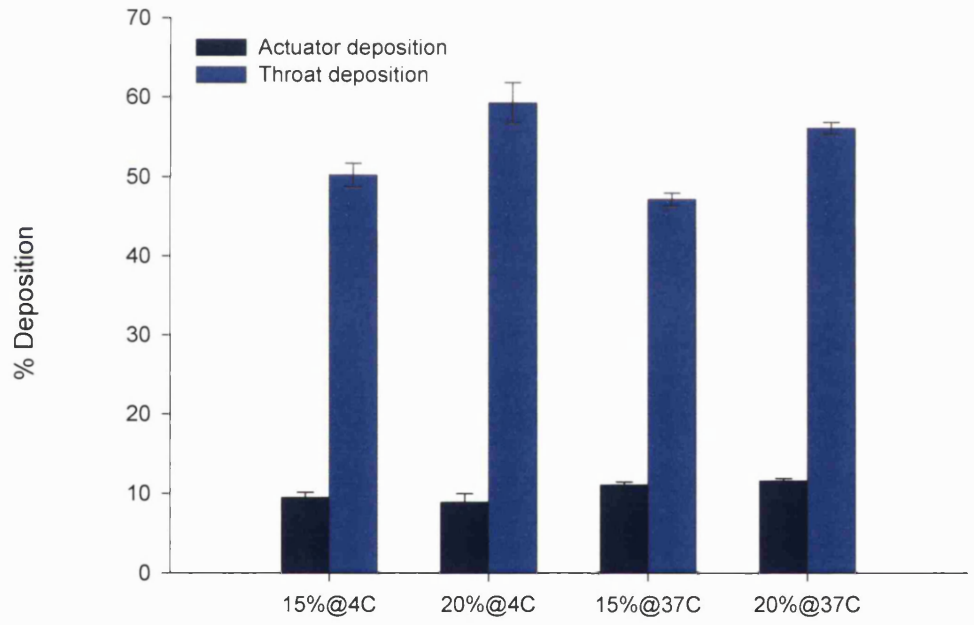

%Deposition	15% : 4°C	20% : 4°C	15%: 37°C	20%: 37°C
Actuator	9.56 (0.69)	8.89 (1.10)	11.03 (0.43)	11.58 (0.43)
Throat	50.43 (1.51)	59.71 (2.56)	47.22 (0.85)	56.14 (0.76)

Figure 4.8: ***The effect of co-solvent level and temperature on the actuator and throat deposition patterns of aerosol clouds generated form a salbutamol maleate solution pMDI***

4. 7.4 Conclusion

The andersen cascade deposition patterns for both the 15 and 20% cosolvent level salbutamol maleate formulations displayed a similar trend irrespective of the temperature of equilibration, and statistical significances are delinetaed where appropriate. To elucidate why these differences occurred, other critical parameters must be investigated: the MMAD and the GSD.

MMAD data generated both differed from and conversely agreed with those in the literature. Data generated by Gupta (Gupta et al 2003) predicted a mass mean aerodynamic particle size of about 1.2-1.3µm (taken from data extrapolation) for BDP solution formulations at co-solvent levels of 15 and 20%; whilst the MMAD increased slightly with co-solvent concentration, and it was highly dependent upon solute concentration. However, in this study an Andersen cascade was not utilised, instead a 3320 APS (TSI Inc. Shoreview, MN) attached to a USP throat via a 20cm extension tube coupling was chosen. Data from these studies may be open to validation and scrutiny, as no calibration was indicated on the optical system, although this may have been performed. (Particle refractive indices should be verified under both dry and solvent laden ''wet conditions, as evaporation will take place during experimentation). The use of a standard USP throat would also not compensate for changes to, and the amortisation of differing equipment. Further, adding an extension tube may add to particle evaporation times as the coupling tube may act as a spacer. Finally all experimentation is assumed to be carried out at ambient conditions again this was not documented and could not be verified.

Documented MMAD's generated in this study ranged from 1.67µm to 2.30µm respectively. For equivalent co-solvent levels to that of the Gupta et al study, non-volatile concentrations would facilitate a drug loading of 0.4% w/w or greater in the final formulation,approximately double that here. Extended comparisons of the data indicated other differences: throat depositions in the Gupta et al study were less than those in this thesis. Namely depositions for the 20% w/w BDP solutions equated to those of the equivalent 15% w/w hydrophilic maleate salt, and those of the 20% w/w co-solvent level maleate salt formulation were not equitable on the corresponding graphical representation. Also the fine particle fractions were different. The 15% w/w hydrophilic maleate salt formulation gave a respirable fraction equivalent to a 10% BDP solution

formulation. Likewise a 20% w/w hydrophilic maleate formulation gave an equivalent respirable fraction to a 15% w/w BDP solution formulation.

However, these data do follow a similar trend to those observed by Brambilla and co-workers (Brambilla et al 1999). They indicated a range of MMAD measurements between 1.1µm to 1.8µm for co-solvent levels of 15% w/w and drug loadings of 0.085% w/w to 0.424% w/w for identical actuator orifice diameters, when formulated as BDP solutions. It should be noted that the actuators from all studies were different thus would have different airflow geometries.

Both of these studies indicated that MMAD increased with non-volatile component and was not significantly affected by co-solvent level; although, both noted there was a slight increase, with increased co-solvent level. Data presented by Lewis (Lewis et al 2004). regarding co-solvent concentrations and the effect on particle size indicated a high p value (0.086), but was not far from significance. Both of these studies were conducted at ambient inhaler temperature, and while ambient temperature was assumed, neither study indicated a laboratory temperature. In this study, temperature equilibration significantly changed the vapour pressure, which significantly altered actuator deposition, throat deposition, the MMAD and GSD. The added effect of the co-solvent further increased the aforementioned effects, and also had an impact on the fine particle dose. Interestingly, an increase in spray orifice diameter had the effect of increasing MMAD, whilst decreasing FPD.

The change in MMAD can be equated to the overall changes in vapour pressure, surface tension and viscosity as a result of temperature change. At low temperature the surface tension and viscosity of the formulation all increase. And a liquid drop will remain intact as long as the fluctuations, which occur in air pressure around the drop surface, are compensated by surface tension. Surface tension forces resist expansion of a liquid surface, and to achieve atomization those of the aerodynamic, centrifugal, or pressure forces must supersede them. At low temperature, the former will this resist change to a greater degree. Intuitively, therefore, the increase in surface tension resists the deformation forces.

Liquid viscosity opposes the deformation because aerosol breakup time increases. Viscosity also has a marked effect on liquid velocity, namely nozzle flow rate decreases, as does the Reynolds number hindering jet instabilities. As the formulation exists the actuator thickening the jet occurs raising the flow area delaying disintegration and

increasing drop size. At high viscosities energy losses are greater and less energy is available for atomization. (Lefebvre 1989).

As liquid jet disintegration and conversion into droplet atomisation is proportional to liquid velocity, and volumetric flow rate is inversely proportional to the square root of liquid density, then the effects of temperature and thus density are important. (Weber 1931) (See equations in appendix A 4.0). There is a substantial change in the densities of the major volatile propellant: 1282kgm^{-3} at 4ºC and 1160kgm^{-3} at 37ºC. In conjunction at high viscosities the Reynolds number is lower and so turbulence on the droplets is therefore less, equating to less inertia and, so, reduced particle breakup

The rate of particle evaporation also changes due to changes in the liquid phase. Within an array of multicomponent aerosol droplets the more volatile component will vaporise faster leaving the less volatile component; in effect mini distillation occurs. It has been proposed that micro-explosions equivalent to flash evaporation take place (Landis and Mills 1974). Thermodynamically, the enthalpy of the liquid mixture is reduced at lower temperatures. Consequently, the heat capacity of the individual droplets within the aerosol cloud also changed and are lower at constant ambient pressure.

Intuitively, a low enthalpy value equates to a low internal energy, therefore reduced evaporation takes place at reduced liquid temperatures. Ethanol has greater heat capacity and enthalpy values compared to the propellant, and its increase in concentration in this respect, explains the increased time for evaporation and therefore size change.

Significant changes in aerosol polydispersity (over all combinations) were noted at both fifteen and twenty percent co-solvent levels, and the degree of cloud particle size dispersion increased for a given co-solvent level and decreased as the temperature was increased. A trend was noted here, as with the MMAD, that the 15% formulation at 4°C was similar in value to that of the 20% formulation at 37°C. The wide range of particle size distributions that occured within the aerosol clouds may be due to droplet-droplet interactions within the cloud and droplet gas flow interactions. As isolated droplets come close to each other, drops can influence particles several radii away and can even impact on each other and coalesce. Alternatively, many other particles may emerge from the collision. This tends to occur at higher co-solvent levels and consequently higher surface tension and viscosity levels. Indeed coalescence has been implicated as an important factor at the injector orifice in petrol engines. The theory predicts increasing average droplet size increases downstream from the injector / orifice, which corresponds with the

data generated here. Although different intrinsic physicochemical data were implicated for the petrol injector, basic principles apply to both systems (O'Rourke and Bracco 1980). One possible reason for the increase in actuator deposition at high temperature may be due to the reduction in surface tension and so increased wetting of droplets and final droplet-droplet coalescence. The increased wetting my also account for particle stick to such a low surface energy material as polypropylene from which the actuator is made.

As the level of co-solvent rises and the temperature drops, the vapour pressure of a liquid droplet is lower, surface tension is greater, viscosity is greater and the temperature gradient between the drop and surrounding air is also increased. As indicated, these will influence the ambient gas temperature, particle momentum and vaporization by heat and mass transfer. Other possible mechanisms may occur whereby at smaller droplets vaporise faster leaving the larger droplets, condensation occurs in the colder vapour rich regions of the spray near to the spray orifice and the longer wavelength disturbances on the jet will take longer to grow and yield larger droplets.

Droplet collisions, primarily two droplets as probability of three droplet collisions are low, can lead to several permutations of interaction: permanent droplet-droplet coalescence, initial coalescence and separation, separation into two other daughter droplets, separation into smaller satellite droplets particle bounce and shatter. Several studies regarding two droplet collisions have been made. Qian and Law (1997) distinguished between five distinct regions of droplet collisions by plotting the Weber number against the impact parameter (the shortest distance given by tangents to the direction of motion at the time of impact). Essentially at small impact parameters and increasing Weber number coalescence is followed by bounce and followed by coalescence again. This is a simplified explanation of a complex phenomenon but helps to explain changes in MMAD and polydispersity.

4.8 Current Semi-Empirical Methods to Predict MMAD's of pMDI's.

The major parameters that describe an aerosol cloud for medicinal purposes are MMAD, GSD, LPD, FPD and the distribution pattern indicated by the stage-by-stage delineation and the corresponding cumulative distribution. At present, the physical processes that result from atomisation of an aerosol cloud are insufficiently appreciated so that the derivation of particle size distributions from basic equations has been limited, and not wholly applicable to HFA systems. It would be advantageous to be able to predict the

MMAD and GSD of a therapeutic aerosol as these parameters have been routinely utilised to correlate to the specific therapeutic area. (Stalhofen et al 1989)

From the data collected, it was apparent that the criteria necessary to describe particle size from the solution system were dependent upon the non-volatile formulation components (drug: salt), low volatile formulation components (ethanol), volatile formulation components (134(a)) and pressure (as a function of temperature) of the system. However, the literature has indicated that the presence of excipients, and changes in physicochemical nature (surface tension, viscosity) and thermodynamics were also fundamental to the atomization process (Brambilla et al 1999). Consideration of all these processes, allows supports the derivation of an expression to determine the equilibrium particle size emitted from a pressurized solution system, analogous to that evaluated by Clark and Lewis. (Clark 1996; Lewis et al 2004). Empirical equations exist for calculating the MMD, SMD and percentile sizes of particles generated from plain orifice atomizers, and it was theorised from the data generated that the MMAD could be predicted from empirical equations. However most of the research has been carried out on compression ignition engines. The fundamental properties and characteristics of such systems that were incorporated to describe the MMAD generated included the following: the vapour pressure, actuator orifice diameter, surface tension and the viscosity of non-volatile and semi-volatile components (Harmon 1955, Giffen and Lamb 1953 Elkotb 1982).

4.8.1 Derivation of an equation to predict MMAD's generated from solution based pressurized metered dose inhalers.

The derivation of an equation providing a complete description of a multicomponent liquid droplet is beset with complications dependent upon the different vaporization rates of the components, resulting concentration gradients within the liquid, constant changes of mass and heat diffusion rates, to name a few of the multitude of variables.

Consider the liquid particle, its composition can be expressed as the number of moles of the individual species where,

$$X_m = \frac{W_{(g)}}{RMM} \qquad \textbf{Equation 4.3}$$

The number of moles of component is X_m , $W_{(g)}$ is the weight of component in grams and the relative molecular mass RMM is in grams per mole.

The mole fraction of a species say Mf(a) (active solid) in a quarternary mixture of (a) active, (e) (ethanol), water (w) and v (volatile component 134(a)) is then ,

$$Mf_{(a)} = \frac{Moles_{(a)}}{Moles_{(a)} + Moles_{(e)} + Moles_{(v)} Moles_{(water)}} \qquad \textit{Equation 4.4}$$

The relationship between the non-and semi-volatile with the energetic volatile component can be described as a ratio between the two, with the universal gas constant utilised to mediate for changing temperatures, volumes and energy distributions of the molecular components parameters, as depicted in equation 4.5.

$$\frac{\left((Mf_{(a)} \cdot R.)(Mf_{(e)} \cdot R)(Mf_{(water)} R)\right)}{Mf_{(v)} \cdot R} \qquad \textit{Equation 4.5}$$

As surface tension and viscosity are important parameters in droplet kinetics and thermodynamics these have been incorporated into the final equation. The surface tension as stated is important in the calculation of the Weber number of the droplets and the viscosity in the calculation of the Reynolds number. These variables along with the diameter of the spray orifice yielded equation 4.7 to predict the MMAD.

$$\frac{P(atmos)}{P(system)} \times \frac{Mf(a) \times Mf(e) \times Mf(water)}{Mf(v)} \times R^2 \times \left(\frac{\sigma(ae)}{\sigma(v)}\right)^x \times \left(\frac{\eta(v)}{\eta(ae)}\right)^x \times d_O = MMAD \qquad \textit{Equation4.6}$$

Where, $P(atmos)$ is the ambient atmospheric pressure, $P(system)$ is the pressure of the pMDI at specified temperature, $Mf(a),(e),(v)$ are the mole fractions of the (a) active the non volatile component, (e) ethanol, the semi volatile component, and (v) 134(a) the volatile component. R is the gas constant, $\sigma(ae),(v)$ are the tensions of the active ethanol mixtures and the surface tension of the volatile component at a specified temperature and finally, $\eta(ae),(v)$ are the viscosity of the active ethanol mixtures and of the volatile component at a specified temperature.The equation, to fit the data, also had a constant x, which equated to values of 0.5 at 4°C and 3.5 at 37°C respectively. Table 4.2 indicates

the values utilised in the calculations of viscosities and surface tensions of ethanol/134(a) mixtures used in the solution formulations.

Table 4.3 illustrates both the actual experimental MMAD data generated and the corresponding theoretically predicted MMAD's from the semi-empirical equation 4.6.

Temp°C	Viscosity / kgS^{-2}		Surface Tension / Nm^{-1}	
	Ethanol	134(a)	Ethanol	134(a)
0	1.77E-03	2.73E-04	2.41E-02	1.15E-02
20	1.20E-03	2.11E-04	2.24E-02	8.69E-03
40	8.34E-04	1.62E-04	2.07E-02	6.06E-03

Table 4.2: ***Thermochemical data utilised in theoretical particle size calculations.***

(Data for propellant 134(a) was taken from the Solvay Fluor data sheet 2005 and for ethanol from the Efunda (engineering fundamentals) web site 2005)

Co-solvent level / %w/w	Temp / °C	Active (%w/w)	Predicted MMAD	Actual MMAD	% change
15	4	Maleate (0.27)	2.01	2.08	+3.0
15	37	Maleate (0.27)	1.69	1.67	-0.99
20	4	Maleate (0.22)	2.44	2.30	-0.94
20	37	Maleate (0.22)	1.91	1.96	+3.0

Table 4.3: ***The predicted MMAD of solution based metered dose formulation containing a novel salt utilising equation 4.7 and experimental studies.***

Predicted MMAD's were calculated from equation 4.7 using vapour pressure data evaluated from placebo formulations, with theory and practice correlating well with only minor deviations. However, to fully validate the particle size distributions proposed by equation 4.7 then a range of formulations at varying temperatures would need to be analysed and data reviewed with the equation. These would include several actives, co-solvent levels and spray orifice diameters as all variables are predicted to change the particle size distribution of the clouds.

4.8.2 Evaluation of the Geometric Standard Deviation.

Determination for a value of the GSD of the particle size of an aerosol cloud would be invaluable in the calculation of the fine particle fraction emitted from a metered dose inhaler as 95% of an aerosol cloud lies within the range of ln MMAD ±2 ln GSD. Therefore amalgamation of both the MMAD and GSD may allow calculation of the therapeutic fraction emitted from the inhaler. The values for the GSD could be related relatively simply as the GSD was 1.19 times the GSD at 4ºC and about 1.31 times the MMAD at 37ºC. Further it was found that a simple relationship resulted between the key parameters and the fine particle fraction: the product of the MMAD and GSD when plotted against the fine particle fraction approximated to a linear relationship (R^2 = 0.95 line of best fit)

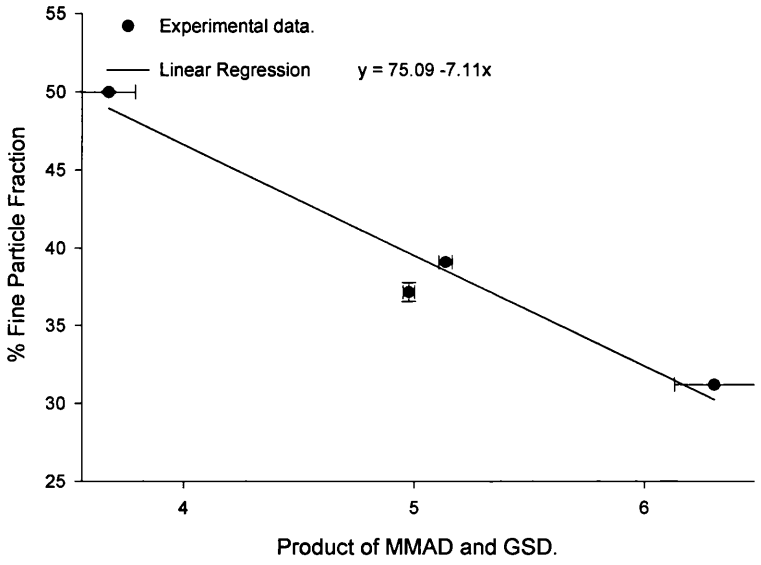

Figure 4.9: A graphical illustration of the relationship between MMAD,GSD and Fine Particel Fraction.

4.8.3 Conclusion

In conclusion, this chapter has evaluated the effect of formulation variables on particle size distribution and associated particle characteristics. Temperature and thus pressure together with concentration changes in co-solvent had a major impact on inhaler output. From these results, an empirical relationship was produced effectively calculating the equilibrium MMAD (as a function of the principle physicochemical properties of the components of the formulation) and the resulting GSD values. One caveat associated

with the data relates to the surface tension and viscosity values utilised in the calculations. Idealised values at 0, 20 and 40ºC were utilised in calculations, as specific data for ethanol and 134(a) were not available.

These results challenge current data. Also, if such major effects are observed at ambient conditions then evaluation under *in-vivo* simulations and the effect of drug character warrant further evaluation.

5 THE EFFECTS OF ENVIRONMENTAL CONDITIONS ON THE AEROSOL CHARACTERISTICS OF NOVEL SOLUTION PMDI'S

5.1 Introduction

It has been postulated from experimental investigations that the environment of the respiratory tract can influence the fate of inhaled aerosol particles (Morrow 1986). *In-vitro* experimentation substantiates theory, as the measured deposition patterns resulting from aerosol generation indicate changes in particle size fractions and polydispersity dependent upon the physicochemical composition of the cloud and the ensuing thermodynamic and kinetic interactions with the testing environment. The human lung creates an essentially warm and humid environment, however, the complexity of the system renders it practically impossible to quantitate and map the localized temperature and humidity profiles present throughout. In fact, it has been shown, the actual temperature and humidity profiles that ensue depend on the route of the passage of air; for example, differences on the aforementioned profiles have been established depending on whether the air has been pre-conditioned by nasal or oral breathing (Proctor and Swift 1977; and Martonen et al 1993).

Changes within the chemical composition of the formulation, both active and excipients, can either accentuate or negate the environmental effects in the presence of varying degrees of water vapour. Indeed, many pharmaceutical preparations have been shown to be hygroscopic in nature, and strongly interact with water vapour present (Hickey and Martonen 1993). Thus, upon interaction of an aerosol particle with the environmental water vapour, particles may change in size, shape and density. As a result, particle deposition both in terms of mass and specific location may be markedly different to conventional estimates (Ferron 1977).

In this thesis, the term thermodynamic environment is used rather than hygroscopicity *per se*, although they have been previously used interchangeably. The rationale for this approach is that hygroscopicity implies growth primarily from the absorption of water and does not consider the effects of condensation and vapour pressure. Rather than growth, particle size retardation may occur via suppression of the evaporation of volatile components from an effective increase in localised vapour pressure.

Independent of the counter-balanced argument between environment or hygroscopicity, the delivery of pharmacologic drugs into environments, which differ from those of ambient temperature (approx. 20-25°C) and relative humidity (30-65%) has received attention from several sources of research (Eisner et al 1990, Ferron and Soderholm 1990, Martonen 1990, Soderholm and Ferron 1992) and alternative associated applications. (Ferron et al 1989, Martonen at al 1989, Martonen et al 1993, Soderholm et al 1991 and Ferron et al 1993).

The implications from the effects of the thermodynamic environment on the fate of aerosol particles are therefore fundamental to their final location site in the lung, residence time at receptor and the eventual translation into clinical efficacy. Further, the primary technique of administration is also an important factor in the overall deposition (namely whether aqueous based from a nebuliser, delivered from a dry powder system or generated from a pressurized propellant multi-component device, and, also whether the incorporation of ancillary spacers or holding chambers are utilised).

5.2 Overview of the Thermodynamic Properties of Inhaled Aerosol Particles

5.2.1 Present Theoretical models: A brief review

Ferron expounded some of the first treatises on the phenomenon of hygroscopicity. The theory developed by Ferron (Ferron 1977) and expanded by co-workers assumed that aerosol particles reached equilibrium within a short time after inhalation, and, that, equilibrium conditions were defined as those when the temperature and water vapour concentrations of the lung environment were the same as at the surface of the particle. The theory is based upon Raoult's law derived water vapour concentration present at the surface of a salt solution as ratio to that of pure water, including the dissociation of the salt into individual ions, associated water molecules and their respective molecular masses. The pressure exerted by a curved surface is greater than that of a flat surface, and this is phenomenon is taken into account into the model. The resulting relationship is depicted in equation 5.0

$$\frac{Deq_a}{Deq_i} = \left(\frac{\rho i}{\rho a.gs}\right)^{1/3} = \left[\frac{\rho i}{\rho a}\left(1 + Mw\frac{\left[H\left(1 + j - jRw\right)\right]}{Ms\left[Rw - H\right]}\right)\right]^{1/3} \qquad \textbf{Equation 5.0}$$

Where $Deq(a),(i)$ are the equivalent diameters of the particle in air and the dry particle, $\rho(a),(i)$ are the densities of the particle and the initial dry particle, $M(s),(w)$ are the molecular weights of the solid and water respectively and i, j, Rw, H are the number of ions which the salt dissociates into, the number of water molecules per salt molecule, the vapour pressure of a curved surface and the relative humidity respectively.

This approach has been used in several studies, however, they all pertain to dry or aqueous base systems (Groom 1981 Hickey et al 1990). In fact, most studies used inorganic salts and their solutions as model compounds during experimental studies, and only a few have utilised actual drug formulations, presumably as this was because of their implications as atmospheric pollutants (Ferron 1977, Ferron et al 1988, Steele and Hamill 1981, Cocks and Fernando, Haenel and Zankl 1979).

The main assumption of the theory was that particles which enter a humid environment (the respiratory tract) of certain sizes reach equilibrium within certain time-frames: those smaller than 0.2μm equilibrated within 1 second, 1.0μm particles equilibrated within 2 seconds and larger particles would not equilibrate within one respiratory cycle. This also assumed that the complex dynamics that occur between particles, such as fluid flow (boundaries and wakes) and mass and heat transfer are effectively uncoupled or ignored.

5.2.2 Improved theoretical models.

Many of the improvements to the original theory described have been based on fluid dynamics and associated computational methods. Many thorough treatises on sprays have been based on other non-therapeutic aerosols, namely those pertaining to combustion of fuels and metal slurries, and although not essentially similar in terms of formulation principles of heat and mass transfer apply (Sirignano 1999). To further complicate the application of theoretical models, *in-vivo* flow fields through the lung are turbulent and unsteady (Martonen et al 1993); but the newer theoretical models do incorporate the aforementioned heat and mass transfer effects into the governing equations. However, the theory holds only for saline solutions and essentially calculates the number of moles of water that constitute a droplet and how mass transfer of environmental particles (water vapour) cross the boundary layer (the layer of water molecules on the particle surface). Interestingly, the results from calculations indicated

that the mass heat transfer coefficients affect the rate of equilibration and not the particle size.

5.2.3 Experimental investigations of environmental influences on aerosol behaviour: An overview of laboratory systems

Particle size changes (specifically growth ratios of the MMAD's) of aerosolised medicaments as a function of both temperature and relative humidity have been documented in the literature (See appendix A 5.0). It is, thus, imperative that the environmental conditions of the model used and experimental system during aerosol experiments need to be tightly controlled and monitored throughout such investigations. Several *in-vitro* methodologies are cited in the literature in relation to temperature and humidity controlled apparatus (Hiller et al 1980, Halbert et al 1982, Bell and Ho 1981, Tang et al 1977, and Hickey et al 1988).

The system developed by Hickey et al. (based on the original concept of Groom et al., 1981), involved the use of two independent controls: one to heat and humidify the air, and secondly to control the temperature of the system. The apparatus was surrounded by a ¼" thick expanded polystyrene structure to provide insulation from the surrounding environment, thus providing dual control of the conditions. A further rationale for this type of approach was that if adjustments were made to one part of the system the isothermal equilibrium of the other was not disturbed. The apparatus also consisted of a 7.85L equilibrium chamber, which retained the aerosol particles for up to 40s, thus providing an 'adequate time' interval for aerosol "growth". The air supplied through the system was also partially diverted and sampled to accurately determine the concentration of the water vapour (the % relative humidity (%RH)). All other usual practices were undertaken during temperature and humidity control; for example the supply and use of clean filtered air, continually monitored of flow rates via calibrated rotameters and adequate equilibration time post experiment to ensure isothermal contact. Other cited references (Hiller, Halbert and Bell) have employed climatically controlled cabinets, which accommodated control of the intake air by direct heating and humidification by using saturated salt solutions. All these controlled airflow studies conditioned the aerosol particles generated for extended periods e.g. Hiller for 30s and Tang for 20s.

The problem with such long residence times is that even with adequate training in breath holding procedures rarely exceed five seconds, and even upon following patient information leaflets will reach ten seconds. The only experimental apparatus, which

monitored short-term equilibration between the aerosol cloud generated and local environment was that of Bell and Ho with times ranging from 0.05s –1s (Bell and Ho 1981).

5.2.4 Experimental Set-up: In-vitro environmental control in this study

Based on equipment set-up and procedures previously described, it was decided to take a pragmatic approach to environmental control. Clearly accurate and precise measurement and isothermal control of the system were pre-requisite, but an exact mimic of the temperature and humidity profiles of mammalian physiology was not. It was decided, therefore, in this study to attain a wide range of temperatures both ambient (lab approx. 25°C) and high (body approx. 37°C) coupled with accurate measurement of relative humidity within a simply engineering scheme. It is true that the absolute water content of air varies with temperature but this was negligible when considered at the limits of temperature measurement: in the region of ± 0.1°C. Aerosol residence time was not increased by the use of holding chambers or spacers, and the aerosol was allowed to transition in "real time" namely it was not interfered with post actuation of the pMDI. This was performed in an attempt to simulate actual patient compliance and reduce the artificial growth that may have occurred in previous studies. Several studies have monitored particle growth in real time but have utilised light scattering methods (Martonen 1990 and Hiller et al 1980). The following sections detail actual experimental procedures and practices.

5.3 Methods and Materials

5.3.1 (a) Control of high temperature and high humidity testing conditions.

All of the recognised temperature and humidity-controlled apparatus cited in the literature have encased equipment in isothermal conditions usually via a controlled cabinet, as it is imperative that the system is in thermal and hygroscopic equilibrium. The importance of keeping the equipment in equilibrium has been previously elaborated upon (Finlay and Stapleton 1999) and has been incorporated into this study. Isothermal control was accomplished by use of a 'walk-in', insulated and externally temperature controlled stability cabinet situated at the University of Bath (Department of Pharmacy and Pharmacology). A schematic of the equipment is shown in figure 5.0.

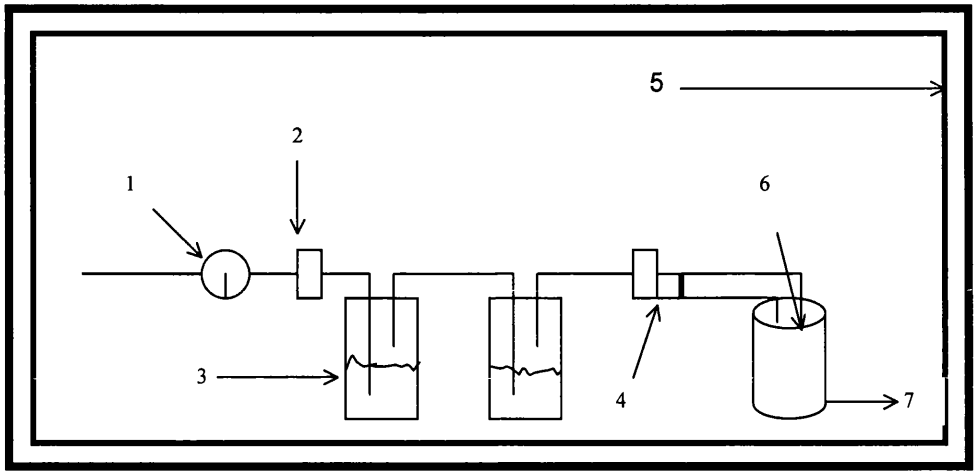

Figure 5.0: A schematic of the temperature and humidity experimental system sampling of novel experimental pMDI formulations.

Temperature control was accomplished externally and was monitored and recorded internally and the measurement verified using both a mercury in glass thermometer, (Fisons UK,) and also a dual temperature and hygrometer device (Digitron R 200, Digitron, Devon, UK.) to ascertain both the temperature of the air and that of the water in the humidifiers. Air was drawn into the apparatus from the room and the flow-rate monitored by a calibrated flow meter (Glass Precision Engineering, Hemel Hempstead UK indicated in the legend as **1**). This was then passed through a 0.2µm filter (Pall, Ann Arbour, Michigan **2**) and then subsequently passed into two bubble humidifiers (**3**), which contained de-ionised temperature equilibrated MilliQ grade water, the temperatures of which were checked prior to experiment. The humidified air then passed through a modified actuator (Norton Healthcare, Waterford, Ireland) (**4**) containing a canister of the model formulation. The warmed and humidified air was then drawn through an Andersen Cascade Impactor (Copley Instruments, Nottingham,UK **6**) via a vacuum pump (Gast, UK **7**) at 28L/min ± 5%. The apparatus was set up in the stability cabinet and left for a minimum of 72 hours to achieve thermal equilibrium. Readings were taken with a calibrated thermometer to verify equilibration and both digital temperature recorder and the glass thermometer agreed to within ± 0.1°C. The temperature and humidity of the air entering the actuator at the point of the spray orifice was also monitored throughout the experimental studies. The vacuum pump was set in operation for a minimum of 5 seconds prior to the actuation of the canister as part of a 'dummy-run' procedure to ensure no dew point condensation on the equipment. The delivery tubes of the equipment showed no signs of dew, and as a final check the cascade impactor was dismantled and found to be

dry. The canister prior to experiment was kept at ambient temperature and inserted into the actuator just before being actuated, consecutively, 10 times, and the aerosol generated was collected on the stages of the Andersen cascade impactor. During transfer from ambient conditions to the environmental test condition, the canister was placed in a custom made polystyrene insulating block to reduce heat transfer to the formulation. The analysis was performed as swiftly as possible, within one minute of set up, so as to maintain the ambient vapour pressure of the formulation and restrain the formulation from reaching thermal equilibrium with the environment, as an increase in temperature would inevitably increase the vapour pressure of the formulation. The actuator, induction port and stages were washed down with methanol whilst in the isothermally controlled environment, and were never removed from it during the study; this ensured isothermal equilibrium was never compromised. The apparatus was then left to dry in the isothermal system and reassembled after a period of 30 minutes, which was the approximate time for chemical analysis of the stages. The whole procedure was repeated three times for each formulation and testing environment combination. For low humidity high temperature conditions the bubble humidifiers were removed from the set up and the relative humidity of the cabinet used as low humidity environment.

5.3.1(b) Control of low temperature and high humidity testing conditions

The same procedure, as outlined above, was repeated for the determination of particle size character at low (ambient) temperature conditions. However, in these studies the equipment was equilibrated at ambient laboratory conditions. Again the water and air temperatures were monitored and experimentation occurred when there was a difference of ±0.1°C between calibrated mercury in glass and digital thermometers. The flow rate and humidity were determined as described above.

5.3.1 (c) Rationale for use of experimental humidity testing conditions

Humidity controls in previously cited studies were achieved via the use of saturated solutions of various salts. The activity of a solution (a description of the vapour pressure) changes with the nature of the salt employed, and is predominately independent of temperature (Robinson and Stokes 1959). Potassium Dichromate has been routinely used as a saturated solution of this salt gives an equilibrium vapour pressure of 98% of pure water (Handbook of Chemistry and Physics). Depending on the humidity required other salts are known to provide specific relative humidities (Davis and Bubb 1978, Hicks

and Megaw 1985, Martonen et al 1982). In this study water was utilised to provide a relative humidity of 100% at the testing temperature, as the objective was to determine the effect of humidity on an aerosolised formulation over a range of environmental conditions, not to mimic exact *in-vivo* conditions. A second valid rationale for the use of water only was that the humidity in the subglottic area has been suggested to be between 99-99.8%. (Porstendorfer 1971).

5.3.1 (d) Hardware modification: Design changes to the actuator.

The actuator used in this study was a modified from a salamol inhaler (Baker Norton, Waterford, Ireland) with a 0.33 mm spray orifice diameter. As airflow was externally acquired, from a controlled source, to mimic "inspired" air, several modifications were made to the actuator: the open end of the actuator was sealed from the atmosphere by covering with a pliable nitrile rubber covering. Secondary sealing of the actuator, from the environment, was achieved by sealing with parafilm. This modification also allowed depression and return, 'full travel' of the valve stem in the lower frustrum of the actuator. Air was drawn through the actuator through holes drilled into the sides of the actuator, and subsequently connected with plastic tube connector fittings, sealed with a silicone polymer. The sealant was allowed to dry and set for 24 hours before use. A diagram of the set up as shown in the figure 5.1.

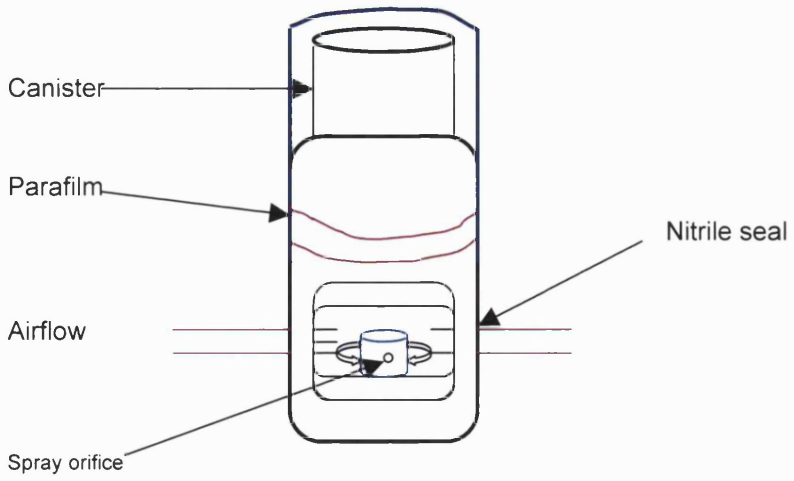

Figure 5.1: A diagram of the modified Salamol (Baker Norton) actuator used in the study.

5.3.1 (e) DataGeneration and Device performance

As per chapter 4, similar methodology was adopted when capturing aerosol particle size data. Namely, 10 consecutive actuations from the same device were performed after 2 priming shots had been taken. The units produced were formulated so that the same canister could be utilised for all 12-aerosol experiments, in order to reduce variability. Tables 5.0-5.4 describe the critical aerosol particle size characteristics: the MMAD, GSD, large particle deposition patterns (namely the actuator and throat depositions), and environmental conditions recorded during experimentation, and both the delivered and emitted dose data are depicted in tables 5.5 and 5.6, for the maleate and oleate salts respectively. Table 5.7 depicts complementary information detailing the composition of the ctual formulations and the theoretical emitted dose.

5.4 Results and Discussion

5.4.1 Introduction

The following aerodynamic data illustrated the in-vitro measurements from the coupled temperature and humidity study matrices. To study the effect of hygroscopicity on aerosol cloud distribution patterns, novel hydrophilic and hydrophobic salbutamol salts were synthesised and formulated as solution based systems, with a minimum mass of ethanol to attain short term stability (See Appendix chapter 3 tables A 3.1(c-e)). Solution systems were chosen in preference to suspension formulations for the following studies as particle size changes could be accurately related to the environment since every particle in a solution aerosol cloud would contain drug. This would allow an accurate and precise description of cloud dynamics in terms of mass and heat transfer effects due to condensation, particle evaporation and interaction with surrounding environment potenetially resulting in hygroscopic growth or droplet suppression from vapour pressure effects (Lange and Finlay 2000).

The differences in molecular masses of the derivatives and the subsequent delivered and emitted doses from the inhaler were based on the dose currently utilised in clinical practice: salbutamol base, 100 μg per actuated dose, again similar to the experimental rationale in chapter 4. Data were systematically evaluated by considering the direct influence of each environmental variable sequentially, with all data percentage normalised. To clarify, deposition was performed by investigating one variable at a time

keeping the other variable constant for both salts. Then the primary particle characteristics were evaluated: the MMAD, GSD, LPF (Large Particle Fractionin terms of actuator and throat deposition) and the FPF (Fine Particle Fraction). Finally, salt deposition patterns were directly compared and normalised.

5.4.2 Primary and secondary mechanisms of particle formation and associated aerosol fractions: A brief summary of definitions

As previously discussed in chapter 4, both the primary and secondary aerosolisation mechanisms were dependent upon the formulation, hardware variables, and the shape and oscillation of the liquid stream. Although fully described in the previous chapter what follows is a brief set of criteria used in the description of data generated. The critical Weber number indicates the demarcation of the division between primary and secondary mechanisms of atomisation. At a high critical Weber number, aerodynamic forces predominate over viscous forces and the particle may undergo further subdivision into satellite droplets. If the sizes of the droplets produced exceed the critical Weber number these may be subject to a similar fate and divide also. This describes the secondary mechanism of particle production. If, however, the aerosol droplet/particle aerosdynamic size does not exceed the critical Weber number (We_{cr}) it will, in theory, remain unchanged in dimension and contine along within the airstream. In this study, primary aerosol deposition is postulated to occur at the spray orifice and is described hereafter as the patterns associated at the actuator, throat and the non-respirable particle fractions namely those on stages 0 and 1 (This it should be noted is not strictly true as secondary atomization may occur throughout these stages, but this is assumed to simplify the process and evaluate the data). For those that do exceed the critical size and do not impact on the higher stages (equivalent to the upper respiratory tract) of the apparatus, but travel to the lower stages (equivalent to the respirable or lower stages of the respiratory tract), undergo secondary atomisation.

Secondary aerosol atomisation, as generalised for this study, can be related to the fine particle or respirable fraction of the aerosol designated by stages 2 to the filter stage. It is true to say, and important to note here, that, a particle produced from the primary atomisation process may account for drug deposition in the respirable phase: from atomisation traverse the apparatus at under the prescribed environment to the lower stages.

In the studies that follow, however, the effective temperature, pressure and viscosity of the environments will change accordingly, which will influence the Weber number and aerosol characteristics. Because the environment around a particle is not exactly known at any one time only "average" particle size distributions can be described, as such changes in stage mass and particle distribution shifts can be utilised to provide inferences the effects of environmental conditions on atomisation.

5.4.3 Tabulated Data Summaries

Tables 5.0–5.4 describe the data generated, normalized where appropriate and summarised relating to the matrix of aerosol experiments for both hydrophilic and hydrophobic salbutamol salts formulated as solution based pressurized metered dose inhalers. Table 5.0 summarises the aerosol clouds mass median aerodynamic particle size and polydispersity data

Environmental Condition	MMAD				GSD			
	Maleate	(SD)	Oleate	(SD)	Maleate	(SD)	Oleate	(SD)
LT:LRH	1.48	0.09	1.27	0.24	**2.46**	0.37	**2.63**	0.11
LT:HRH	1.35	0.10	1.42	0.20	**2.74**	0.06	**3.10**	0.15
HT:LRH	1.11	0.22	0.87	0.08	**2.30**	0.42	**3.69**	1.81
HT:HRH	1.21	0.15	1.13	0.14	**2.20**	0.13	**3.20**	0.63

Table 5.0: ***The effective mass mean aerodynamic sizes and cloud polydispersity of hydrophilic (maleate) and hydrophobic (oleate) salbutamol aerosol formulations at 10% w/w ethanol levels.***

Table 5.1 summarises, succinctly, the critical parameter data into a format that enabled interpretation in fundamental terms, when conjugated with the appropriate graphical data, of the primary and secondary atomisation processes, as arbritrarily designated earlier: the primary indicated by the actuator and throat deposition, and secondary by the fine particle fraction.

For clarity, when data is discussed on an intra-formulation percentage basis, reductions and increases delineated refer to changes from the first environmental condition quoted; when discussed on an inter-formulation basis changes are referred back to the hydrophilic salt

Critical Parameter (%deposition)	LT:LRH		LT:HRH		HT:LRH		HT:HRH	
	Maleate	Oleate	Maleate	Oleate	Maleate	Oleate	Maleate	Oleate
Actuator	8.97	6.86	16.33	16.84	22.00	19.54	27.35	20.37
Throat	44.24	17.29	25.96	7.70	12.74	8.82	11.78	7.52
FPF	42.76	72.33	52.88	67.87	63.24	67.43	57.42	67.01

Table 5.1: ***The effective percent located deposition for critical aerosol characteristics of hydrophilic (maleate) and hydrophobic (oleate) salbutamol aerosol formulations at 10% w/w ethanol levels.***

Table 5.2 illustrates the temperature and humidity profiles during aerosol experiments for both salt formulations.

Environmental Condition	Experimental Testing Conditions (Recorded values)			
	Maleate		Oleate	
	T°C	%RH	T°C	%RH
LT:LRH	25.2	30.3	24.6-24.7	29.6-30.1
LT:HRH	24.8	100.0	21.8	100.0
HT:LRH	38.4	25.6-28.6	38.7-39.0	25.5-30.9
HT:HRH	36.8-37.1	94.2-100.0	37.6-37.8	94.7-100.0

Table 5.2: ***The experimental testing conditions recorded during aerosol measurements of hydrophilic (maleate) and hydrophobic (oleate) salbutamol aerosol formulations at 10% w/w ethanol levels.***

Table 5.3 reviews the percentage normalized individual stage deposition data for the maleate salt formulations analysed over the range of testing conditions.

ACI stage	LT:LRH		LT:HRH		HT:LRH		HT:HRH	
	Maleate	(sd)	Maleate	(sd)	Maleate	(sd)	Maleate	(sd)
Actuator	8.77	1.57	16.33	2.73	22.00	3.63	27.35	3.26
Throat	42.91	9.61	25.96	6.07	12.74	2.87	11.78	6.40
Stg 0	2.28	0.42	2.45	0.75	1.17	0.59	1.93	0.31
Stg 1	1.69	1.29	2.38	0.73	0.85	0.20	1.52	0.22
Stg 2	0.68	0.22	2.02	0.18	0.69	0.16	0.80	0.55
Stg 3	1.91	0.62	2.18	0.08	1.57	0.49	1.08	0.43
Stg 4	7.34	1.90	7.89	1.09	4.67	0.48	5.82	0.5
Stg 5	14.61	5.15	17.91	2.3	19.44	4.60	24.02	3.66
Stg 6	10.17	1.15	9.59	1.37	16.90	3.09	13.02	0.47
Stg 7	3.45	0.14	5.26	1.16	9.21	1.12	6.39	0.57
Filter	6.13	1.06	8.02	1.40	10.77	3.67	6.29	3.50

Table 5.3: ***Andersen Cascade Impaction, stage recovery data (% normalised drug loadings) of a 10% w/w salbutamol maleate aerosol formulation.***

Table 5.4 indicates the percentage normalized stage deposition data for the oleate salt formulations over the testing range conditions.

ACI stage	LT:LRH		LT:HRH		HT:LRH		HT:HRH	
	Oleate	(sd)	Oleate	(sd)	Oleate	(sd)	Oleate	(sd)
Actuator	6.86	2.54	16.74	3.57	19.54	5.93	20.34	2.61
Throat	17.30	1.61	7.70	2.44	8.82	5.82	7.52	4.46
Stg 0	1.35	1.10	3.41	0.47	3.39	3.79	2.85	2.27
Stg 1	2.17	0.83	4.27	0.66	0.82	0.74	2.25	0.87
Stg 2	1.63	1.04	2.44	1.11	0.49	0.34	3.38	0.63
Stg 3	8.23	1.37	7.79	0.57	3.13	1.49	4.04	1.10
Stg 4	10.43	1.76	10.98	0.84	6.07	2.53	6.03	1.00
Stg 5	15.92	1.13	14.44	2.32	13.36	6.22	16.59	1.16
Stg 6	17.34	1.51	14.10	1.15	17.85	2.16	15.78	3.62
Stg 7	7.43	2.20	5.52	1.13	6.96	0.57	5.74	1.59
Filter	11.34	5.50	12.60	2.50	19.59	4.69	15.45	5.42

Table 5.4: ***Andersen Cascade Impaction, stage recovery data (% normalised drug loadings) of a 10% w/w salbutamol oleate aerosol formulation.***

The dose data for both formulations are given in tables 5.5 and 5.6 respectively. These tables depict the actual mean delivered dose by mass and the percentage delivered and emitted doses allowing inter-formulation comparisons. To complement the data generated, table 5.7 idicates the actual formulations utilised and the associated theoretical dose based on the composition. The theoretical dose is what would be expected if the inhaler were operating in an optimal manner.

Environmental Testing Condition	Actual Delivered Dose (µg)	(sd)	Mean Delivered Dose %	(sd)	Mean Emitted Dose %	(sd)
LT;LRH	100.8	**3.76**	93.94	2.90	85.79	3.8
LT;HRH	133.48	**5.05**	126.59	8.87	105.90	6.77
HT:LRH	88.82	**29.27**	74.40	9.65	68.96	25.51
HT:HRH	93.96	**10.02**	89.20	4.66	64.91	6.96

Table 5.5: ***Intra-formulation shot dose data for a 10% w/w salbutamol maleate pMDI aerosol (Delivered and emitted dose data are percentage normalised).***

Environmental Testing Condition	Actual Delivered Dose (µg)	(sd)	Mean Delivered Dose %	(sd)	Mean Emitted Dose %	(sd)
LT;LRH	193.90	28.08	85.03	12.71	78.99	9.10
LT;HRH	245.96	5.4.2	116.01	3.99	96.64	7.08
HT:LRH	225.45	8.4.6	110.23	4.93	88.60	6.22
HT:HRH	191.43	55.48	108.68	3.68	100.43	3.08

Table 5.6: ***Intra-formulation shot dose data for a 10% w/w salbutamol oleate pMDI aerosol (Delivered and emitted dose data are percentage normalised).***

Drug	Active Mass / g	Ethanol Mass /g	134(a) Mass /g	Dose Theory / µg
Salbutamol Maleate	0.0272	1.4144	12.7241	110.22
Salbutamol Oleate	0.0418	1.0759	9.0088	236.93

Table 5.7: ***Formulation composition and theoretical delivered dose form experimental aersosol formulations.***

5.4.4. The effect of temperature variation and constant relative low humidity testing conditions on the deposition patterns of salbutamol salt formulations.

Figures 5.2 and 5.3 illustrate the influence of varying temperature and and low humidity testing conditions on the particle size distribution patterns of the novel solution inhaler formulations.

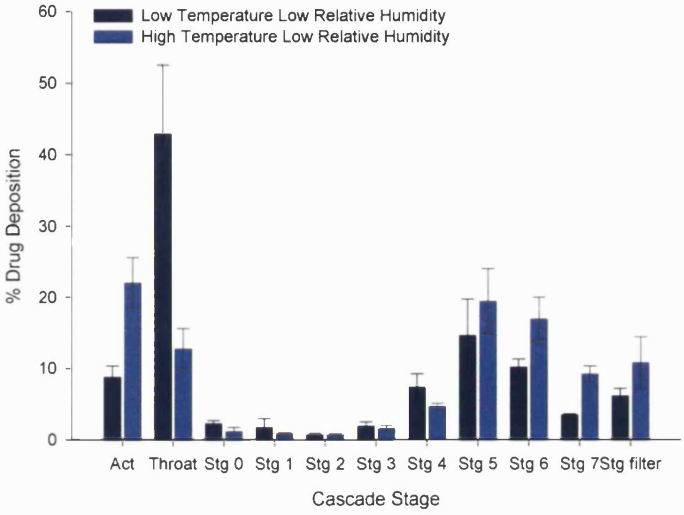

Figure 5.2 ***Intra formulation comparison of salbutamol maleate at low relative humidity with varying temperature.***

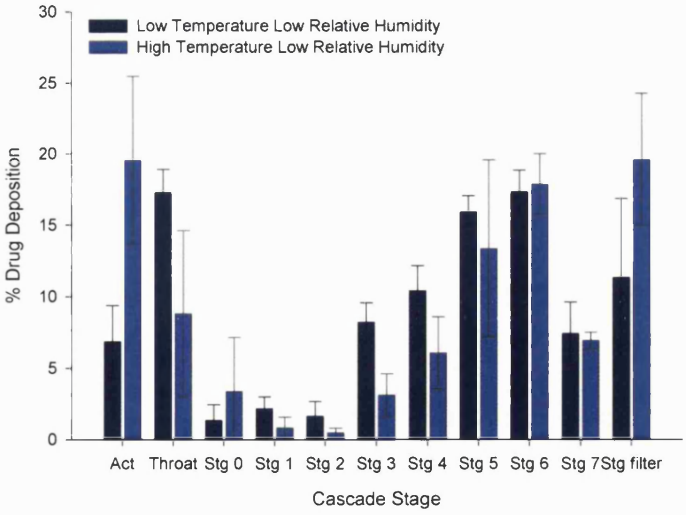

Figure 5.3: ***Intra formulation comparison of salbutamol oleate at low relative humidity with varying temperature.***

5.4.4 (a) *Evaluation of the data relating to the Hydrophilic salt*

The low temperature, low relative humidity deposition pattern can be considered the "gold standard" or baseline deposition profile, as these are the conditions, which would be expected to be encountered under a normal lab-testing regimen. The actual environmental readings for these replicated experiments were constant and fluctuated very little, as the temperature remained static at 25.2°C and, in conjunction, relative humidity remained constant at 30.3%. (See table 5.2). Importantly, it should be noted that the deposition pattern that presented iself was not typical of a pressurized solution based system as the majority of drug deposition was centered on stage 5 of the impactor. The effect of temperature was pronounced at the primary deposition stages, with significant changes being observed on the actuator and throat resulting in p values <0.001 for both stages. Significance was also observed on stages 6 and 7 returning p values of 0.033 and 0.001 respectively. Upon testing at elevated temperature the actuator deposition increased by approximately 13.2% and the throat dropped by about 30.2%. The distribution pattern for the aerosol particles for the two temperatures were similar with deposition centered at stage 5 of the impactor, and that varying the temperature while maintaining conditions of low relative humidity did not significantly affect the relative deposition profile within the *in-vitro* apparatus. The only difference was that an increase, on an identical stage-by-stage deposition, occurred as the temperature was increased. This may be associated with the variations within the primary mechanism due to the increase in environmental temperature potentially "flash evaporating" the volatile propellants, possibly improving, i.e. reducing throat deposition, ultimately leading to a therapeutic benefit from a clinical viewpoint.

5.4.4(b) *Evaluation of the data relating to the Hydrophobic salt*

At low relative humidity and low temperature, the oleate salt produced a different particle size deposition profile. The environmental testing conditions fluctuated slightly more see table 5.2, although in real terms this equated to only 0.1ºC and 0.5% RH, which was within experimental error. Significant difference in deposition patterns as evaluated by ANOVA indicated that this only occurred for the actuator and stage three and returned values of $p<0.01$ and $p<0.001$ respectively. Distribution patterns followed a similar trend as per the maleate salt for the fine particle fraction, with the actuator and throat deposition patterns changing accordingly. The actuator decreased by approximately 12.7% and the throat increased by about 8.5%. Stage three decreased by about 5.1%.

5.4.5. The effect of temperature variation and constant high relative humidity testing conditions on the deposition patterns of salbutamol salt formulations.

Figures 5.4 and 5.5 illustrate the effects of varying temperature and high humidity testing conditions on the particle size distribution patterns of the novel solution inhaler formulations.

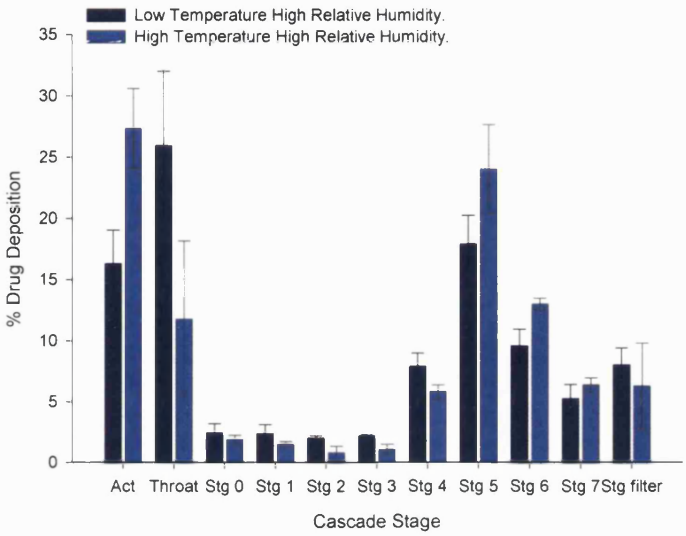

Figure 5.4: ***Intra formulation comparison of salbutamol maleate at high relative humidity with varying temperature.***

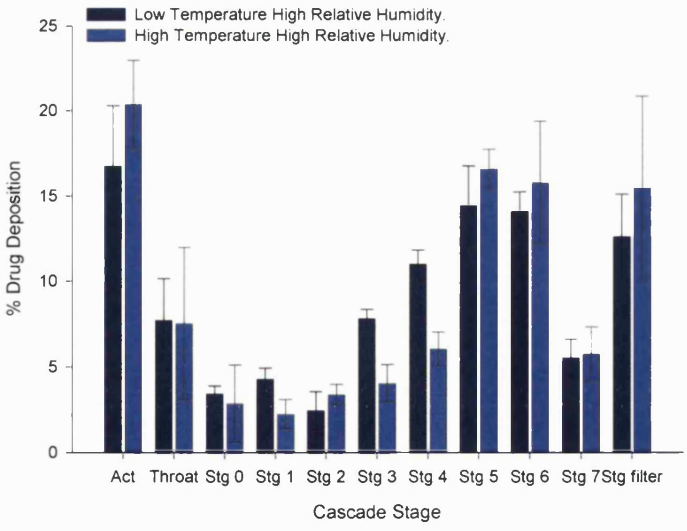

Figure 5.5: ***Intra formulation comparison of salbutamol oleate at high relative humidity with varying temperature.***

5.4.5 (a) *Evaluation of the data relating to the Hydrophilic salt.*

The deposition patterns from these set of conditions followed a similar distribution profile to the low relative humidity condition, with maximal drug deposition centered on stage 5. Again the trend was observed that when the temperature of the environment was increased the actuator and throat depositions reversed in aerosol deposited. Significant cascade stage reductions were observed for only the actuator and stage 2, which both achieved p values of 0.001. The percentage change for these stages equated to a realative increase of 11.0% and an drop of 1.2%. The throat stage although not significant decreased by about 14.2%. Table 5.2 indicated the relative environmental testing conditions. And indicated that both the temperature and humidity remained relatively constant throughout with fluctuation over a temperature range of 0.3ºC and a humidity of 5.8% RH. Such fluctuations may have been attributable to leaks within equipment seals.

The high temperature and high relative humidity condition had the highest actuator and lowest throat deposition when compared to all other combinations. From an aerosol mechanistic viewpoint it can be theorised that the increased vapour pressure of formulation resulted in rapid and violent droplet break-up, evident from comparison of the data for both the MMAD and large particle fractions, as illustrated in tables 5.0 and 5.1. The MMAD underwent a reduction from 1.48 to 1.11µm at low RH and 1.35 to 1.21µm at high RH. In conjunction there was an increase in actuator deposition about 11% when the temperature was increased and a change in fine particle fraction, about 4.5%, occured. It was inferred, therefore, from these observations that increased intake air temperatures may directly affect the primary atomisation mechanism from the changes illustrated in the data. At high relative humidity, namely, higher mole fraction of water in the entrained air the aerosol cloud experienced a reduction at the upper stage plates probably by a mixture of suppression of droplet evaporation and hygroscopic growth. This in turn may have modified and increased the effect of secondary dispersion/particle generation mechanisms. The water vapour in the atmosphere present may have retarded evaporation and enhanced absorption of water molecules into the salbutamol maleate salt droplet.

5.4.5 (b) *Evaluation of the data relating to the Hydrophobic salt*

Deposition patterns for the hydrophobic salt indicated significant changes on stages 3 and 4 of the impactor with maximal drug loading on the actuator and for stage 5 within the impactor both environmental conditions. P values for both these stages equated to <0.001

and 0.009 respectively and in terms of percentage changes of 3.7 and 5.0% Table 5.2 illustrates the testing conditions documented during experimentation. As per the maleate salt the low temperature high relative humidity testing condition was relatively static, but the temperature varied by 0.2ºC and the relative humidity by 5.3% accordingly. Temperature fluctuation can be attributed to the control of the room as temperature mapping had not been performed prior to experimentation and the vacuum pump close to the apparatus may have attributed to such fluctuations. Again the variations in the humidity may have been due to equipment seals The change in mass median aerodynamic diameter was greater fo this combination of salt and environmental condition as compared to the hydrophilic counterpart: 1.42 to 1.13 microns for the oleate and 1.35 to 1.21 microns for the maleate. The additional combination of little change in fine particle fraction and the reduction in MMAD indicated potential suppressive mechanism.

5.4.6. The effect of relative humidity variation and constant low temperature testing conditions on the deposition patterns of salbutamol salt formulations.

Figures 5.6 and 5.7 illustrate the effects of constant low temperature and varying humidity testing conditions on the particle size distribution patterns of the novel solution inhaler formulations.

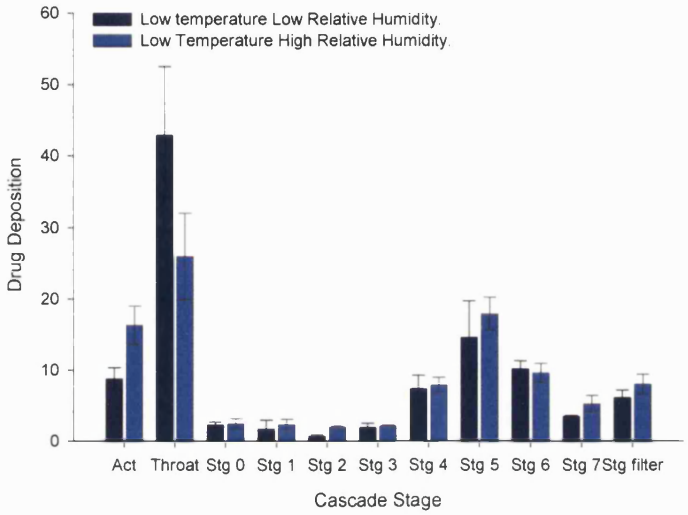

Figure 5.6 ***Intra formulation comparison of salbutamol maleate at low temperature with varying relative humidity.***

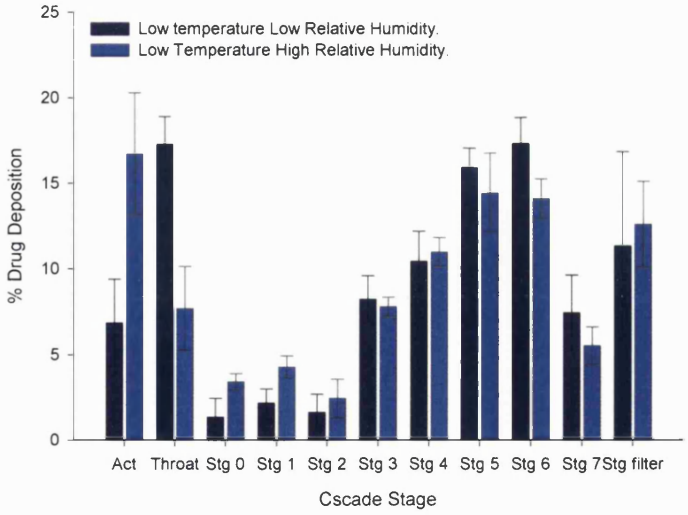

Figure 5.7: ***Intra formulation comparison of salbutamol oleate at low temperature with varying relative humidity.***

5.4.6 (a) *Evaluation of the data relating to the Hydrophilic salt*

The effect of high relative humidity when the temperature was controlled at a low and ambient level indicated significant differences in deposition pattern for the actuator and stage 2, which attained significance values of $p<0.001$ and $p=0.002$. This equated to percentage increases of 7 and 1.3% respectively. The throat stage although not displaying a significant change did result in a 16.9% decrease when the humidity was increased. At the low temperature testing condition the MMAD decreased from 1.48 to 1.35 microns. At high temperature with increasing humidity the MMAD experienced an increase from 1.11 to 1.21 microns. Such an decrease when hygroscopic growth is postulated is discussed later but is theorised to result from particle density changes. The large particle fraction, as a sum of actuator and throat depositions as shown in table 5.1, increased by approximately 10% when the humidity was increased.

5.4.6 (b) *Evaluation of data relating to the Hydrophobic salt*

In the previous studies the deposition pattern of the oleate salt at all testing conditions indicated an overall smaller particulate aerosol: higher drug loading on the higher secondary mechanism/deposition stages. Significance for this salt under these conditions was achieved only at stage 2 exhibiting a p value of 0.004. From a percentage perspective the largest changes were centered on the actuator and the throat, which returned values of an increase of 9.9% and a decrease of 9.6% respectively. Unlike the hydrophilic salt stages 5 and 7 experienced a decrease in percentage deposition.

Changes were also observed in the MMAD as shown in table 5.0 as the mass median aerodynamic particle size increased in an upward trend from 1.27 to 1.42. Such a trend, effectively a growth rate ratio of 1.12 or 12% may be inferred from interpretation of the size distribution graph. The increase on the primary stages may result presumably from an increased water vapour concentration and therefore the atmospheric vapour pressure suppression of the subsequent vapourisation of the volatile components.

This hypothesis is at least partially confirmed, as salbutamol oleate is highly water insoluble and as such would be an unlikely site for nucleation of water molecules. However a 12% particle size change is relatively large compared to those previous studies of Kim et al (Kim et al 1985) who found a difference of only 4% with a solution aerosol Bronkometer®, (Isoetharine Mesylate) Breon Labs, New York, NY. However there are major differences between these studies and the aforementioned were that the

propellant cited was a CFC and the RH of the experiment was 90% approximately. Thus some effects of particles as cloud condensation nuclei may occur particularly at small MMAD's. In addition the throat deposition was about 18.3% less than the hydrophilic under these environmental conditions.

5.4.7 The effect of relative humidity variation and constant high temperature testing conditions on the deposition patterns of salbutamol salt formulations.

Figures 5.8 and 5.9 illustrate the effects of constant high temperature and varying humidity testing conditions on the particle size distribution patterns of the novel solution inhaler formulations.

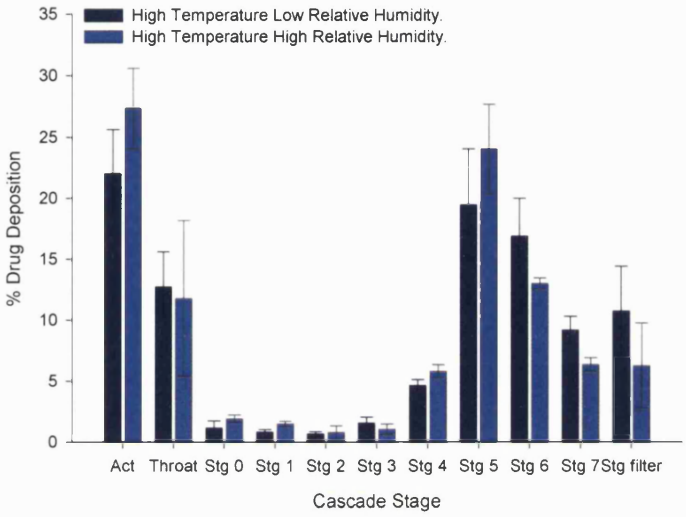

Figure 5.8: ***Intra formulation comparison of salbutamol maleate at high temperature with varying relative humidity.***

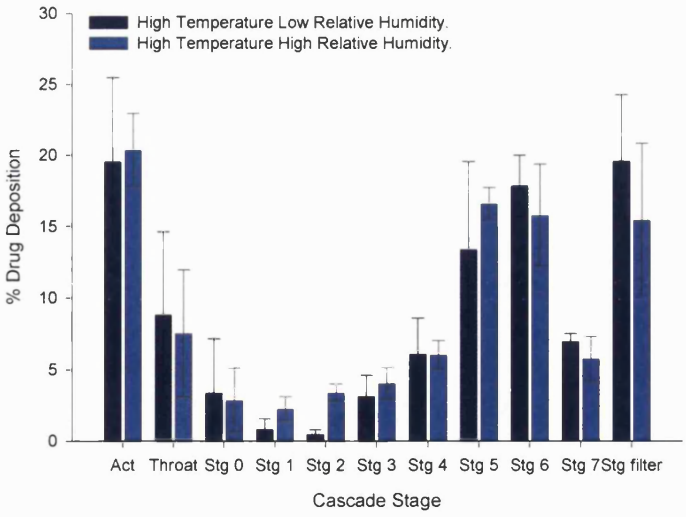

Figure 5.9: ***Intra formulation comparison of salbutamol oleate at high temperature with varying relative humidity.***

5.4.7 (a) *Evaluation of data relating to the Hydrophilic salt*

Upon varying the relative humidity at high temperatures (≈38-39°C), for the hydrophilic salt (salbutamol maleate) throat deposition patterns indicated a similar trend. Although not significant when conditions were varied the actuator deposition increased by 5.4% and the throat decreased by 0.95% from low to high humidity. The only significant change was noted on stage 7 which returned a p value of 0.001. All other stage deposition patterns followed a similar trend with stage 5 occupying the maximum drug loading, which increased by approximately 4.6%, with the high relative humidity condition having slightly lower deposition on the higher stages. In effect the particle deposition tended towards the lower stages The relative percentage changes for stages 6,7, and filter were 3.9, 2.8 and 4.5%. Fluctuations in humidity were evident at both testing conditions as indicated in table 5.2, and a growth rate ratio of 1.09 or 9%, resullted when the humidity increased. The fine particle fraction increased by approximately 10%.

5.4.7 (b) *Evaluation of data relating to the Hydrophobic salt*

At these testing conditions the oleate salt exhibited a similar trend in deposition pattern for all stages. The fine particle fractions wereapproximately equal and changed very little The growth rate ratio, calculated from data in table 5.0, was 1.30 or 30 % for these intra-testing conditions. The only significant change resulted on stage 2, which produced a p value of 0.001 and a percentage change of 2.9%.

It should be noted that the main stage deposition for the low humidity condition was the filter stage. This condition had the highest filter stage of all, for the oleate salt under all testing conditions. The high relative humidity also had it main drug loading on the filter stage but the preceding stages 5 and 6 were approximately equal, unlike the low RH. This can be quantified from the data in table 5.3. A point to note as for the hydrophilic salt was that there was fluctuation around the measured relative humidity in approximately the same order of magnitude as depicted in table 5.2.

5.4.8 The effect of environmental testing conditions on the MMAD and of salbutamol salt formulations.

Figures 5.10 and 5.11illustrate the effects of varying environmental testing conditions on the MMAD and GSD of the novel solution inhaler formulations.

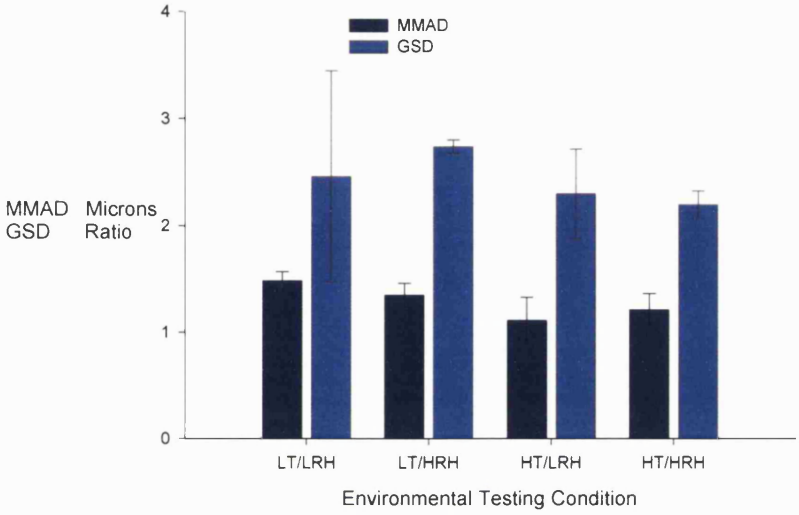

Figure 5.10: ***Intra formulation comparison of the particle size and polydispersity of salbutamol maleate.***

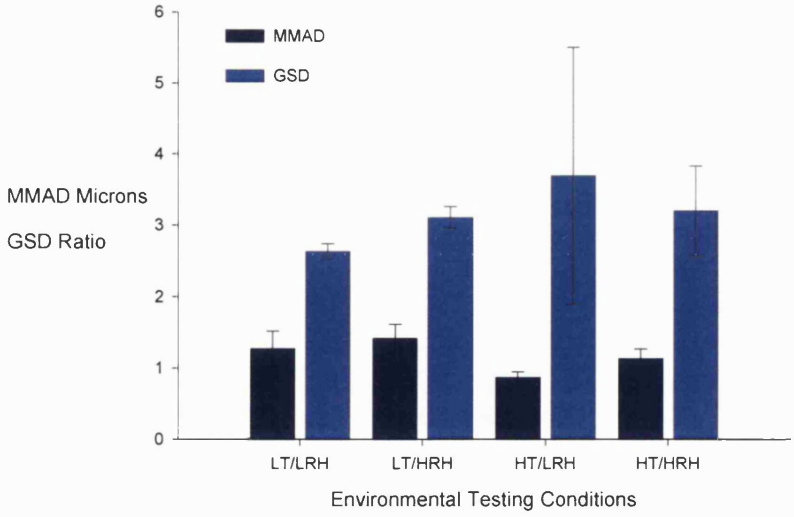

Figure 5.11 ***Intra formulation comparison of the particle size and polydispersity of salbutamol oleate.***

5.4.8 (a) *Evaluation of data relating to the Hydrophilic salt*

In general, the lower temperature environments produced higher MMAD's and the effect of humidity varied depending on the temperature of the entrained. At constant low temperature, the MMAD decreased by approximately 9% when the RH was increased. (See tables, 5.0 and 5.2 accordingly relating to the following discussions). Conversely, at constant high temperature the particle size increased by approximately 9% when the relative humidity was increased. When RH was kept at a low and constant value and temperature varied, an increase in temperature caused a 25% reduction in MMAD. When the RH was kept at an elevated value a corresponding increase in temperature resulted in a 10% reduction in MMAD.

No significance for MMAD was observed for any intra temperature combination as a p value of 0.066 was calculated.

Polydispersity was shown to decrease at static conditions of humidity when temperature was increased. Under static conditions of temperature polydispersity decreased at high relative humidity and increased under low temperature and high relative humidity. Considering the data systematically, low temperature comparisons indicated an 11% increase in GSD for the maleate salt when humidity was increased. When the high temperature testing environments were considered a change of about 4% resulted at high humidity. When the humidity was held constant, and low, increasing the temperature dropped the MMAD by 7% and at high temperature a reduction of about 20% occurred. No significant difference was observed as indicated by a p value of 0.188

5.4.8 (b) *Evaluation of data relating to the Hydrophobic salt*

Data for this salt indicated that significant differences were observed between the low temperature high relative humidity and high temperature low relative humidity conditions when compared, as indicated by a p value of 0.025.These were the only data sets that indicated significant changes. Again, the trend as with the hydrophilic maleate salt was that lower temperatures produced higher MMAD's. Taking the data in tables 5.0 and 5.2, at constant low temperature the MMAD increased by about 12%; when the relative humidity was increased the MMAD increased by about 30% respectively. When the relative humidity was kept at a constant low value, increasing the temperature caused a drop in MMAD of 31%; at a constant high relative humidity value the MMAD was reduced by approximately 20% when the temperature was increased.

Aerosol polydispersity was different from that of the hydrophilic salt and no statistical significance was encountered for any combination of the environmental testing conditions. Considering the low temperature testing conditions, increasing the relative humidity resulted in an increase in about 18% and at static high temperature increasing the RH resulted in a drop of approximately 13%. Alternatively, when the testing conditions were constant at a controlled low/ambient relative humidity increasing the temperature resulted in a 40% increase in cloud dynamics. Finally at high relative humidity increasing the temperature did not affect the GSD greatly as the change was only 3%.

5.5. Inter formulation comparisons of the Particle Size Distributions produced from Novel solution pMDI's.

Figures 5.12 and 5.13 illustrates the normalized deposition data comparing the inter-formulation deposition patterns for the novel solution formulations when tested at low temperature and varying relative humidity conditions.

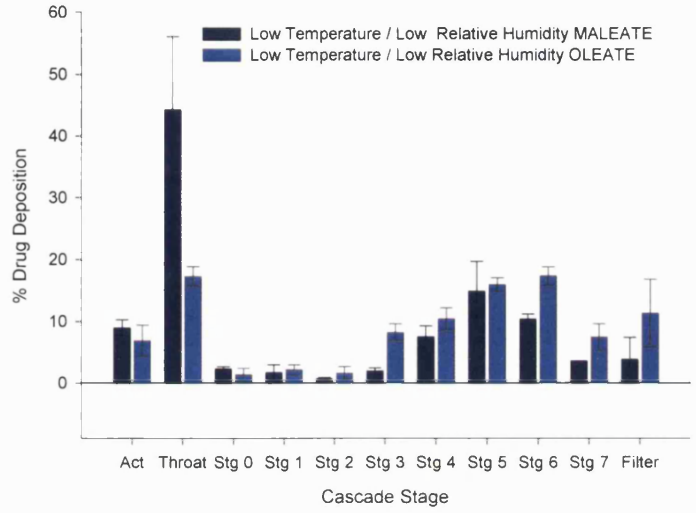

Figure 5.12 ***Inter formulation comparison of salbutamol salts at low temperature and low relative humidity.***

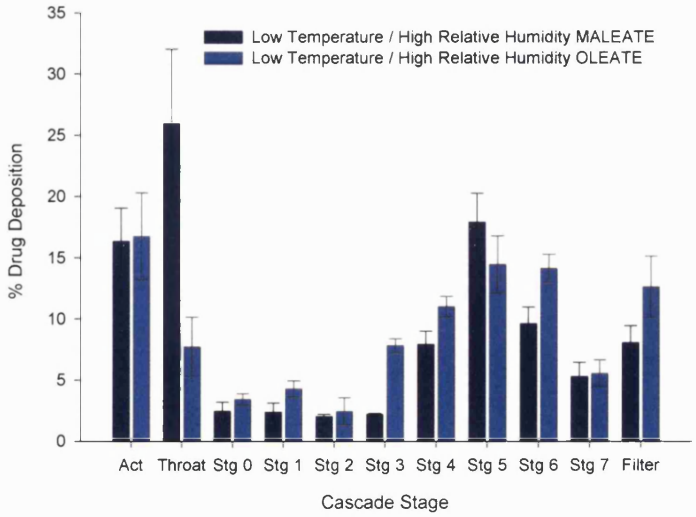

Figure 5.13 ***Inter formulation comparison of salbutamol salts at low temperature and high relative humidity.***

Figures 5.14 and 5.15 illustrates the normalized deposition data comparing the inter-formulation deposition patterns for the novel solution formulations when tested at high temperature and varying relative humidity conditions.

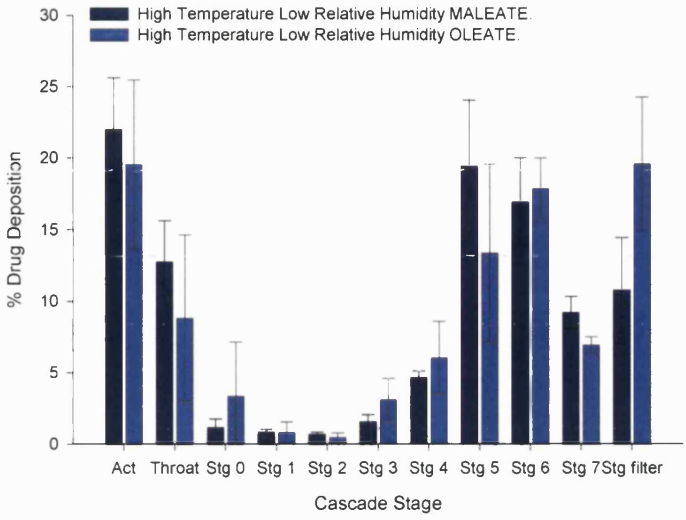

Figure 5.14: ***Inter formulation comparison of salbutamol salts at high temperature and low relative humidity.***

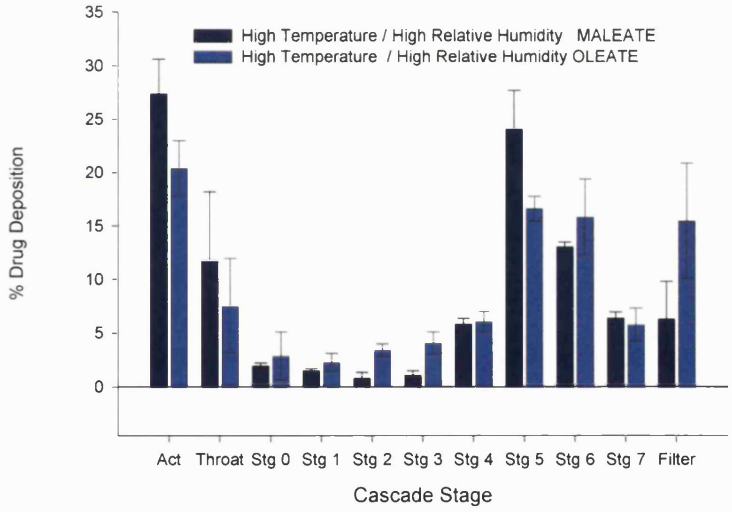

Figure 5.15 ***Inter formulation comparison of salbutamol salts at low temperature and high relative humidity.***

5.5.1 General Discussion

From the data generated and summarized in figures 5.14 -.517 and tables 5.0-5.4, it was shown that the salt derivative within the aerosolised formulation had a significant effect on both the primary and secondary mechanisms of atomization, and subsequent deposition patterns of the aerosolisation of solution based pMDI systems. It was also determined that the effect of temperature on the cloud generated also imparted a significant, and, if manipulated, a beneficial effect on cloud dynamics. By beneficial effect, the resulting implications are that unwanted distribution of drug on stages such as the throat and reassignment of drug to other particle size distributions were possible. Such a redeployment of drug may be beneficial depending on disease state. The following discussion relates to the inter-comparison graphical representation of deposition.

5.5.2 Inter formulation comparisons: The effects of environmental testing conditions on particle deposition patterns from novel solution pMDI's.

The deposition patterns exhibited by both salt formulations were widely different. Considering the pattern at low temperature and low humidity and ambient lab conditions the oleate gave a deposition pattern that was finer namely more drug was loaded on the higher (6,7 and filter) stages, with deposition patterns rising from stage 3 and centered at a maximum around stage 6 of the impactor. The maleate formulation, with a lower effective solid concentration would have been expected to give a smaller MMAD and similar deposition pattern, but this did not occur. At this condition, significant changes in deposition pattern were evaluated using a two-tailed heteroscedastic t-test, with t at 95% confidence intervals. The stages that indicated significance were the throat (t stat 4.31; t crit 4.55), stage 3 (t stat –7.23; t crit 3.18) and stage 6 (t stat –6.54; t crit 2.88). In percentage terms the changes indicated a reduction for the throat of approximately 25.6% and increase of 6.3 and 7.2% for stages 3 and 6 respectively.

When the effects of hygroscopicity were considered at low temperature and high relative humidity, or more correctly at high mole fraction of water vapour within the intake air, data indicated different aerososlisation mechanisms. Actuator recovery increased on both, roughly doubling, to around 16% for the hydrophilic salt and an almost three fold change for the hydrophobic salt. The throat deposition of both salts significantly reduced from around 43-26% for the maleate salt and 17-8% for the oleate. The throat deposition in

relative terms was still greater than that of the actuator and increased from 9-16% for the maleate and 7-17% for the oleate. The FPF's also changed: 43-53% for the maleate and 72-68% for that of the oleate. Statististically, several stages indicated significance in particle size changes: the throat (t stat 4.83; t crit 3.18), stage 1 (t stat –3.32; t crit –2.78), stage 3 (t stat 16.92; t crit 4.30), stage 4 (t stat –3.89; t crit 2.78) and stage 6 (t stat –4.38; t crit 2.78). In percentage terms this equated to a reductions for the throat of approximately 18.3%, for stage 1of approximately 1.9% and increases for stages 3, 4 and 6 of 5.6, 3.1 and 4.5% respectively.

The high temperature low relative humidity condition indicated no statistical difference on any of the impactor stages between the salts. Also there were no major changes in percentaage deposition for any stage. Only stages 6 and the filter indicated appreciable paercentage changes, as these resulted in a decrease of 6.1 and 8.8% respectively. Taking the effects of high temperature and low relative humidity, opposed to low temperature and high relative humidity, the oleate was relatively unchanged, and deposition on the actuator increases slightly from 19.5 to 20.4%, and the throat reduces from 8.8 to 7.5%. The maleate however, increased by 5.3% on the actuator and by only decreased by 0.95% on the throat. The changes from this to the final condition, high temperature and high relative humidity, were relatively small and insignificant.

The high temeprature high relative humidity condition returned three stages that significantly differed from each other: the throat (t stat 2.90; t crit 2.78), stage 2 (t stat– 5.37; t crit 2.71) and stage 3 (t stat –4.35; t crit 3.18).

5.6 The effect of environmental testing condition on the major primary and secondary particle production mechanisms

Figures 5.16 and 5.17 illustrate the effects of environmental testing conditions on the major primary and secondary particle production mechanisms for the novel pressurised solution formulations

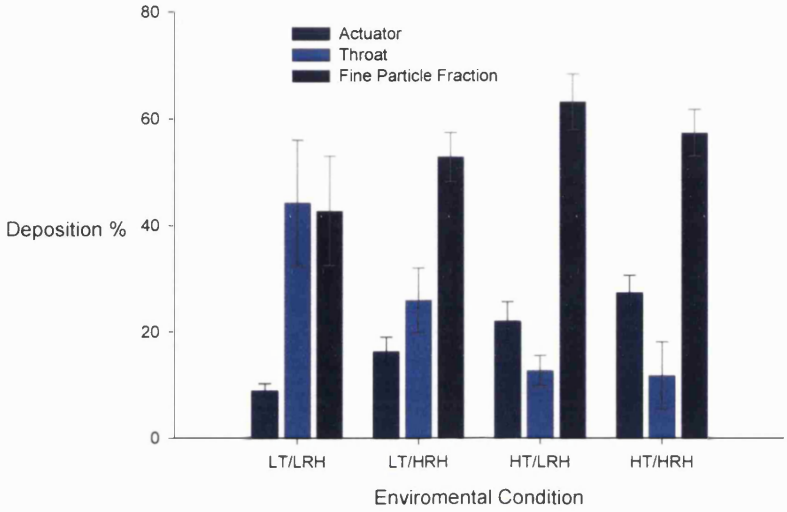

Figure 5.16: ***Intra formulation comparison of the primary aerosol characteristics of salbutamol maleate.***

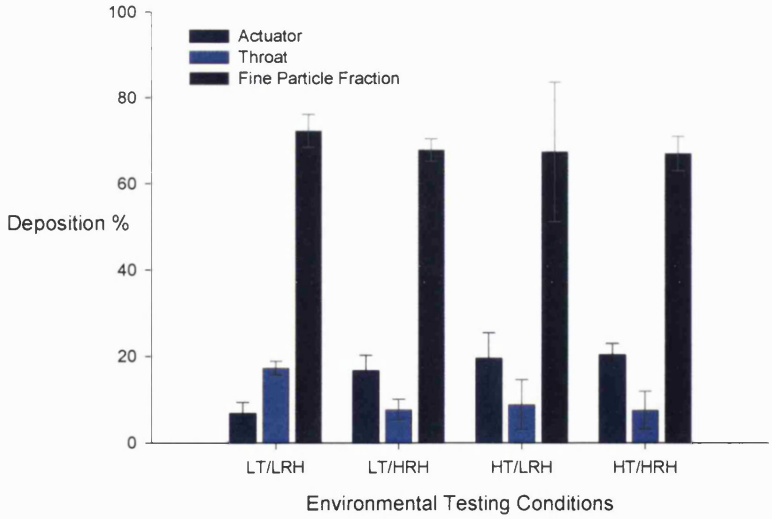

Figure 5.17: ***Intra formulation comparison of the primary aerosol characteristics of salbutamol oleate.***

5.6.1 (a) Evaluation of the data relating to the Hydrophilic salt

When tested at ambient lab conditions the highest throat, lowest actuator and lowest fine particle fraction was obtained for the hydrophilic salbutamol maleate salt. Upon maintaining low conditions of relative humidity, but when the temperature was increased a complete change in the primary mechanism and large particle deposition pattern was observed. Table 5.4 summarises the normalized stage deposition data and provides a direct comparison for intra and inter salt formulations. Actuator deposition increased from about 9% to 22%, the throat deposition decreased from 43% to 13% and the fine particle fraction increased from 43 to 64% respectively. When the relative humidity was at the extreme value, in the region of 100%, and the temperature varied between 24.8°C and 36.8-37.1°C, a similar trend was observed, whereby the actuator deposition increased from approximately 16% to 27% the throat decreased from about 26 to 12% and the fine particle fraction increased from around 53% to 57%.

Considering the reverse, when temperature was kept at a low ambient value about 24.8-25.2°C and humidity varied 30.2% and 100% relative humidity, under high humidity conditions the actuator deposition increased, the throat deposition was reduced and the fine particle fraction increased. The approximate relative percentage changes were 9% increasing to 16% for the actuator, 44% decreasing to 26% for the throat and 43% increasing to 45% for the fine particle fraction.

In general, the actuator and throat deposition was affected by both temperature and humidity, but more so by temperature, as was the fine particle fraction. At both high temperature and humidity the fine particle fraction was about 6% lower than the maximum value. Statistically, actuator, throat and fine particle fraction data sets exhibited statistical differences.

For the actuator a pvalue of <0.001 resulted for the following combinations: low temperature low relative humidity and both high temperature low relative humidity and high tempertaure hgh relative humidity. And also for the low temperature high relative humidity compared to the high temperature high relative humidity testing conditions. The particle size deposition patterns of the throat returned a p value of 0.001 for the low temperature low relative humidity condition compared to both the high temperature low relative humidity and high temperature high relative humidity conditions. The fine particle

fraction data, p= 0.02, had only one set of conditions that reached significance: the low temperature low relative humidity when compared to the high temperature low relative humidity conditions.

The extent of aerodynamic force, calculated in the throat region, can be seen from the change in Weber number from 4°C through to 37°C. As temperature is increased for the hydrophilic salt the Weber number increases. A simplified calculation, based on standard data, illustrates this change:

$$We = \frac{2R\rho(\Delta U)^2}{\sigma} \qquad \textit{Equation 5.1}$$

Where all usual nomenclature applies and calculations are based on dimensions and suppliers physical and chemical data:

2R= D = 10μm particle, ΔU^2 = 9040ms^{-1}, D of USP Andersen throat 19 mm ρ=0.0174,0.0323, 0.0504 kgm^{-3} at 4,25 and 37°C and σ = 4.23x10^{-4}, 3.10x10^{-4}, 2.29x10^{-4} kgs^{-2} at 4, 25 and 37°C for a 10:90 ethanol 134(a) solution.

Assuming a dry environment, (as humidity alters gas viscosity) for a 10 micron particle at 4°C, We = 11.2, at 25°C We = 28.2, and finally at 37°C, We = 59.6. For a 5 micron particle at the ascending temperatures described the We = 5.58, 14.1 and 29.8 respectively. (For a 1 micron particle the We_{cr} is 1/10th the 10 micron particle value)

These trends were confirmed from comparison of the data in table 5.1 by comparing LT: LRH and HT: LRH environments. The actuator data indicated an increase of approximately 2.45 fold (the We_{cr} drops by about 2.11) due to the increase in $We_{cr.}$ The throat data also indicated a reduction by approximately 3.47 fold. This may be due to the larger particles exceeding the critical dimensions and undergoing breakup. The MMAD values from table 5.0 indicated a reduction in MMAD, about 0.75 times the LT: LRH when compared to the HT: LRH value, as a result of the increased particle breakup. From the idealized calculation it becomes evident that as the We_{cr} decreases the particle size decreases and so smaller particle experience less aerodynamic force.

Humidity had a similar effect,by increasing the actuator deposition and reducing the throat deposition, but in this instance to a lesser extent, see table 5.1 LT:HRH conditions versus

the corresponding low RH data. This may be due to an increase in viscosity of the dispersed phase potentially hindering atomisation. This effect can be observed in the HT:HRH condition, which has the greatest actuator deposition. The FPF increases from LRH to HRH at the extremes of temperature and the MMAD decreases (as a result of probable density changes that will be discussed later) from, which one can infer hygroscopic growth as the water-soluble species may act as nucleation sites for water vapour molecules.

5.6.1 (b) Evaluation of the data relating to the Hydrophobic salt

The particle size deposition patterns for the hydrophobic salt were, in general, less affected by temperature and humidity than its hydrophilic counterpart, as the data depicts in table 5.4 The throat deposition was higher in relative terms than the actuator for the low temperature low relative humidity conditions. All other conditions had the reverse trend with higher actuator deposition and lower throat deposition, and overall the relative percentage changes were small. The actuator deposition changed, and increased, from 6% at low temperature to 16%, 19% and 20% for low temperature high relative humidity, high temperature low relative humidity and high temperature high relative humidity environments respectively. The throat decreased from 17% to 7%, and 8% to 7% for these conditions respectively.

The We_{cr} numbers calculated above also apply to the oleate or hydrophobic salt. As the formulations were similar in overall volatile component composition: 10.62: 89.38 (ethanol: 134(a)), for the hydrophobic salt versus 9.98: 90.02 for the maleate salt then any differences should, in theory, be due to the physicochemical and colligative properties of the derivative. The reduced amount of deposited drug as compared to the hydrophilic counterpart at LT:LRH would indicate a reduction in surface tension for particles of this formulation. This seems counterintuitive given the salt is at a concentration of 0.41%w/w as compared to 0.19% w/w for the hydrophilic derivative.

Statistical differences were only observed on the actuator for this data set, which returned a value of 0.01 for combinations of the low temperature low relative humifidt condition when compared to bith the high temperature low relative humidity and high temperature high relative humidity.

Again tables 5.0 and 5.1 summarise the critical data. As with the hydrophilic salt, the hydrophobic salt formulation once aerosolised undergoes modification via the primary mechanism indicated by similar changes in actuator and throat deposition: an increase to 17% at the actuator and a reduction on the throat.

5.6.1 (c) Conclusion: The effects of the environment of the major primary and secondary particle production mechanisms

In conclusion, at this stage, evaluation of the growth rate per se can be derived from the calculated "growth rate ratios": the change from low to high RH at constant temperature (see table 5.0). As a surrogate and, as far as possible, a direct, correlation to *"in-vivo"* conditions both salts indicated an increase when HT: LRH was evaluated against HT: HRH. For the hydrophilic/maleate salt this generated a ratio of 1.09; for the hydrophobic/oleate this resulted in a value of 1.30. Both results are in the orders determined by previous workers in the field, (See literature values in appendix A.5.0), even though different experimental conditions and laboratory equipment were utilised. The "growth" of the hydrophobic organic salt solution may in part be correlated to the hypothesis set out in appendix 5.1. whereby Bell and Ho suggested that the reduction in growth of isoproterenol saline solutions with glycerol was retarded probably due to surfactant molecules hydrogen bonding to water molecules on the particles surface reducing water bv vapour molecules transferring to the particles core. In this particular case, as the formulation contains no hydrophilic active molecule only excipients namely ethanol; so, it is postulated here that the surfactant portion of the derivative aligns at the particle surface in a humid or water laden environment and said molecules bind to the surface possibly via van der Waals or dipole interactions at the double bond. This may help to reduce the surface pressure and so evaporation and, or, may lock water molecules on to the particle surface effectively increasing the MMAD. The comparison between the throat depositions of both salts at LT: LRH indicated a significant change in deposition. As discussed, this may be due to a reduction in surface tension of the emitted particles. This seems plausible as surfactants reduce surface free energy. The maleic acid molecules contain a free hydroxyl group that may form both intra and inter molecular hydrogen bonds redressing the balance of the competing vapour pressure effects of the curved surface. Matrix effects may also occur, but analysis of the particle during its trajectory (experimentally difficult) and post plate deposition would be required.

5.7 Data evaluation and discussion of the possible mechanisms resulting in the particle size deposition patterns of novel solution pMDI' formulations

From the preceding data, it was shown that temperature and humidity influenced both the primary and secondary aerosolisation processes, which may directly affect aerosol delivery when preconditioned within in the respiratory tract. Furthermore, the effect of drug salt derivative, contrary to related experimental investigations, had a major impact on particle deposition within an *in-vitro* apparatus with varying environmental testing conditions. This was confirmed from both data evaluated on an inter-formulation, stage-by-stage basis when the major parameters, section 5.6, were statistically evaluated. For these parameters, not previously documented, significant differences for the actuator, throat and fine particle fractions. These differences are depicted in table 5.8

Parameter	Maleate	Oleate			P Value
	Environmental Condition				
Actuator	LT:LRH	HT:LRH	HT:HRH		
	HT:LRH	LT:LRH			<0.001
	HT:HRH	LT:HRH			
Throat	LT:LRH	LT:HRH	HT:LRH	HT:HRH	<0.001
	LT:HRH	LT:HRH	HT:LRH	HT:HRH	
Fine particle Fraction	LT:LRH	LT:LRH	LT:HRH	HT:LRH	HT:HRH	0.004

Table 5.8: ***Statistical differences encountered for key particle size parameters when compared on an interformulation basis.***

The main objective of the study was to evaluate the effect of hygroscopicity on the delivery of salbutamol salts to the lung. Hygroscopicity, in aerosol mechanics, is standard nomenclature for describing the interactive effects of water molecules with droplets and sprays, and in this study has shown to have a significant effect when coupled with temperature.

General Discussion: Possible effects of Drug derivative effects on cloud dynamics

Before discussing the effects of hygroscopicity and the impact of environmental testing conditions on drug delivery, consideration should be given to the process of atomization and cloud dynamics based purely on the character of drug the derivative alone: review of the data generated under standard conditions (the control conditions) described as those of low temperature and low relative humidity. Theoretically, deposition patterns for the two salts should follow similar trends, even though the concentrations of the active were different. Concentration effects have been shown historically to affect MMAD, and theoretically, the oleate should have had a larger MMAD. This was not however observed in this study.

Primary atomisation is described by the oscillations and perturbations that affect the liquid jets that emanate from the spray orifice, whereas secondary atomisation proceeds via disintegration of the initial droplets, which exceed a critical size and further disintegrate, influenced by aerodynamic forces. Data suggested the effect of salt derivative was affecting the secondary atomisation process, to a greater degree, with varying environmental conditions. (It should be noted that the testing apparatus removed a large portion of aerosol droplets from the initial burst produced from atomization; these resulted in particle sizes greater or equal to 9 microns in mass weighted diameter). It is likely that these particles would have undergone further breakup. This could be rationalised, as the actuator deposition data were similar for both formulations, but the review of the subsequent impactor stages indicated heavier drug loading on lower plates and a fundamental character namely the MMAD was significantly different. The LT: HRH condition was an exception, but results are discussed, further, later. Also, the dose impacted to a greater degree on the throat stage for the hydrophilic salt: salbutamol cis butenediaotae / maleate. The throat deposition was over double that for the hydrophobic derivative at low temperature conditions, but was similar although still slightly increased at high temperature variations. MMAD values for particle depositions were greater for the maleate salt at all testing environments except for the low temperature high relative humidity.

For this process to occur, it is theorised that an increase in injection pressure on the emerging liquid ligament from the orifice would be required resulting from a change in liquid mass flow rates. This suggests that the mass flow rate through the orifice may have been significantly greater then for the oleate salt and thus, in turn, impart a greater

coefficient of discharge upon actuation. A further implication here is that the densities of the liquids in the metering chamber are different, as the mass flow rate is related to the square root of the liquid density; however, density changes of the magnitude required are unlikely, and not supported by individual shot weight data. The individual salts, however, do have different densities: 1.305 vs. 1.095 gcm^{-3} for the maleate and oleate, respectively. This may have an important effect on the microscopic, individual droplet scale.

Again, on a microscopic scale viscosity may be very different. The increased concentration of the hydrophobic-based surfactant derivative would be expected to produce a more viscous drug solution. Also the increased concentration of hydrophobic drug derivative may affect heat transfer from the surrounding environment by changing the heat capacity, and thus possibly affecting an increase in size. Viscosity has a complex effect on particle size distributions. In general, it lowers the Reynolds number and dampens instabilities in liquid jets dischsrged from an orifice. This in turn would delay disintegration and increases particle size. Therefore a more viscous oleate solution would be expected to again produce a larger MMAD. However the data contradicts the preceding hypothesis. However, in a hollow cone such as an actuator tube and spray orifice, viscosity can increase flow rate by increasing the liquid film and surface area over and around the orifice. Increasing the mass flow rate would accelerate spray, increase the discharge coefficient, increase the velocity of liquid discharge and decrease the MMAD. (Lefebvre 1989). The surface chemistry of the derivative may also be important here, assisting in rationalization of the pressure change-viscosity theory. The oleate is a surfactant-based acid adduct. This may in turn affect as indicated above flow by spreading and subsequently depositing on the mouthpiece. Here shear stress values could be different, for the different formulations and drug concentrations. Rapid multiple actuations as performed in this study, may precipitate drug on the actuator orifice and mouthpiece. For a solid material namely the maleate salt, a potential reduction or slow down in discharge rate may result and ultimately may affect particle size. A surfactant would behave differently. A liquid coating, the oleate salt, may reduce shear stress between the passage of formulation and the walls of the spray orifice. Energetically, the minimum amount of energy required for atomisation is equal to the product of the surface tension and the surface area. An increase in surface area would therefore reduce the critical value. A spreading liquid surfactant will increase surface area in relation to a solid deposited, suggesting the surfactant formulation may remain 'wet' upon aerosolisation. The aerosolized droplets for different salt forms may therefore have different morphologies post aerosolisation as a result of the possible production of a "dry" hydrophilic particle and a "wet" hydrophobic particle. This effect has indeed been

observed by scanning electron micrographs of particles deposited on stage plate 4 of the cascade impactor. These are illustrated for the maleate and oleate salt in figures 5.18 A and B, respectively. The scanning electron micrographs illustrated the unexpected changes in particle morphology, which may result from variations in the structure of the salt. The maleate produced classic spray dried amorphous spheres, whereas the oleate indicated a liquid amorphous morphology.

Figure 5.18 A: A scanning electron micrograph of salbutamol maleate recovered from a cascade impactor stage 4.

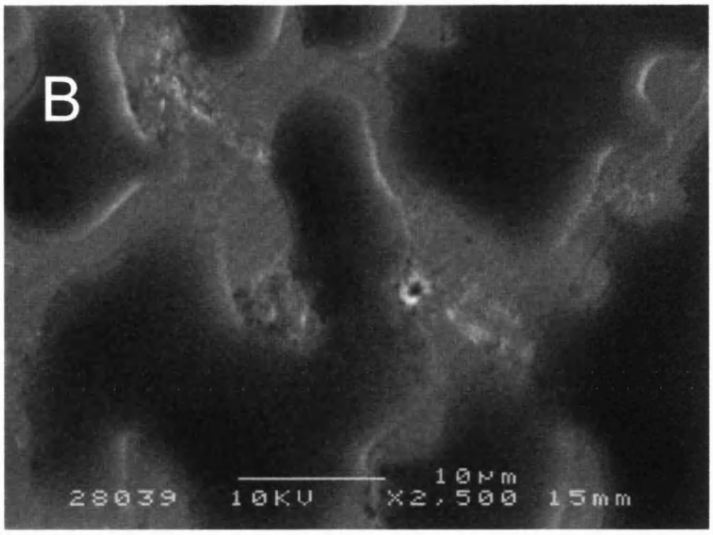

Figure 5.18 B: A scanning electron micrograph of salbutamol oleate recovered from a cascade impactor stage 4.

The SEM of the fixed oleate salt figure 5.18 B indicates the presence of "liquid pools and streams" possibly due to the lower viscosity of the aerosol droplets upon collection. An alternative explanation may be that the collapse of the salbutamol oleate hydrophobic salt particles resulting from a phase change due to the uptake of moisture and temperature changes during SEM preparation. A phase change at effectively ambient temperature would require physicochemical properties similar to mixtures of natural lung surfactants. (For an amorphous material, a glass transition temperature is more applicable related to the viscosity of the material exceeding a critical value) In conjunction, it may be possible that with even a small amount of water vapour in the testing atmosphere (30.3% in this case), molecules of vapour may adsorb to the particle surface and remain trapped until deposition providing a liquid air interface for subsequent spreading. To verify this fact bespoke experimentation would need to be performed over a range of humidities and on all impactor stages. Ultimately, surface chemistry of the different derivatives indicated significance differences and their choice in the future must be considered in aerosolised therapy. The severe and dramatic differences in distribution patterns and FPD signified, it was hypothesized, that aerodynamic forces on the oleate derivative were greater than that of the maleate. It was inferred from these data that the surface tension, (Weber number) and the viscosity (Reynolds number) figures of the maleate droplet were greater than that of the oleate. Thermodynamics may have also impacted on particle size distributions. Upon aerososlisation, particles may have experienced a drop in temperature due to propellant evaporation, which could subsequently act as cloud condensation nuclei. Two phenomena may occur post actuation: all volatile components may vaporize leading to the rapid precipitation of a solid particle, or the highly volatile component vaporizes preferentially leaving an ethanol and drug liquid droplet. Either way, an increase in MMAD and in fine particle fraction should result. From the data a dry particle is theorised for the maleate and a liquid particle for the oleate; this can be explained by the following rationale and is supported by the SEM micrographs in figures 5.18A and B. A decrease in MMAD occurred for the hydrophilic aerosol, but the fine particle dose increased. This apparently contradictory behaviour can be explained by hygroscopic growth. As the dry hydrophilic aerosol particle sorbs water the density decreased from about 1.305 gcm^{-3} to approximately 1.0gcm^{-3}. As the aerodynamic diameter is equivalent to the product of the density and the particle diameter then a simple calculation predicted a drop of MMAD to roughly 1.30 (1.35 actual) for the maleate, and an increase to 1.35 for the oleate (1.42 actual). In-vitro deposition data confirmed this supposition. Further, the fine particle dose increased from 42 to 53% for the maleate but dropped slightly from 72 to 67% for the oleate.

The Effects of Environmental Conditions on Drug Delivery

Air temperature of the environment was shown to have a significant effect on cloud behaviour, since as temperature increased so did the formulation vapour pressure and so would the rate of evaporation of the volatile formulation components. Under these conditions the MMAD should therefore decrease with increasing temperature. This was substantiated for both salts, with the added effect of increasing MMAD when water vapour was present. A question now presented itself: was the increase at high relative humidity due to vapour suppression, did hygroscopic growth occur or did a combination of the two processes occur?

The data suggested a vapour suppressive type mechanism for the hydrophobic unsaturated fatty acid derivative. Consider the high temperature varying humidity deposition profile (figure 5.9) coupled with the actuator, throat and fine particle fraction (figure 5.13). The actuator, throat and fine particle deposition remained relatively unchanged over the environmental testing conditions. The stage depositions indicated similar patterns, which increased at the higher stages, but the low relative humidity condition dominated the very fine particle dose. For the oleate the MMAD increased: the growth ratio was 1.12 for the low temperature conditions and 1.30 at high temperature under elevated humidity testing conditions. As the active is water insoluble it is possible that the water vapour as intimated adsorps physically to the surface via dipole-dipole interactions, and potentially forms an electrostatic attraction between the unsaturated double bond and the oxygen-hydrogen bonds of the water vapour molecules. The latter assumption would need to be confirmed by NMR studies as ethanol present may alter molecular orientations. The surfactant present may interfere with the heat transfer, namely evaporation and diffusion at the particle interface.

For the hydrophilic unsaturated carboxylic acid, the data, it is inferred, indicated two different mechanisms. The actuator deposition increased with temperature and humidity (figures 5.2, 5.4, 5.6, and 5.8). In conjunction, the fine particle dose increased with humidity until the combination of high temperature and low humidity condition and dropped slightly at the high temperature high humidity condition. (Figure 5.8 and table 5.1). The inter stage depositions (figure 5.17) indicated a greater loading for the high humidity condition at stage five with a decrease over the very fine particle dose stages.

Hygroscopic growth or activation of an aerosol particle to enable growth into a larger droplet occurs when the environmental supersaturation exceeds the critical supersaturation of the particle. This process is controlled by the rate of generation of potential supersaturation, the net rate of mass transport of water vapor to the ensemble of particles, the thermodynamic driving force for condensation, and the release of latent heat. During aerososlisation environmental supersaturation may occur and condensation of water vapor onto the activated cloud droplets the linitial aerosol particles may occur, in a manner similar to cloud activation by soluble aerosol particles. For water soluble species the formation of a dry particle is proposed, which dissolves and subsequently grows. The insoluble species, it is proposed, does not grow via a hygroscopic mechanism, and remains as a wet droplet protected by the formation a surfactant layer on the surface. Water vapour concentration and pressure may cause a layer of water molecules to physically adsorb to the droplet surface. To corroborate the prior assumptions and illustrate hygroscopic versus vapour suppression mechanisms, the reader is directed to tables 5.0 and 5.1 and figures 5.12 and 5.13 respectively. Comparing the low relative humidity and varying temperature environments the data changes are similar with the exception of the throat, which has been explained by viscosity changes and the increasing critical Weber number We_{cr}.

Humidity affects both salts when comparing LT: LTH and LT: HRH, but for the hydrophobic salt this is suppressive as the FPF remains unchanged: 72% versus 68%. The FPF for the maleate salt however increased from 43 to 53%, and although not significant was a major increase. The change in MMAD, a reduction, it was conjectured resulted from a change in density via water uptake.

Comparing the range of conditions, there was increase from LT: LRH to HT: HRH: ambient laboratory versus those mimicking physiological *"in-vitro"*. The individual GRR's were 0.75 for the hydrophilic and 0.89 for the hydrophobic respectively, but the inter formulation GRR's over these conditions indicated an increase of 1.07 for the hydrophilic salt. The respirable fraction also indicated a change as the FPF increased by about 15% for the hydrophilic salt, a significant increase over the hydrophobic salt, which increased by about only 5% with the results not effectively attaining significance.

Overall, the data indicates that testing at the normal lab conditions does not give an accurate reflection of particle size changes that occur when these two novel solution based pressurized inhalers were tested. Also the selection of drug derivative is critical in determining the cloud dynamics of solution-based pMDI's.

6 CONCLUSIONS AND RECOMMENDATION FOR FUTURE WORK

The aim of this thesis was to investigate the effects of temperature and humidity on the fundamental, characteristic properties of aerosol particle clouds emitted via novel HFA solution based inhaler formulations of salbutamol.

The basis of this pharmaceutics study covered the following areas:

(i) The chemistry of bronchodilator synthesis and crystallisation,
(ii) Physico-chemical characterisation,
(iii) The effect of formulation variables and modelling of aerosol clouds, and
(iv) The effects of simulated environmental conditions on the particle size distribution of aerosol clouds generated by pressurized solution systems.

General Conclusion to Chapter one

The introductory chapter highlighted that pressurised inhaler technology has been largely static, over the last four decades, and also the chemistry of drug selection and formulation science has largely been empirically based. The bronchodilator salbutamol sulphate, it was inferred, was chosen merely on the differences in pKa value in order to expedite rapid crystallisation, and not based on the rationale of its pharmaceutical properties. The change from CFC to HFA propellants has also had a major impact on formulation development of pMDIs. This complication, has been mainly related to the partial solubility of the active ingredients in HFA propellants, and that the majority of the accepted surfactants are insoluble. Thus, the rational for drug salt selection has been largely overlooked and been based on commercial drivers and challenging technical issues.

Further Work associated with chapter one

Further work in this area should focus on literature searches and investigations into archived work on inhalation therapy, e.g. the Egyptian Ebers, probably the oldest medical texts in existence, indicate the use of vapour inhalation. Mechanisms into producing drug vapours or compounds which sublime may improve deposition and reduce losses in the throat; systemic drug delivery would also benefit from this approach to drug delivery.

The search for novel surfactants, although not within the scope of this thesis, utilised not only to stabilise suspensions, but more appropriately to enhance solubility would be of interest to manipulate particle growth kinetics. Polyfluorinated carboxylic acids, under the trade name Fomblin HC have been cited in the literature for this purpose. However, other toxilogically safe fluorinated materials may also be evaluated for this purpose. The US military have utilised fluorinated hydrocarbons to enhance breathing in high-pressure sub-aqua applications and it is feasible that these compounds are HFA soluble.

General conclusions to chapter two

Chapter two focused on the selection and synthesis of novel bronchodilator derivatives. Salbutamol was chosen as the drug of choice since this has been the gold standard in relief therapy for asthma and RAO's for several decades. The selection of salt derivatives, although not new, was novel in this application of solution-based systems.

In this thesis, several novel salt derivatives of salbutamol were synthesised, and the choice of reaction conditions allowed the development of a pre-formulation screening tool to be incorporated into the synthetic method. Of the all the derivatives synthesised, the carboxylic salts proved to be the most soluble in ethanol. Further, it was established that unsaturated carboxylic acids were highly soluble with the reasons for enhanced solubility discussed. Indeed, stereoselectivity was shown in this study to have an influence on physical solution stability and solubility. Cis-trans isomerism was important as fumaric acid, trans butenedioic acid, proved to be insoluble, whereas, the cis form maleic acid was shown to be highly soluble.

It was shown that by careful selection of solvents and anti-solvent systems that even highly soluble salts could be manufactured in-situ within the pMDI canister. Although not a structured part of the research, formation of particles from a batch manufacturing process perspective for labile compounds may be of commercial and technological interest. Further, given the fact crystallisation could be achieved in-situ, as was visually observed by particle induction in the canister, it could be possible with careful reaction thermodynamics and kinetics to produce monodisperse particles. Altering the process conditions, of not only the salt solution, but also the anti-solvent (HFA 134(a)) namely its temperature and pressure may provide a means of modifying particle size and its behaviour.

The drug derivatives have also been extensively characterised as documented in this chapter. Structural identification was conclusively proved by X-Ray crystallography.

Further work associated with chapter two

The area of crystallisation is a complex interplay of thermodynamics and kinetics, and has been shown to be highly influenced by selection of solvent systems. At present, no work in this thesis has been performed investigating the existence of polymorphism of the salt derivatives. By utilising different anti-solvent systems different polymorphs may be synthesised. Indeed, in this thesis, melting points from DSC when compared to standard compounds indicated differences. The effect of polymorphism will impart many differences in character and may improve solubility. Alternatively, other inhalation systems such as dry powder inhalation preparations may benefit from selective salt formation. This may provide a novel means of influencing particle interactions with carrier excipients, plastics and polymers such as those found in reservoirs and blisters, while maintaining environmental stability and delivery. The effect of structural stereoselectivity has been demonstrated on solubility, but chiral effects have not been investigated. As the R-enantiomer is the pharmacologically active molecule, further work involving this compound should be investigated not only in terms of solubility, but, also, in cloud formations and deposition patterns from aerosol clouds. The effect of reaction conditions on drug synthesis in the final container should possibly be investigated. From initial experiments, it was observed that manipulating the amount of ethanol, and water in the final contained could produce 2 phase systems. It is possible that the final material may be crystallised for suspension-based systems by carefully controlling the rate and temperature of addition of anti-solvent (HFA134(a)); the handling of concentrated drug solutions prior to manufacture may have advantages over micronised powders. The use of sonication energy on crystal character has been investigated, (Mar and Ulrich 1999) and could potentially be utilised to produce crystals of a specific size and quality for inhalation.

Further work may centre on investigating the effects of solvate, hydrate or polymorph production from synthesis or conversely from long-term storage in different solid and liquid propellant systems. As particle morphology upon deposition has been shown to change, investigations into effects on pharmacokinetics and pharmacodynamics may be beneficial.

General conclusions to Chapter Three

As the antithesis to chapter two, where the main focus was on preparation and crystallisation of salts from solution, in this chapter the enhancement of solubility in polar and non-polar solvent systems was the main objective. The HFA propellants are poor solvents for the majority of surfactants, but have been shown to dissolve certain drugs to varying degrees Ultimately, this can decrease the physical stability of suspension formulations, and the mechanisms for these changes were considered. Ironically, the HFA propellants intrinsic characteristics should be better solvents per se This is discussed and evaluated in **appendices A 3** and concluded is not the whole argument.

A novel approach has been taken to model the solubility of components in solution based metered dose inhalers using data obtained in pure propellant, pure co-solvent, and mixtures thereof. Theoretically, it was proposed that if the solubility of the active in the formulation mixture exceeded the drug concentrate at a predetermined temperature then solubility and solution integrity would be maintained. Both theory and experiment correlated well, and deviations were discussed via the formation of metastable regions.

Further work associated with chapter three

Progression of work associated with this chapter would focus on the improvement of the solubility apparatus, and the solution solubility model, so that accurate solubility predictions may be reached by relating both the chemical structure, and drug concentration in tandem. This would assist as evidence from visual studies, rather than formulation selection on visual studies alone. Solubility theory could be extended by investigation into effect of polymorphism and surface energy properties.

General conclusions to Chapter four

Chapter four reviewed, briefly, the general mechanisms of liquid disintegration into aerosols of aerosol clouds, and the effect of formulation variables on the particle size distributions of novel solution based pMDI systems, when compared to a suspension based system of similar composition: a hydrophilic salt within a propellant co-solvent mixture of 15% w/w co-solvent and 85% propellant 134(a). In general, there were little differences between identical co-solvent level formulations. Inter co-solvent levels indicated a statistical significance when analysed at both 4°C and 37°C respectively. MMAD's and polydispersity increased with the level of co-solvent added, but were lower at higher temperature and thus higher vapour pressures. This may be related to viscosity and surface tension effects, and to a change of the critical Weber number of the aerosol droplets. A total mass balance incorporating stem deposition was not analysed, and this may have accounted for the discrepancies seen in high ethanol formulations.

Fine particle dose recoveries followed the anticipated trend. Higher vapour pressures and lower co-solvent levels gave higher fine particle fractions. The effect of formulation variables was shown to statistically effect particle deposition when formulations were equilibrated at high and low temperatures, as compared to ambient. Finally, a semi-empirical equation has was derived that predicted the MMAD of aerosols based upon drug character and excipient physicochemical constants that held to with ± 3% of experimental results.

Further work associated with chapter Four

The semi-empirical equation derived should be expanded upon, by comparing additional experimental data of novel and conventional formulations with the theory. Additional components that alter surface tension and viscosity should be incorporated to test the robustness of the theory and expand upon it, and alternative particle sizing methods such as laser diffraction could be employed to evaluate the differences of MMAD. Ranges of actuator orifice diameter, and valve build (metering chamber) should also be tested, as they have been previously shown to impart effects on aerosol formation. Fundamental physicochemical assessment of vapour pressures of ethanol and 134(a) mixtures over a range of temperatures would also be invaluable, as data so far has been generated at

ambient. Clear deviations from the positive vapour pressure erstwhile described have been shown.

General conclusions to Chapter five

The testing environment clearly affected the aerosol clouds generated from the novel solution pMDI's. In addition, it was also noted that the salt derivative itself, when formulated at the lowest acceptable co-solvent level necessary to attain short-term stability, had a marked effect particle size distribution, and it was inferred that the salt derivative itself was affecting both primary Equated to the large, non-respirable dose and secondary (respirable dose range) aerososlisation mechanisms.

Hygroscopicity and its effects of aerosolised on salt forms of medicaments were a primary goal of this thesis, providing the question: what changes occur in fundamental aerosol parameters, when evaluated under non-standard testing conditions?

Data generated indicated that a particle size increase occurred for the hydrophobic (Oleate) salt when humidity was increased at both temperature extremes. Whereas, the hydrophilic (Maleate) salt, which would have been expected to increase actually decreased at low temperature and increased in relative terms less than its hydrophobic counterpart, at high temperature. Explanations for this behaviour are postulated by the fact that the aerosol particles are essentially different after discharge from the actuator orifice: the hydrophilic are "dry" post actuator and the hydrophobic are "wet". This was partially confirmed from SEM images of the cascade impactor stage 4. As a dry particle, the density would decrease on acquisition of moisture from its surroundings, and the MMAD would also decrease. For a wet particle (ethanol only, assuming the propellant is effectively removed and the less volatile co-solvent remains) the particle density conversely would increase and the MMAD also increase. The differences in experimental MMAD may be due to the fact that the surfactant (hydrophobic salt) partitions between the liquid vapour interface and may increase the critical supersaturation and decrease the size preferable for growth.

During the discussion of chapter five a question presented itself: did the change in MMAD at high temperature result from hygroscopic growth or retardation of propellant/co-solvent evaporation? The data from figures 5.18 A and B indicated a suppressive mechanism for the hydrophobic salt. This was justified by considering the data at high temperature high relative humidity, and high temperature low relative humidity's respectively. No change in

fine particle fraction was observed (secondary aerosolisation mechanism), nor any significant changes in actuator or throat deposition (primary aerosolisation mechanism).

For the hydrophilic salt it was postulated that hygroscopic growth occurred. This statement was qualified by the fact that similar data reviewed (figure 5.3) indicated an increase in fine particle dose, which at high temperature would be unlikely. The increases in MMAD of the particles rather than suppression of volatiles evaporation were confirmed from the data in figure 5.5. Here the actuator deposition increased at these conditions, rather than decreased.

Further work associated with chapter five

Particle changes not only in distribution, but morphology were observed. Investigations into particle morphology and pharmacokinetic effects warrant further study. Delivery of surfactant containing species may be of benefit not only in valve function and device performance, but may alter the adsorption and duration kinetics of the drug, as aerosol growth kinetics is a complex and multi-functional discipline. Two different salt forms have been shown to exhibit different dynamic growth characteristics contrary to theory. The effect of salt form indicated changes not only particle size, but also particle polydispersity and deposition on the pMDI hardware. Further work should be undertaken to review processes essential for production of a monodisperse aerosol. The reduction of throat deposition by actuator modifications, utilising humidified air would be therapeutically advantageous to the asthmatic population as a whole.

APPENDICES FOR CHAPTER 1

A 1.1: Anatomical and Physiological characteristics of the human lung model adapted from Weibel.

Airway Branch Gen.	No per Gen	Diameter (cm)	Length (cm)	Total Area (cm^2)	Total Volume (cm^3)	Cumulative Volume (cm^3)
Trachea	0	1	1.8	12.0	2.54	30.5
Main Bronchus	1	2	1.22	4.76	2.33	11.25
Lobar Bronchus	2	4	0.83	1.90	2.13	3.97
Lobar Bronchus	3	8	0.56	0.76	2.00	1.52
Seg Bronchus	4	16	0.45	1.27	2.48	3.46
Seg Bronchus	5	32	0.35	1.07	3.11	3.3
Bronchus	6	64	0.28	0.90	3.96	3.53
Bronchus	7	128	0.23	0.76	5.10	3.85
Bronchus	8	256	0.186	0.64	6.95	4.45
Bronchus	9	512	0.154	0.54	9.65	5.17
Bronchus	10	1,024	0.130	0.46	13.4	6.31
Term Bronchus	11	2,048	0.109	0.39	19.60	7.56
Term Bronchus	12	4,096	0.095	0.33	28.8	9.82
Bronchiole	13	8,192	0.082	0.27	44.5	12.45
Bronchiole	14	16,384	0.074	0.23	69.4	16.40
Bronchiole	15	32,768	0.066	0.20	113.0	21.70
Ter Bronchiole	16	65,356	0.060	0.165	180.0	29.70
Res. Bronchiole	17	1.31×10^5	0.054	0.141	300.0	41.80
Res Bronchiole	18	2.62×10^5	0.050	0.117	534.0	61.80
Res. Bronchiole	19	5.24×10^5	0.047	0.099	944.0	93.20
Alv.duct	20	1.49×10^6	0.045	0.083	1,600	139.50
Alv.duct	21	2.10×10^6	0.043	0.070	3,220	224.30
Alv.duct	22	4.19×10^6	0.041	0.059	5,880	350.00
Alv.sac	23	8.39×10^6	0.041	0.050	11,800	591.00

A 1.2: Adrenergic receptor sub-types and their function.

Effector Organ	Response	Adrenergic Receptor involved
Heart		
Rate of contraction	Increase	β_1
Force of contraction	Increase	β_1
Blood vessels		
Arteries	Constriction	α_1
Skeletal muscle	dilation	β_2
Veins	Constriction	α_2
Bronchial tree	Dilation	β_2
Splenic capsule	Contraction	α_1
Genito-urinary		
Uterus	Contraction	α_1
Vas Deferens	Contraction	α_1
Prostatic capsule	Contraction	α_1
Kidney		
Urinary Bladder	Rennin secretion	β_1
Detrussor	Relaxation	β_1
Trigone	Contraction	α_1
Uterer	Contraction	α_1
GI tract	Relaxation	α_2
Eye		
Radial Muscle	Contraction	α_1
Ciliary muscle	Relaxation	β_1
Liver		
Fat cells	Lipolysis	β_1
Pancreatic insulin release	Decrease	α_2

APPENDICES FOR CHAPTER 2

A 2.1: DSC melting point data of salbutamol salts synthesised and screened.

SALT ANION	MELTING POINT (approx.) °C
Acetate	ND
Fumarate	ND
Lactate	ND

NB the Fumarate was insoluble in ethanol even though its only difference to the maleate was the trans arrangement of the carboxylic acid groups.

Adipate	192
Stearate	108

NB The adipate and state mp differs from that described by Jashnani et al probably due to the solvents used in the synthesis

Mesylate	Degrades after 124
Besylate	Degrades after 138
Tosylate	Approx 160
Succinate	186
Nitrate	147
Phosphate	201
Hydrochloride	188
Maleate	130
Sulphate	200
Oleate	77

A 2.2: ***I.R. band assignments for stretching and bending vibrations with associated intensities.***

Functional Class	Stretching Vibrations			Bending Vibrations		
	Range (nm)	Intensity	Assignment	Range (nm)	Intensity	Assignment
Alkanes	2850-3000	str	CH_3, CH_2 & CH 2 or 3 bands	1350.1470 1370.1390 720-725	med med wk	CH_2 & CH_3 deformation CH_3 deformation CH_2 rocking
	3020-3100 1630-1680 1900-2000	med var str	=C-H & $=CH_2$ (usually sharp) C=C (symmetry reduces intensity) C=C asymmetric stretch	880-995 780-850 675-730	str med med	=C-H & $=CH_2$ (out-of-plane bending) cis-RCH=CHR
Alkynes	3300 2100-2250	str var	C-H (usually sharp) C□C (symmetry reduces intensity)	600-700	str	C-H deformation
Arenes	3030 1600 & 1500	var med-wk	C-H (may be several bands) C=C (in ring) (2 bands) (3 if conjugated)	690-900	str-med	C-H bending & ring puckering
Alcohols and Phenols	3580-3650 3200-3550 970-1250	var str str	O-H (free), usually sharp O-H (H-bonded), usually broad C-O	1330.1430 650-770	med var-wk	O-H bending (in-plane) O-H bend (out-of-
Amines	3400-3500 (dil. soln.) 3300-3400 (dil. soln.) 1000-1250	wk wk med	N-H (1°-amines), 2 bands N-H (2°-amines) C-N	1550.1650 660-900	med-str var	NH_2 scissoring (1°-amines) NH_2 & N-H wagging (shifts on H-bonding)
Aldehydes and Ketones	2690.2840(2bands) 1720-1740 1710-1720	med str str	C-H (aldehyde C-H) C=O (saturated aldehyde)			
	1690 1675	str str	C=O (saturated ketone) aryl ketone	1350.1360 1400.1450 1100	str str med	$-CH_3$ bending $-CH_2$ bending C-C-C bending
	1745 1780	str str	-unsaturation cyclopentanone cyclobutanone			
Carboxylic acid and Derivatives	2500-3300 (acids) overlap C-H 1705-1720 (acids) 1210-1320 (acids)	str med-str	O-H (very broad) C=O (H-bonded) O-C (sometimes 2-peaks)	1395.1440	med	C-O-H bending
	1785-1815 (acyl halides)	str	C=O			
	1750 & 1820 (anhydrides) 1040-1100 1735-1750 (esters) 1000-1300 16301695(amides)	str str str str	C=O (2-bands) O-C C=O O-C (2-bands) C=O (amide I band)	1590.1650 1500.1560	med med	

A 2.3: Atomic coordinates ($x10^4$) and equivalent isotropic displacement parameters ($Å^2 x\ 10^3$) for (jt2x) Salbutamol Oleate. U (eq) is defined as one third of the trace of the orthogonalized U^{ij} tensor.

	x	y	z	U(eq)
C(1)	9936(2)	7164(1)	10068(2)	26(1)
C(2)	8429(2)	6703(1)	9375(2)	26(1)
C(3)	9402(1)	6791(1)	9085(2)	20(1)
C(4)	9496(2)	7201(1)	7943(2)	27(1)
C(5)	9336(1)	5503(1)	8201(2)	20(1)
C(6)	9948(1)	4889(1)	7848(2)	20(1)
C(7)	9402(1)	4327(1)	7166(2)	19(1)
C(8)	8772(1)	3896(1)	7695(2)	19(1)
C(9)	8228(1)	3405(1)	7081(2)	17(1)
C(10)	7584(1)	2926(1)	7684(2)	21(1)
C(11)	8295(1)	3352(1)	5880(2)	19(1)
C(12)	8912(2)	3783(1)	5334(2)	22(1)
C(13)	9466(2)	4254(1)	5975(2)	22(1)
C(14)	2058(2)	5851(1)	9055(2)	26(1)
C(15)	3022(2)	6085(1)	9271(2)	35(1)
C(16)	3615(2)	5660(2)	8515(2)	40(1)
C(17)	4609(2)	5840(2)	8737(2)	39(1)
C(18)	5207(2)	5367(2)	8002(2)	43(1)
C(19)	6198(2)	5513(2)	8238(2)	43(1)
C(20)	6787(2)	5023(2)	7548(2)	44(1)
C(21)	6851(2)	5209(2)	6284(2)	44(1)
C(22)	7425(2)	5870(1)	6058(2)	37(1)
C(23)	7882(2)	5984(1)	5124(2)	35(1)
C(24)	7874(2)	5522(1)	4050(2)	35(1)
C(25)	7702(2)	5966(1)	2941(2)	33(1)
C(26)	6791(2)	6334(1)	2866(2)	32(1)
C(27)	6612(2)	6784(1)	1773(2)	35(1)
C(28)	5688(2)	7144(2)	1703(2)	38(1)
C(29)	5510(2)	7639(2)	660(2)	39(1)
C(30)	4589(2)	7978(2)	598(2)	43(1)
C(31)	4438(2)	8519(2)	-389(3)	57(1)
N(1)	9823(1)	6042(1)	8970(1)	17(1)
O(1)	10390(1)	4563(1)	8849(1)	21(1)

O(2)	7988(1)	2260(1)	8095(1)	26(1)
O(3)	7751(1)	2868(1)	5297(1)	25(1)
O(4)	1548(1)	6219(1)	8360(1)	26(1)
O(5)	1807(1)	5291(1)	9571(1)	33(1)

A 2.4: X-Ray Crystallographic summary data for salbutamol Oleate

Identification code	jt2x	
Empirical formula	C31 H55 N O5	
Formula weight	521.76	
Temperature	100(2) K	
Wavelength	0.71073 Å	
Crystal system	Monoclinic	
Space group	P 21/c	
Unit cell dimensions	a = 14.9781(11) Å	□= 90°.
	b = 18.3004(14) Å	□=93.2510(10)°.
	c = 11.5501(9) Å	□ = 90°.
Volume	3160.8(4) $Å^3$	
Z	4	
Density (calculated)	1.096 Mg/m^3	
Absorption coefficient	0.073 mm^{-1}	
F(000)	1152	
Theta range for data collection	1.36 to 28.29°.	
Index ranges	-19<=h<=18, -15<=k<=24, -14<=l<=12	
Reflections collected	19250	
Independent reflections	7296 [R(int) = 0.0569]	
Completeness to theta = 28.29°	92.8 %	
Refinement method	Full-matrix least-squares on F^2	
Data / restraints / parameters	7296 / 0 / 341	
Goodness-of-fit on F^2	0.918	
Final R indices [I>2sigma(I)]	R1 = 0.0554, wR2 = 0.1343	
R indices (all data)	R1 = 0.1146, wR2 = 0.1504	
Largest diff. peak and hole	0.720 and -0.347 $e.Å^{-3}$	

A 2.5: Atomic coordinates (x 10^4) and equivalent isotropic displacement parameters ($Å^2$ x 10^3) for salbutamol maleate. (U (eq) is defined as one third of the trace of the orthogonalized U^{ij} tensor)

	x	y	z	U(eq)
C(1)	-2156(5)	9076(4)	7744(4)	49(1)
C(2)	-1205(5)	9841(3)	6235(4)	42(1)
C(3)	-1023(7)	10581(3)	7849(5)	58(2)
C(4)	-967(5)	9717(3)	7318(3)	33(1)
C(5)	1330(5)	9191(2)	8409(3)	27(1)
C(6)	2692(5)	8540(3)	8347(3)	38(1)
C(7)	3399(5)	8448(3)	9353(3)	30(1)
C(8)	2845(5)	7799(3)	9942(4)	41(1)
C(9)	3342(5)	7722(3)	10870(3)	39(1)
C(10)	4382(5)	8313(3)	11256(3)	34(1)
C(11)	4981(5)	8982(3)	10692(3)	33(1)
C(12)	4482(5)	9032(3)	9723(3)	29(1)
C(13)	5952(6)	9682(3)	11135(5)	55(2)
N(1)	674(4)	9324(2)	7423(2)	28(1)
O(1)	3739(4)	8815(2)	7660(3)	50(1)
O(2)	4801(4)	8280(3)	12205(3)	50(1)
O(3)	7372(4)	9368(2)	11590(3)	44(1)
O(4)	3166(5)	6957(3)	3061(3)	37(1)
O(5)	1788(4)	6216(3)	4136(3)	34(1)
C(14)	2473(6)	6918(3)	3840(4)	26(1)
C(15)	2505(7)	7701(4)	4472(4)	34(1)
C(16)	1859(7)	7848(4)	5321(4)	38(1)
C(17)	837(6)	7276(4)	5934(4)	29(1)
O(6)	594(4)	6496(2)	5684(3)	31(1)
O(7)	347(6)	7589(3)	6729(3)	31(1)
O(4')	3880(20)	7359(13)	3309(14)	59(5)
O(5')	3020(20)	8322(10)	4276(14)	50(5)
C(14')	3010(30)	7537(12)	3986(17)	48(6)
C(15')	2200(30)	6846(15)	4546(16)	45(6)
C(16')	1390(30)	6867(13)	5372(14)	38(5)

A 2. 5 (continued)

C(17')	1064(19)	7623(10)	6013(12)	23(4)
O(6')	1381(18)	8351(9)	5738(11)	37(4)
O(7')	-120(20)	7587(10)	6550(12)	31(4)

A 2.6: X-Ray Crystallographic summary data for salbutamol maleate

Identification code	jt1x	
Empirical formula	C17 H25 N O7	
Formula weight	355.38	
Temperature	100(2) K	
Wavelength	0.71073 Å	
Crystal system	Orthorhombic	
Space group	P na21	
Unit cell dimensions	a = 8.4487(8) Å	□= 90°.
	b = 15.4327(15) Å	□= 90°.
	c = 13.8712(13) Å	□ = 90°.
Volume	1808.6(3) $Å^3$	
Z	4	
Density (calculated)	1.305 Mg/m^3	
Absorption coefficient	0.101 mm^{-1}	
F(000)	760	
Theta range for data collection	1.97 to 28.29°.	
Index ranges	-11<=h<=7, -19<=k<=16, -17<=l<=18	
Reflections collected	10650	
Independent reflections	3861 [R(int) = 0.0335]	
Completeness to theta = 28.29°	96.0 %	
Refinement method	Full-matrix least-squares on F^2	
Data / restraints / parameters	3861 / 8 / 227	
Goodness-of-fit on F^2	1.029	
Final R indices [I>2sigma(I)]	R1 = 0.0790, wR2 = 0.2077	
R indices (all data)	R1 = 0.1099, wR2 = 0.2318	
Absolute structure parameter	0(2)	
Largest diff. peak and hole	0.920 and -0.367 $e.Å^{-3}$	

A 2.7: HPLC equipment

Equipment	Make	Model
Pump	Jasco	PU 980
Autosampler	Jasco	AS950
Detector	Jasco	UV 975 UV/Vis
pH meter	Jenway	3305
Reagents	Supplier	Batch Lot / No
Methanol / HPLC grade Fisher	Various	
Water	Lab prepared MilliQ	resistivity >15MΩ
Glacial Acetic acid (G.A.A)	BDH	K25686717 838

A 2.8: HPLC analytical methodology settings used in solubility determinations

Mobile Phase:	60:40:1	MeOH: H_20: G.A.A
Column:	Spherisorb C18	12.5 x 5cm i.d.
Flow rate:	1.25 ml/min	
Run time:	4 mins	
Detection Wavelength	276	
Needle wash solvent:	100% MeOH	

APPENDICES FOR CHAPTER 3

A 3.1: ***Statistical data: One-way Analysis of Variance for determination of optimal solution solubility equilibration times***

Source	DF	SS	MS	F	P
	2	0.0000025	0.0000012	0.98	0.400
Error	14	0.0000178	0.0000013		
Total	16	0.0000203			

Individual 95% CI's For Mean based on Pooled Std Dev

Level	N	Mean	Std Dev	----------+---------+---------+------
1	5	0.001923	0.001820	(----------*----------)
2	6	0.001067	0.000898	(----------*----------)
3	6	0.001101	0.000317	(----------*----------)
				----------+---------+---------+------
Pooled Std Dev = 0.001127				0.00080 0.00160 0.00240

Tukey's pairwise comparisons

Family error rate = 0.0500
Individual error rate = 0.0203
Critical value = 3.70

Intervals for (column level mean) - (row level mean)

	1	2
2	-0.000929 0.002642	
3	-0.000964 0.001668	-0.001737

A 3.2: Physicochemical properties of pMDI media and their effect on solvent power

The change facilitated in the search for non-ozone depleting propellants identified two HFA's as suitable candidates, as they appeared to possess the necessary physicochemical properties required. Primarily they had a comparative toxicity to their CFC counterparts, they were non-ozone depleting, non-flammable, and had sufficient vapour pressures. However, it became apparent that they were not going to be direct substitutes (Dalby et al 1990). The reduced power of the solvents with respect to dissolution of conventional pharmaceutical surfactants, even though they were relatively polar, was not anticipated (Byron et al 1994). Such reasons need to be interpreted from intrinsic physico-chemical properties. These inherent characteristics are indicated in table A 4.1.

Table A 3.1 compares the major physicochemical properties of both the HFA and CFC propellants. On first inspection, the HFA's have comparable boiling points, solubility parameters, and display superiority with respect to dipole moments and dielectric constants. Therefore they should elicit a similar propensity for surfactant dissolution, and none of the conventional markers of solubility explained practical observations.

One potential reason for the reduction in solubility was proposed by Vervaet and Byron (Vervaet and Byron 1999). They suggested the polarisability of the HFA's are smaller than their CFC counterparts. The high electronegativity of the fluorine atoms reduces the number of van der Waal's interactions (induced dipoles), and, thus, the effective polarisability (Byron et al 1994). However, this explanation has been postulated from vapour phase data and does not account for the liquid solubility. Indeed, it is true that larger molecules (an increase in atomic number and size i.e. the change from fluorine to chlorine) do exhibit greater polarisabilties. Conventional surfactants by their nature are highly oxygenated polymeric compounds and oxygen itself being electronegative would result in electron cloud-cloud repulsion. The non-polar CFC11 with its high polarisability volume, small molecular size, less polar nature and lower electronegativity would enhance its approach and interaction with surfactants.

The affinity for water is also greater for the HFA's than the CFC's, likely due to hydrogen bonding, which exists because of the aforementioned electronegativity values, assisted by the anomalous covalent structure of water. Fluorine itself corroborates this observation this producing hydrated fluoride derivatives whereas other halides are anhydrous.

Intrinsic Property	CFC 11	CFC 12	CFC 114	HFA 134(a)	HFA 227ea
Boiling Point (°C)	24	-30	4	-26	-16
Vapour Pressure (kPa)	89	566	182	572	390
Density (Kg cm^{-3})	1490	1330	1470	1230	1420
Viscosity (Pa s^{-1})	430	200	300	210	270
Surface tension (Nm^{-2})	0.018	0.009	0.011	0.021	0.027
Enthalpy (kJ mol^{-1})	25.1	17.2	22.1	18.6	19.6
Dielectric constant (J^{-1} C^{-1} m^{-1})	2.3	2.1	2.2	9.5	4.1
Dipole moment (D) (1D = Cm^{-1})	0.24	0.51	0.58	2.1	1.2
Induced Polarisation (m^{-3} mol^{-2} x 10^5)	2.8	2.3	3.2	6.1	6.1
Solubility Parameter (Hilderbrand units)	7.5	6.1	6.4	6.6	6.2
Kauri-Butanol Value	60	18	12	9	13
Log P (oct / water)	2.0	2.2	2.8	1.1	2.1
Water solubility (ppm)	130	120	110	2200	610
Polarisability Volume (10^{-24} cm^{-3} molecule vapour)	9.5	7.9	8.5	5.4	5.8

Table A 3.1(a): Physicochemical properties of pMDI media

The fact that the solubility of conventional surfactants is reduced within the new propellants is not the whole story. Induced polarization, increased dielectric constants and dipole moments refute poor solvent power and indicate improved solvent characteristics. Thus various respiratory medicaments are, to some degree, soluble in HFA's, which has necessitated the total solubilisation of medicaments with use of a co-solvent, usually ethanol, to obviate Oswald ripening.

Dissolution and hence the disruption of long-range electrostatic interactions resulting from coulombic charges between ions, is decreased in a solvent or solvent system as the effective field strength is reduced. (Chemical potential therefore and resultant energy is favoured by interaction of ionic atmospheres). Solvents with high relative permittivity values (Dielectric constants) perform this function well (Genzer and Kolafa 2003). For example, in aqueous systems coulombic fields are reduced by nearly 2 orders of

magnitude (water has a high dielectric constant). And, in conjunction, the presence of the "ionic atmosphere" of an ion tends to "shield" it further reducing the electrostatic potential, as the coulombic interaction falls off as the distance from the nucleus according to:

$$\frac{1}{r} \longrightarrow \left(\frac{1}{r}\right)\exp\left(\frac{-r}{r_D}\right)$$

Equation A 3.1(a)

Where, r is the distance and r_D the shielding or Debye length

.The Debye-Huckel theory allows calculation of the shielding length for dilute aqueous electrolytes utilising the dielectric constant. This is given the following expression.

$$r = \sqrt{\left(\frac{\varepsilon RT}{2\rho L^2 e^2 I}\right)}$$

Equation A 3.1 (b)

Where, r is the shielding radius (nm), R is the universal gas constant, T temperature, L is Avogadro's constant, ρ is the density of the medium, e is the charge on a proton, and I the Ionic strength. To illustrate the "effective strength" of the propellants and the necessity for the requirement of a co-solvent, the shielding length was calculated for the salbutamol salts in CFC 11, HFA 134(a) and ethanol respectively, assuming the ions were spherical points. And the approach of the relationship between dilute aqueous solutions and and organic systems were equivalent. The results for individual salts are tabulated in table A 3.1(b)

	Shielding length CFC 11 / nm	Shielding length HFA 134(a) / nm	Shielding length Ethanol /nm
Salbutamol Maleate	5.40×10^{-10}	1.14×10^{-9}	2.14×10^{-9}
Salbutamol Oleate	4.40×10^{-10}	9.29×10^{-10}	1.75×10^{-9}

Table A3.1(b) Shielding lengths (r_D / m) of various propellant/co-solvent components used in pMDI formulations.

The calculated Debye lengths are in general agreement with practical observations. The effects of ion concentration and permittivity are illustrated: as the concentration of ions are increased, the Debye length is decreased from increased shielding, and when the relative permittivity is high, the ionic atmospheres are diffuse and the central nuclear charge effect suffers from a reduction in strength. HFA 134(a) therefore, from these crude calculations, is approximately 2.1 times more effective at shielding than the CFC 11 for each salt at their therapeutic concentration; and, the co-solvent is approximately 3.98 times as effective as shielding as the CFC11 but only 1.88 times as 134(a)

Formulation EtOH / %w/w	Storage condition	Timepoint	Observation
10/12.5	25 °C	initial	clear some dust fibres
10/12.5	25°C	3 days	clear some dust fibres
10/12.5	25°C	10 days	large crystals 0.2-0.5mm
15/20/30	25°C	Initial 10 days	clear some dust fibres
15/20/30	-23.5°C	14 days	clear some dust fibres
15/20/30	-23.5°C	56 days	clear some dust fibres

Table A 3.1(c) The visual Solubility of Salbutamol Maleate in Ethanol / HFA 134(a) (active concentration approx. 0.25% w/w RMM 355.38)

Formulation EtOH / %w/w	Storage condition	Timepoint	Observation
10/12.5	25°C	initial	clear some dust fibres
10/12.5	25°C	3 days	clear some dust fibres
10/12.5	25°C	10 days	No crystals. A ring of oleate formed at the liquid vapour interface
15 / 20	25°C	Initial 10 days	No crystals. A ring of oleate formed at the liquid vapour interface
30	25°C	Initial 10 days	clear some dust fibres
30	-23.5°C	14days	clear some dust fibres
30	-23.5°C	56 days	clear some dust fibres

Table A 3.1(d) The visual Solubility of Salbutamol Oleate in Ethanol / HFA 134(a) (active concentration approx. 0.37% w/w RMM 521.78)

Formulation EtOH / %w/w	Water / ppm	Timepoint	Observation
15	5000	Initial	Clear
		8wks @-23.5ºC	Crystals / uniform 2PS
15	50000	Initial	2 PS
		8wks @-23.5ºC	2PS
20	5000	Initial	Clear
		8wks @-23.5ºC	clear
20	25000	Initial	Clear
		8wks @-23.5ºC	2PS clears on warming
20	50000	Initial	2 PS
		8wks @-23.5ºC	2PS
30	5000	Initial	Clear
		8wks @-23.5ºC	Clear
30	25000	Initial	Clear
		8wks @-23.5ºC	Clear
30	50000	Initial	Clear
		8wks @-23.5ºC	Clear

Table A 3.1(e) The visual Solubility of Salbutamol Maleate in Ethanol / HFA 134(a) / Water systems (active concentration approx. 0.25% w/w RMM 355.38)

Tables 3.1(c-e) inclusive illustrate the visual observations that relate formulation composition to solution stability.

APPENDICES FOR CHAPTER 4

A4.1 Equations predicting particle size and volumetric flow rate

A 4.1 (a) Particle size

$$Dm = 6do(\mathrm{Re})^{0.15} \qquad \textit{Equation A4.0}$$

(Panasenkov 1951).

Where, D_m is the Median diameter, d_o is the spray orifice diameter, R_e is the Reynolds number.

A 4.1 (b) Volumetric Flow rate

$$U = \frac{Q}{a} \qquad \textit{Equation A 4.1}$$

Where, Q is the Volumetric flow rate, a is the cross sectional area of the spray orifice.

A 4.1(c) Volumetric flow through a restriction

$$Q = C_d a_d \left[2\frac{\Delta P}{\rho}\left(1 - \frac{a_o}{a_1}\right)\right]^{0.5} \qquad \textit{Equation A 4.2}$$

Where, C_d is the drag coefficient, a_d, is the area of the orifice, ΔP is the pressure gradient, ρ is the density of liquid, a_o the orifice cross sectional area a_1 is the inlet cross sectional area.

A 4.2 The effect Formulation variables on aerosol delivery

A 4.2 (a) Metering volume

There are several metering valve variants. Variations occur not only with the method of valve chamber filling, but also in valve componentry and geometry. The volume of the metering chamber nominally extends from 25-100µl, and contains a representative amount of suspended or solubilised drug. Problems occur with valves and formulations as they can loose drug from the reservoir (commonly known as loosing its prime). If this occurs, drug variation in subsequent doses, and a smaller dose may be delivered. This property is valve and formulation dependent, but has been attributed to the viscosity of formulations leaking from metering chamber-filling orifices. Alternative valve designs are available, but, again, each has its limitations. (Schultz et al 1994) Various elastomers and resins inherent in metering valves can interfere with suspension formulations by nature of drug-surface-valve component interactions. In addition, the volume of the metering valve has been shown to influence on deposition pattern, presumably due to mass and heat diffusion parameters changing. (Newman et al 1982 and Moren 1978).

A 4.2(b) Study specific variables

A 50µl inverted use metering valve (Bespak Kings Lynn) 20mm diameter of the capillary action type was used in this study, as this is a generally available commercially. The ferrule, core, spring, body, metering chamber seats and gaskets are standard HFA ethanol compatible materials.

A 4.2 (c) Vapour pressure

Propellant system vapour pressure has been shown to be arguably one of the most important factors in aerosol dynamics. (Polli et al 1969, Harnor et al 1993 Clark 1996). First principles of thermodynamics help us understand the rationale, as the molar Gibbs free energy (the chemical potential) increases with pressure and can be expressed by equation A 4.2

$$\mu(p) = \mu^{\phi} + RT\ln\left(\frac{f}{p}\right) \qquad \textbf{Equation A 4.3}$$

Where $\mu(p)$ is the chemical potential at pressure p, μ^{ϕ} is the standard chemical potential, R is the universal gas constant, T is the temperature, and f the fugacity.

(NB: Fugacity, the equivalent of "activity" for a component in a mixture of gases. It has the same physical meaning as the activity for a component in a solution)

In suspension systems the lowest particle size is limited by the size of individual or particle agglomerate, therefore, in theory there should be more "flexibility" in solution systems with respect to particle size manipulation. It has been shown that increasing the vapour pressure (274 to 502Kpa) of formulations containing Teflon spheres significantly increased the whole lung deposition, and reduced that of the extrathoracic region. (Newman et al 1982) It is hypothesised that the delivery of polydisperse or monodisperse aerosols may be achievable by careful control of formulation and hardware.

A 4.2 (d) Study specific variables

Vapour pressures utilised in this study varied according to temperature, and were measured experimentally using placebo formulations, crimped with a continuous spray valve tested with a pressure gauge (Pamasol Switzerland). Pressures ranged from approximately 1-7 bar dependent on formulation and temperature.

A 4.2 (e) Temperature

The easiest way to manipulate vapour pressure,aerosol dynamics and drug delivery is by temperature control. Particle size distributions from pMDI's are routinely measured at ambient temperature (unless under research conditions), and are rarely taken to extremes of temperature for investigation: at freezing point, and at the upper end body temperature were the vapour pressure of 134(a) is in excess of 10 bar. It is known that mixtures of ethanol and HFA's strongly deviate from Raoult's law as higher equilibrium pressures are experienced (Tzou 1998). This may, ultimately, be to the advantage as a change in temperature may allow optimal delivery with a particular formulation blend. It was an objective of this chapter to investigate temperature extremes for blends of novel salt derivatives.

A 4.2 (f) *Study specific variables*

In this study formulations were stored at three temperatures: -23.5, 4 and 37oC. Temperatures of 4 and 37oC were chose, as these are important for stability (4°C), and also emulate physiological temperature (37°C). The ultra low temperature was chosen, as this was an extreme of temperature and very close to the boiling point of HFA 134(a) where maximum instability may occur. Results from this temperature have not been documented as the majority of the aerosol cloud was deposited on the throat of the apparatus, and data did not approximate to log normal distributions. Previous low temperature studies have been performed on HFA suspension systems, (Stein and Stefely 2003) presumably utilising Airomir. A value of approximately 60% fine particle fraction was evaluated experimentally after equilibration at –20°C.

A 4.2 (g) *Co-solvent level*

The addition of co-solvents is necessary to aid dissolution of the drug. The first regulatory approved suspension and solution systems (3M Pharmaceuticals) contained ethanol at varying levels. Recently Smyth and Hickey (Smyth and Hickey 2003) and Gupta (Gupta et al 2003) investigated the effect of co-solvent in order to assess solubility effects, and also resulting particle size distributions, based of model drug alternatives and beclomethasone respectively. Smyth and Hickey concluded that drug solubility may be improved with addition of ethanol, and, due to the deviation from ideality of the mixtures utilised, formulations of up to 20% w/w ethanol were practically useful. In the former study, the concentrations of active in the formulations was at 0.01% w/w, and illustrated an increase in MMAD and GSD with increasing ethanol and a decrease in fine particle fraction. There was no correlation between device and throat deposition. Gupta et al, however, noted that MMAD increased significantly with active concentration, but did not with increasing ethanol level. They also indicated an increase in throat deposition of 125% when ethanol levels were increased by 15%, and a decrease in respirable fraction from about 50 to 25% when the ethanol level was increased from 5 to 20%, indicating that the efficiency of solution pMDI's decreases with increased ethanol concentration. They also generated a variable, which they termed the "maximum respirable mass" (MRM). This is a product of drug solubility and delivered dose and is obviously is drug, formulation and actuator dependent.

A 4.2 (h) *Study specific variables*

Co-solvent levels were varied according to initial stability studies. Values ranged fro 15-30% w/w respectively.

A 4.2 (i) *Non-volatile additives: actives and excipients*

As previously intimated, the addition of low volatility additives affects the spray and resultant cloud distribution. As the drug mass is fixed in the formulation due to constraints of clinical dosage and physicochemical properties then the only alternative available to change particle size distribution is the use of physiologically acceptable excipients. Brambilla (Brambilla et al 1999) found, that, addition of glycerol to solution formulations containing steroids and anticholinergics increased the MMAD. Addition of such excipients will affect several parameters relating to liquid ligament deformation and droplet formation: surface tension of the ligaments will change, the molar volume of the liquid will increase, which from the Kelvin equation will endeavour to reduce the pressure of the droplet, and the resulting vapourisation rate will decrease. As a multi-component system, the mass and heat diffusion rates will also change. Convective droplet vapourisation, interaction with gas flows, and alterations of particle drag will combine to affect primary and secondary atomisation.

A 4.2 (j) *Study specific variables*

Drug loading varied according to a therapeutic equivalent to the free base, where 1.00 was equivalent to 100µg of freebase, calculated from the relative molecular masses of the maleate salt and oleate respectively. The equivalents are calculated and presented in table 4.0:

Compound	Relative Mol Mass	Therapeutic Equivalent	Drug loading %w/w Based on 10g fill wt
Salbutamol Base	239.31	1.00	0.175
Salbutamol Maleate	355.38	1.485	0.259
Salbutamol Oleate	521.78	2.180	0.382

Table A 4.2 The relative drug loading values for salbutamol salts equivalent to 100 microgram's freebase.

A 4.2 (k) *Actuator design*

The actuator design is integral to the development of the aerosol cloud. It is debatable, but the actuator orifice, sump and valve stem arrangement are deemed to be some the most important factors. Airflow through the actuator, the design of the mouthpiece, and mouthpiece extensions are also important as they emulate spacer devices. It is theorised that these reduce orophayrngeal deposition by allowing evaporation and deceleration of larger droplets to occur. (Byron 1990). The spray orifice diameter has been shown to influence the MMAD as smaller diameters produce smaller particles and finer sprays (Clark 1992); and droplet diameters have been derived empirically and been shown to vary proportionally to the orifice diameter. Empirical equations relating MMD based on spray orifice diameter and liquid flow rate are illustrated in appendices 4.1 - 4.3 respectively. Effectively the volumetric flow rate and hence the liquid velocity relative to the gas decreases. This will reduce the critical value of the Weber number and, so, ligament break up and droplet formation occurs quicker forming smaller droplets.

A 4.2 (l) *In-vitro Vs In-vivo correlations*

It is well known that particle deposition in the lung is dependent upon aerodynamic particle size, (Task Group in the lung 1966), and the parameters of MMAD and fine particle fraction do not totally correlate from *in-vitro* to *in-vivo* clinical efficacy. However, at present, in vitro testing materials are not ideal, and the differences are thought to stem from the use of unrealistic metallic throats. Improvements have been suggested by the use of anatomic throats from replica casts. (Olsson et at 1996) In fact replica lung casts are routinely used in research. (Martonen 1983). In this study, standard pharmacopeial aerosol testing techniques have been used with slight modifications where indicated.

APPENDICES FOR CHAPTER 5

A 5.1 Particle growth ratios for a selection of inhaled medicaments

Drug aerosol	Particle growth Ratio	Relative Humidity (%) (reference)
Albuterol	1.08	90 (Kim et al 1985)
Beclomethasone dipropionate	1.33	98 (Hiller et al 1980)
Cromolyn Sodium	1.31	98 (Smith et al 1980)
Epinephrine	1.11	90 (Kim et al 1985)
Isoetharine Phenylephedrine	1.10	90 (Kim et al 1985)
Isoproterenol Phenyephedrine	1.24	90 (Kim et al 1985)
Isoetharine sulphate	1.13	98 (Hiller et al 1980)
Metaproterenol	1.10	90 (Kim et al 1985)
Metaproterenol sulphate	1.29	98 (Hiller et al 1980)
Triamcinalone Acetonide	1.17	90 (Kim et al 1985)

Table A 5.0: Particle growth ratios of several medicinal aerosol formulations.

A 5.2 Particle size distribution changes via the use of both hydrophobic and hydrophilic drug derivatives

The particle size analysis of hydrophilic and hydrophobic aerosols has been has been of interest for several years. Atmospheric physicists and aerosol hygienists were probably the first groups to recognize the effects of hygroscopicity on atmospheric pollutants, and the incidences of respiratory disease in industrial urban areas. (Milburn et al 1957). Ferron, has thoroughly modelled the effects of deposition on salt particles; and, Martonen has extensively investigated the effects of hygroscopicity on pharmaceutical aerosols. (It should be noted several other authors have also extensively investigated such effects) On studies of aqueous based saline and isoproterenol hydrochloride solutions (some containing glycerin) in the upper respiratory tract, Bell and Ho studied the effects of dry monodisperse aerosols under different conditions of temperature and humidity and flow turbulence: investigation of effect of the Reynolds number. Experimental data indicated that isopreterenol solutions containing glycerin "grew" at a slower rate than both saline and isopreterenol alone. The growth rate also increased when the Reynolds number. Particle growth diameters and particle growth ratios, of solutions described at different Reynolds numbers are given in table A 5.1

Isopreternol hydrochloride (Conc %)	Excipient	Particle Growth Diameter	R.H (%)	Particle Growth ratio	Reynolds Number
1.0	NA	0.010	93	1.15	1100-1200
1.0	NA	0.045	92	1.65	1100-1200
1.0	NA	0.250	93	2.15	1100-1200
0.5	Glycerol	0.02	93	1.10	1100-1200
0.5	Glycerol	0.120	95	1.40	1100-1200
0.5	Glycerol	0.225	94	1.60	1100-1200
1.0	NA	0.010	93	1.40	2100-3200
1.0	NA	0.150	93	2.45	2100-3200
1.0	NA	0.315	93	2.80	2100-3200
0.5	Glycerol	0.07	93	1.60	2100-3200
0.5	Glycerol	0.21	93	2.05	2100-3200
0.5	Glycerol	0.37	95	2.20	2100-3200

Table A 5.1: The effect of relative humidity on particle growth diameter of aqueous based aerosolised isopreterenol solutions

The mechanism for the retardation of growth proposed centred on the fact that the glycerol hydrogen bonded to the water molecules at the surface of the droplet, and, so, environmental water molecules diffused more slowly across the interfacial boundary into

the core. This theory has been also suggested by (Otanyi and Wang 1984) whereby they studied saline droplets with the addition of cetyl alcohol. Polydisperse aerosols were preconditioned in a controlled environment and passed into an elutriator for analysis. Growth rate of saline droplets was retarded by up to 99.5% resulting from a covering with a monolayer of surfactant.

Another study focused on fatty acid additives with dry powder formulations. A solid formulation, produced by solvent evaporation revealed post chemical analysis a surfactant matrix effect rather than surface-active effect (Hickey et al 1990). Aerosol experiments indicated a reduction in growth ratio for increasing fatty acid content. It was concluded that by varying the residence time of the aerosol in the system the growth rate kinetics could be possibly monitored. Corresponding in-vivo studies, using disodium fluorescein with varying amounts of capric acid coating, in beagle dogs, indicated enhanced uptake (Clark and Byron 1985). Two probable hypotheses resulted from the study: either the coating enhances particle uptake or since the coating resists moisture adsorption the particles deposited deeper in the lung .

Glycerol when formulated in solution based metered dose inhalers and tested at ambient conditions has been shown to increase the MMAD, primarily due to aerosol kinetics. The effect of humidity on aqueous glycerol aerosols has however been investigated. (Davis and Bubb 1978 and Lin and Cox 2003).

The effects of low and high humidity on metered dose bronchodilator solution and suspension aerosols was investigated by Hiller et al (Hiller et al 1980). Data indicated, (generated from a 30s holding time), that that both the number of particles in the measured range and the aerodynamic dose increased for both dosage forms, however the shift for the solution aerosols was greater indicating that the particles had increased instability presumably resulting from a high amorphous content, as compared to crystalline delivered medicaments.

References

Andersen Samplers Inc. (1979). Operating manual for Andersen Samplers inc.1 ACFM Ambient particle Sizing Samplers, Atlanta, Georgia, USA.

Apel, P., S., Rabin, J., R., Trickey, S., B., and Oddershede, J. (2002). Shape-Dependent Molecular Polarisabilities. *Int J. Quantum Chemistry.* 86: 35-39

Ariens, E. (1990).. Stereoselectivity in pharmacodynamics and pharmacokinetics. *Schweiz. Med. Wochenschr.* 120; **5**:131-134.

Asmus, M., J., and Hendeles, L. (2000). Levalbuterol nebulizer solution: is it worth five times the cost of albuterol? *Pharmacotherapy.* Feb 20; **2**: 123-129.

Atkins, P., J. (1991). The development of new solution metered dose inhaler delivery systems. In: *Proceedings of the Second Annual Respiratory Drug delivery Symposium.* Dalby, R., N., and Evans, R. (Eds). Continuing Pharmacy Education. University of Kentucky, Lexington. 416-445.

Atkins, P., W. (1982). Physical Chemistry, Second Edition. Oxford University Press.

Auerbach, I., Springer C., and Godfrey, S. (1993). Total population survey of the frequency and severity of asthma in 17 year old boys in an urban area of Israel. *Thorax.* **48**: 139-141.

Basbaum, C., B., and Finkbeiner N., E. (1989). In: Lung Cell Biology. Masaro, E. (Ed). Marcel Dekker, New York. 37-39.

Beale, J.,P., and Stephenson, N.,C. (1972). X-ray analysis of Th 1165a and salbutamol. *J.Pharm. Pharmacol.* 24; **4**: 277-280.

Beasley, R., Pearce N., and Crane, J. (1997). International trends in asthma mortality. *Ciba Found Symp.* **206**: 140-150.

Bell K., A., and Ho A., J. (1981). Growth rate measurements of hygroscopic aerosols under conditions simulating the respiratory tract. *J. Aerosol Sci.* **12**: 247-254.

Boyden, E,A. (1971). The structure of the pulmonary acinus in a child of 6 years and 8 months. *Am. Jour. Anat.* **132** : 275-299.

Brambilla, G., Ganderton, D., Garzia R., Lewis, D., Meakin B., and Ventura, P. (1999). Modulation of aerosol clouds produced by inhalation aerosols. *Int. J. Pharm.* **186**: 53-61.

Brown, A., B., York P., Sheilds, L., Doherty, C., and Frampton, C. (1994). Structural characterisation of a series of novel salbutamol salts. *Pharm Res.* Vol 11 (10); **S151**: PT 6084.

Brown, A., B., York, P., and Doherty, C. (1994). Solubility and dissolution properties of a series of novel salbutamol salts. *Pharm Res.* Vol 11 (10); **S151**: PT 6083.

Byron, P., R. (1990). Aerosol formulation, generation and delivery using metered systems. In: Byron P., R. (Ed.) Respiratory Drug delivery. Boca Raton, Fl, CRC Press: 167-206.

Byron, P., R. (1994) Dosing reproducibility from experimental albuterol suspension metered dose inhalers. *Pharm Res.* **11**: 580-584.

Byron, P.R., Miller, N.C., Blondino, F.E., Visisch, J.E., Ward, G.H. (1994) Some aspects of alternative propellant solvency. In: Byron P.R., Dalby. R.N., Farr S.,J. (Eds). Respiratory Drug Delivery IV. Interpharm Press, Buffalo Grove, IL .231-242.

Campbell, A.B., and Soyka, L.F., (1976). Selective beta 2-receptor agonists for the treatment of asthma-therapeutic breakthrough or advertising ploy? A commentary. *J.Paedr.* 89; **6**:1020-1026.

Campbell, M., J., Cogman, G., R., Johnston, S., L., and Holgate S., T. (1997). Age specific trends in asthma mortality in England and Wales 1983-1995: Results of an observational study. *Br. Med. J.* **314**: 1439-1441.

Clark, A., R. (1992). The physics of aerosol formation by MDI's-limitations of the current approach. *J. Biopharm. Sci.* **3**: 69-76.

Clark, A., R. (1996) MDI's : The physics of Aerosol Formation. *J.Aer Med.* 9; **1**: S19-S26.

Clark, A., R. and Byron, P., R. (1985). Drug absorpbtion from inhalation aerosols administered by positive pressure ventiliation. II. Effect of disodium fluorescein aerosol particle size on fluorescein absorption kinetics in the beagle dog respiratory tract. *J. Pharm.Sci.* **74** : 939-942.

Clay, M., M., Pavia, D., and Clarke, S., W. (1986). Effect of aerosol particle size on bronchodilation with nebulised terbutaline in asthmatic subjects *Thorax.* 41; **5**: 364-368.

Clay, M., Pavia D., Newman, S., P., and Clarke S., W. (1983). Factors influencing the size distribution of aerosols from jet nebulisers. *Thorax.* **38**: 755-759.

Cocks, A., T., and Fernando R., P. (1982). The growth of sulphate aerosols in the human airways. *J.Aerosol Sci.* **13**: 9-19.

Corrigan, O., I. (1997). Salt forms: Pharamceutical aspects. In: Swarbrick, J., and Boylan, J., C. (Eds.) Encyclopedia of pharmaceutical technology 2nd edition, Marcel Dekker Inc, USA.

Crompton, G., K. (1982). Problems patients Have Using Pressurised Aerosol Inhalers. *Eur. J. Respir. Dis.* 63; **suppl 119**: 1-4.

Cyr, T., D., Duhaime, R., M., Graham, S., J., Ormsby E., D., Lawrence, R., C., and La Belle, M., J. (1997). Metered Dose Inhalers. Part 3. Metaproterenol Sulphate: Particle size distribution and dose uniformity. *L. Pharm. Biomed. Anal.* **15**:1709-1718.

D'Alzono, G., E., Nathan, R., A., Henochowicz, S., Morris, R.,J., Ratner, P., and Renard S.,I. (1994). Salmeterol Xinafoate as maintenance therapy compared with albuterol patients. *JAMA* .**271**: 1412-1416.

Dalby, R. (1992). Special considerations in the formulation of suspension type metered dose inhalers. *Aerosol Age.* **October**: 22-89.

Dalby, R., N., Byron, P., R., Shepherd, H., R., Papadopoulous, (1990). CFC Propellant Susbstitution: p 134(a) as a potential replacement for p 12 in MDI's *Pharm. Tech.* 14; (26,28,30,32,33).

Dalby, R., N., Phillips, E., M., and Byron, P., R. (1991). Determination of Drug Solubility in Aerosol Propellants. *Pharm. Res.* 8; **9**: 1206-1209.

Davies, D., S. (1975). Pharmacokinetics of inhaled substances. *Postgrad. Med. J.* 51; **suppl 7**: 69-75.

Davis, S., S., and Bubb, M., D. (1978). Physico-chemical studies on aerosol solutions for drug delivery III. The effect of relative humidity on the particle size of inhalation aerosols. *Int. J. Pharm.* **1**: 303-314.

Dhand, R., Malik, S., K., balakrishnana, M., and Verma, S., R. (1988). High speed Photographic analysis of aerosols produced by metered dose inhalers. *J.Pharm. Pharmacol.* 40; **6**: 429-430.

Dunbar, C., A., Watkins, A., P, and Miller, J., F. (1997). Theoretical investigation of the spray formed from a pressurised metered dose inhaler. *Atomisation sprays* **7**: 417-436.

Dunnill, M.S., Masserella, G.R., and Anderson, J.A. (1969). A comparison of the quantitative anatomy in normal subjects, status asthmaticus, in chronic bronchitis and emphysema. *Thorax.* **24**: 176-179.

Efunda Website. Engineering Fundamentals: Properties of ethanol. www.efunda.com.

Eisner, A., D., Graham, R., and Martonen, T., B. (1990). Coupled mass and energy transport phenomena in aerosol/vapour-laden gases. I. *J.Aer. Sci.* **21**:883.

Elktob, M., M. (1982). Fuel atomisation for spray modelling. *Prog. Enegy. Combust. Sci.* 8; **1**: 61-91.

Evans M.,J., Shami S.,G., Wilson B., and Plopper C.,G. (1989). The role of basal cells in the attachment of columnar cells to the basal lamina of the trachea. *Am. J. Respir. Cell. Mole. Biol.* **1**: 463-469.

Evans, M., J., Shami S.,G., Cabral – Anderson L., J., and Dekker, N., P. (1986). Role of non ciliated cells in the renewal of the bronchial epithelium of rats exposed to NO_2. *Am. J. Pathol.* **123**: 126-133.

Fair, J., R., Steinmeyer, D., E., Penney, W., R., and Crocker B., B. (1984). Liquid gas systems. In: Green D., W. (Ed). *Perry's Chemical Engineering Handbook,* 6th ed, Mc Graw-Hill, New York: 18.4-18.57.

Ferrayoli, C., G., Palcio, M., A., Bresina, M., F., Palacios, S., M. (2000). Resolution of Racemic Albuterol via Diastereomeric Salts Formation with Di-*p*-toluoyl–D-Tartaric acid. *Enantiomer.* **5**: 289-291.

Ferron G., A., Kreyling G., and Haider B. (1988). Inhalation of salt particles. II: growth and deposition in the human respiratory tract. *J.Aerosol Sci.* **19**: 611-631.

Ferron, G., A. (1977). The size of soluble aerosol particles as a function of the humidity of the air. Application to the human respiratory tract.*J. Aer. Sci.* **8:** 251-267.

Ferron, G., A., and Solderholm, S., C. (1992). Estimation of the times for evaporation of pure water droplets and for stabilisation of salt solution. *J.Aer. Sci.* **21**: 415

Ferron, G., A., Oberdorster, G., and Henneberg, R. (1989). Estimation of the deposition of aerosolised drugs in the human respiratory tract due to hygroscopic growth. *J.Aer. Med* . **2**: 271.

Ferron, G.,A., Karg E., and Peter, J., E. (1993). Estimation of polydisperse hygroscopic droplets in the human respiratory tract. *J.Aer. Sci.* **24**: 665.

Finlay, W., H., and Stapleton, K., W. (1999) Undersizing of droplets from a vented nebuliser caused by aerosol heating during transit through an Andersen impactor. *J.Aerosol.Sci.* **30**: 105-109.

Finnerty, J.P., and Holgate, S., T. (1989). Pathophysiology of Asthma. In: D'Arcy, P.F., McElnay, and J.C., (Eds). The pharmacy and Pharmacotherapy of Asthma. Ellis Horwood, UK..

Fishman, A.,P. (1985). Pulmonary circulation. In: Fishman A.,P., and Fisher A.,B. (Eds) Handbook of Physiology Section 3. The respiratory System Volume 1. Circulation and Non-respiratory functions, Bethesda, M.D .*American Physiological Society*: 93-165.

Ganderton D., and Kassem N., M. Dry Powder Inhalers (1992). Adv in dry powder inhalers. *Adv. Pharm. Sci.* **6**: 195-191.

Ganderton, D. (1992). The generation of respirable cloud from course powder aggregates *J. Biopharm. Sci.* **3**: 101-105.

Genzer, J., and Kolafa J. (2004) Molecular dynamics of potential models with polarisability: comparison of methods. *J. Mol. Liq.* **109**: 63-72.

George C.F. (1981). Drug metabolism by the gastrointestinal mucosa. *Clin Pharmacokin.* **6**:259-274.

Giffen, E., and Lamb, T., A., J. (1953). The effect of air density on spray atomisation. *Motor industry Research Association report,* 1953/5.

Gonda, I. (1988). Therapeutic Aerosols. In: Aulton, M., E. (Ed). Pharmaceutics: The science of dosage form and design. Churchill Livingston, Edinburgh, London, Melbourne and New York.

Greening, A., P., Ind, P., W., Northfield, M., and Shaw, G. (1994). Added Salmeterol versus higher- dose corticosteroid in asthma patients with symptoms on existing inhaled corticosteroid. *Lancet.* **344**: 219-224.

Griffiths, W., D., Mark D., Marshall, I., A., and Nichols, A., L. (1998). Aerosol particle size-calibration procedures In: Griffiths, W., D., Mark D., Marshall, I., A., and Nichols, A., L. (Eds). Aerosol Particle Size Analysis, good calibration Practices. Published by the RSC for AEA technology. Bookcraft Bath.

Groom, C., V. (1981). The characterisation of inhalation aerosols. PhD thesis. University of Aston, Birmingham UK.

Grover, R.,F., Wagner, W.,W., McMurty, I., and Reeves, J.,T. (1984). Pulmonary circulation. In: Shepherd J.,T, Abboud F.,M, (Eds). Handbook of Physiology Section 2. The cardiovascular System Vol III. Peripheral circulation and Organ Flow. American Physiological Society. Bethesda, MD. 103-116.

Gupta, A., Stein, S., W., and Myrdal, P., B. (2003). Balancing Ethanol Co-solvent Concentration with Product Performance in 134(a) Based Pressurised Metered Dose inhalers. *J.Aer.Med.* 16; **2**:167-174.

Haenel, G., and Zankl, B. (1979). Aerosol size and relative humidity: Water uptake by a mixture of salts. *Tellus.* **31**: 73-187.

Haenlein. A. (1932). Disintegration of a liquid jet. *NACA TN 659.*

Halbert, M., K., Mazumder, M., K., and Bond, R., L. (1982). Inhalation simulation and the effects of lung environmental conditions on consumer aerosol products and NaCl aerosol. *Environ. Res.* **29**: 263-271.

Handbook of chemistry and physics. 85th Edition, CRC press, LLC.

Harmon, D., B. (1955). *J. Franklin. Inst.* **259**: 519.

Harnor, K., J., Perkins A., C., Wastie, M., Wilson, C., G., Sims, E., E., Feely L., C., and Farr, S., J. (1993) Effect of vapour pressure on the deposition pattern from solution phase metered dose inhalers. *Int. J. Pharm.* **95**: 111-116.

Hawkins, C., J., and Klease, G., T. (1973) relative potency of (-) and (±) salbutamol Guinea Pig Tracheal tissue. *J. Med . Chem.* 16; **7**: 856-857.

Hickey, A., J. (1988). Practical aspects of aerosol characterisation in an environment of controlled temperature and relative humidity. *Drug Dev. Ind. Pharm.* **14 (2&3):** 337-352.

Hickey, A., J., and Jones, L., D. (2000). Particle size analysis of pharmaceutical aerosols. *Pharm. Tech.* **24**: 48-58

Hickey, A., J., and Martonen T., B. (1993). Behaviour of hygroscopic pharmaceutical aerosols and influence of hydrophobic additives. *Pharm.Res.* **10**:1-7.

Hickey, A., J., Concessio, N., M., Van, N., M., and Platz, R., M. (1994). Factors influencing the dispersion of dry powders as aerosols. *Pharm. Technol.* 18; **8**: 58-82.

Hickey, A., J., Gonda, I., Irwin, W., J., and Fildes, F., J., T. (1990). Effect of Hydrophobic coating on the Behaviour of a Hygroscopi aerosol Powder in an Environment of Controlled Temperature and Relative Humidity. *J.Pharm.Sci* 79; **11**:1009-1014.

Hicks, J., F., and Megaw W., J. (1985). The growth of ambient aerosols in the conditions of the human respiratory system. *J.Aerosol Sci.* 16; **6**: 521-527.

Hiller F, C., Mazumder, M., K., Wilson, J., D., and Bone, R., C. (1980). Aerodynamic size distribution, hygroscopicity and deposition estimates of beclomethasone dipropionate aerosol. *J. Pharm. Pharmacol.* **32**:605-609.

Hiller, F., C., Mazumder, M., K., Wilson, J., D., and Bone, R., C. (1980). Effect of low and high relative humidity on metered dose bronchodilator solution and suspension aerosols. *J. Pharm.Sci.* **69** : 334-337.

Hinze J., O. (1972). 'Turbulent and fluid particle interaction'. *Prog. Heat Mass Transfer.* **6**: 433-452.

Holgate, S. T. (1999) The inflammation-repair cycle in asthma: the pivotal role of the airway epithelium. Ch 2 In: Holgate S.,T., Boushey H., A., and Fabbri L., M. (Eds). Difficult Asthma. Martin Dunitz. London, England.

Holgate, S.T. (2003). *Plenary lecture, Proc. Drug. Delivery. Lungs*, DDLXIII, Westminster, London, UK..

Horsfield, K., DartG, Olson, D.,E., Filley, G.,F., and Cumming, G. (1971). Models of the human bronchial tree. *J. Appl. Physiology.* **31**: 207-217.

Howlett, D., J. (1996). *Proc Drug Delivery to the Lungs VII.* Westminster, London UK. 105-109.

Jashnani, R., K., Dalby, R., N., and Byron, P., R. (1993). Preparation, characterisation and dissolution of two novel albuterol salts. *J. Pharm. Sci.* Jun 82; **(6)**: 613-616.

Jepperson, A.B., Johansson, U., and Waldeck, B. (1984). Steric aspects of agonism and antagonism at beta-adrenoceptors: experiments with the enantiomers of terbutaline and pindolol. *Acta. Pharma. Toxicol.* **54**: 285

June, D. (1997). Achieving the change: Challenges and successes in the formulation of CFC-free pMDI's. *Eur Respir. Rev.* **7**: 32-34.

Keller, M. (1999). Innovations and perspectives of metered dose inhalers in pulmonary drug delivery. *Int. J. Pharm.* 186: 81-90.

Kerem, E., Tibshirani, R., Canny, G., Benum L., Reisman, J., Schuh, S., Stein, R., and Levinson, H. (1990). Predicting the need for hospitalization in children with acute asthma. *Chest.* 98; **6**: 1355.

Kim, C., S., Trujillo, D., and Sackner M., A. (1985). Size aspects of metered-dose inhaler aerosols. *Am. Rev. Respir. Dis.* **132**: 137-142

Konig, P. (1988). Inhaled Corticosteroids- Their present and future role in the management of asthma. J. *Allergy, Clin. Immunol.* **82**: 297-306.

Lalor, C., B., and Hickey, A., J. (1998.). In: Colbeck . I. (Ed). Physicochemical Properties of Aerosols. Chapman and Hall. London, UK.

Lambert. M., W. (1955). Accessory bronchiole-alveolar communications. *J. Pathol Bacteriol.* 70: 311-314.

Landis, R., B., and Mills, A., F. (1974). 'Effects of International Diffusion and resistance on the vaopurisation of binary droplets. **Paper B 7.9**. Fifth International Heat Transfer Conference, Tokyo, Japan.

Lange, C., F., and Finlay, W., H. (2000). Overcoming the adverse effect of humidity in pressurised metered dose inhalers during mechanical ventilation. *Am. J. Respir. Crit. Care Med.* 161; 5: 1614-1618.

Leach, C. (1998). Improved delivery of inhaled steroids to the large and small airways. *Respir. Med.* 92; **suppl A**: 3- 8.

Leach, C., L., Davidson, P., and Boudreau, R. (1998). Improved targeting of the airways with CFC-free HFA beclomethasone metered dose inhaler compared with CFC-beclomethasone. *Respir. Med. 92 (Suppl A).*

Lefevbre, A., H. (1989). Atomisation of droplets and sprays. Combustion an international series. Hemisphere Publishing Company, U.S.

Lewis, D., A., Ganderton, D., Meakin, B., J., and Brambilla, G. (2004). Theory and practice with solution systems. *Proc Respiratory Drug Delivery IX.* River Grove, IL.

Lewis, D., Brambilla, D., Ganderton, D., Howlett, D., and Meakin, B. (2000). Through Can Life Variation In Delivered Dose From pMDIs. *Proc from Respiratory Drug Delivery VII.* Palm Harbor, FL.

Lin, J-C., and Cox, K. (2003). Hygroscopic growth and evaporation of propylene glycol aerosol in the human respiratory tract. *Proc.* Respiratory Drug Delivery Tucson Arizona.

Lynden-Bell, R., M. (2000) Studies of solvation in the atomistic simulation group at Queens University Belfast. (Web-search)

Mar, W., O., and Ulrich, J. (1999) Allpication of ultrasonics in the online determination of supersaturation. *Crys.Res Tech.* 34; **3**: 379-389.

Martin, H.,B. (1966). Respiratory bronchioles as the pathway for collateral ventilation. *J. Appl. Physiol.* **21**: 1443-1447.

Martindale Extra Pharmacopoeia (2002).

Martonen T., B. (1990). Development of surrogate lung systems with controlled thermodynamic environments to study hygroscopic particles: air pollutants and pharmacologic drugs. *Part. Sci. Tech.* **8**: 1-20.

Martonen T., B., Bell K., A., Phalen R., F., Wilson A., F., and Ho A. (1985). Growth rate measurements and deposition modelling of hygroscopic aerosols in human tracheobronchial models. *Ann. Occup. Hyg.* 26; **1-4**: 93-108.

Martonen T., B., Zhang Z., and Hwang D. (1994). Hygroscopic behaviour of secondary cigarette smoke in human nasal passages. *STP Pharm Sci.* **4**: 69.

Martonen, T., B. (1982). Analytical model of hygroscopic particle behaviour in the human airways. *Bull Math Biol.*44: 425-428

Martonen, T., B. (1983).. Measurement of particle dose distribution in a model of a human larynx and tracheobronchial tree. *J. Aerosol Sci.* **14**: 11-22.

Martonen, T., B. (1992). The behaviour of cigarette smoke in human airways. *Am Ind. Hyg .Assoc. J.* **53**: 6-15.

Martonen, T., B., and Katz, I. (1996). Thermodynamics of Inhaled Drugs Part I: Aerodynamic Behaviour. In: Hickey A., J. (Ed). Inhalation Aerosols. The Physical and Biological Basis for Therapy. Marcel Dekker, Inc. New York.

Martonen, T., B., and Yang, Y. (1996). Deposition Mechanics of Pharmaceutical particles in Human Airways. Part I: Aerodynamic Behaviour. In: Hickey A., J. (Ed). Inhalation Aerosols. The Physical and Biological Basis for Therapy. Marcel Dekker, Inc. New York.

Martonen, T., B., Menache, M., G., Hofman, W., Eisner, A., D. (1989). In: Crapo, J., D., Smolko, E., D., Miller, F., J., Graham, J., A., and Hayes, A., W. (Eds). Extrapolation Modelling of Inhaled particles and Gases. Lung Dosimetry. New York, Academic Press.

Martonen, T., B., Zhang, Z., and Lehmann, R. (1993). Fluid dynamics of the human larynx and upper tracheobronchial airways. *Aerosol Sci. Tech.* **19:** 133.

McFadden, E.,R., Jr. (1981). Beta 2 receptor agonist: metabolism and pharmacology. *J Allergy Clin Immunol.* **68**:91-7.

Menkes, H., A., and Macklem, P.,T. (1986). Mechanics of breathing. In: Fishman A.,P., Macklem P.,T., Mead J., Geiger S.,R., (Eds).Handbook of Physiology Section 3. The respiratory System Vol III. American Physiological Society. Bethesda, MD. 337-353.

Merck Index Ninth Ed. (1976). Merck and Co. Inc. Rahway, N.J., U.S.A

Meyrick, B., Sturgess, J., M., and Reid, L., M. (1969). A reconstruction of the duct system and secretory tubules of the human bronchial sub-mucosal glands. *Thorax.* **24**: 729-736.

Milburn, R., H., Crider, W., L., and Morton, S., D. (1957). The retention of hygroscopic dusts in the human lung. *Arch. Ind. Health.* **15**: 59-62.

Miller, N., C. (1990) The Effects of Water in Inhalation Aerosol Suspension Systems. In: Byron P., R. (Ed). *Respir. Drug. Del.* CRC Press. Boca Raton, FL. Appendix. 250-257.

Mitra, S., Ugur, S., Ugur, O., Goodman, H.,M., McCullogh, J.,R., and Yamaguchi H. (1998). (S)-Albuterol increases intracellular free calcium by muscarinic receptor activation and a phospholipase C-dependent mechanism in airway smooth muscle. *Mol. Pharmacol.* 53; **3**: 347-54.

Moren, F. (1978). Drug deposition of pressurised inhalation aerosols II. Influence of vapour pressure and metered volume. *Int J. Pharm.* **1**: 213-218.

Moren, F., and Andersson, J. (1980). Fraction of dose exhaled after administration of pressurized aerosols. *Int. J. Pharm.* **6**: 295-300.

Morris, K., R., Fakes, M., G., Thakur, A., B., Newman, A., W., Singh A., K., Venit J., J., Spagnuolo, A., T., and Serajuddion A., T., M. (1994). An integrated approach to the selection of optimal salt form for a new drug candidate. *Int. J. Pharm.* **105**: 209-217.

Morrow, P., E. (1980). Factors determining hygroscopic aerosol deposition in airways. Physiol Rev. **66**: 330-376.

Newacheck, P., W., Budetti, P., and Halfon, N. (1986). Trends in activity limiting conditions among children. *Am. J. Public. Health.* **76**: 178-184.

Newman S., P., Pavia D., Moren F., Sheanhan N., E., and Clarke S., W. (1981). Deposition of pressurised aerosols in the human respiratory tract. *Thorax* **36**: 52-55.

Newman, S., P., and Clarke, S., W. (1983). Therapeutic aerosols I. Physical and practical considerations. *Thorax.* **38**: 881-886.

Newman, S., P., Moren, F., Pavia, D., Corrado, O., and Clarke, S., W. (1982). The effects of changes in metered volume and propellant vapour pressure on the deposition of pressurised inhalation aerosols. *Int. J. Pharm.* **11**: 337-344.

Newman, S., P., Pavia D., Moren F., M., Shehan N., F., and Clark, S., W. (1981). Deposition of pressurized aerosols in the human respiratory tract. *Thorax.* **36**: 52-55.

Newman, S., P.,Pavia D., and Clarke, S.,W. (1980). Simple instructions for using pressurized aerosol bronchodilators. *J. Roy. Soc. Med.* **73**: 776-779.

Nowaseb, S. (1998). The effect of chirality on the fine particle fractions of DPI formulations of mandelic acid and lactose monohydrate mixtures. *Proc from Drug Delivery to the Lungs IX.* Westminster, London. 76-80.

O'Rourke, P., and Bracco, F., V. (1980). "Modelling drop interactions in thick sprays and a comparison with experiments", Stratified Charge Automotive Engines Conference. *The Inst Mech Eng.*

Olssson, B., Borgstrom, L., Asking, L., and Bondesson, E. (1996). Effect of inlet throat on the correlation between fine particle dose and lung deposition. *Proc. Respir Drug Delivery V.*Pheonix, AZ.

Otanyi, O., and Wang, C., S. (1984). Growth and deposition of aerosol droplets covered with a monolayer of surfactant. *Aerosol Sci. Tech.* **3**: 155-156.

Page, C., P., and Morley, J. (1999). Contrasting properties in albuterol stereoisomers. J Allergy Clin Immunol. Aug; **104 (2 Pt 2):** S31- 41.

Panasenkov N., J. (1951). *Zh. Tekh. Fiz.* **21**: 160.

Peitsch, W. (1991). In: Size Enlargement by Agglommeration. John Wiley, New York, NY.

Phillips, E., M., Byron, P., R., Fults, K., and Hickey, A., J. (1990). Optimised Inhalation Aerosols. II. Inertial testing methods for particle size analysis of pressurized inhalers. *Pharm. Res.* **10**: 454-456.

Phipps, P., R., and Gonda I. (1990). Droplets produced by medical nebulisers. Some factors affecting their size and solute concentration. *Chest* **97**:1327-1332.

Pischtiak, A. (1999). Solvay Fluor und Derivative. Chemical data Sheet for CFC and HFC Propellants.

Polli, G., P., Grim ,W., M., , Bacher, F., A., and Yunker M., H. (1969). Influence of formulation on aerosol particle size. *J.Pharm.Sci.* **58**: 484-486.

Porstendorfer., J. (1971). Unterschungen Zur Frage Wachstums Von Inhalierten Aerosolteilchen in Atemkrat. *Aerosol Sci.* **2:** 73-79.

Proctor, D., F., and Swift, D., L. (1977). Temperature and water vapour adjustment. In: Respiratory Defense Mechanisms, Part I. 95. Brain J., D., Proctor D., F., and Greid L., M. (Eds)., Marcel Dekker inc, New York.

Qian, J., and Law. J. (1997). "Regimes of Coalescence and Separation in Droplet collision". *J .Fluid. Mech.* **331**: 59-80.

Rayleigh, F. R. S. (1882). On the equilibrium of liquid conducting masses charged with electricity. *Philos. Mag.* **14**:184-186.

Reed,C.E. (1978). Physiology and pharmacology of $beta_2$ adrenergic agents_*Chest* **73**: 914-918.

Remington's Pharmaceutical Sciences. (1970). Gennaro, A., F. (Ed). Mack publishing Company, Easton, Pennsylvannia.

Riker Laboratories, Inc. (1960). Self-propelling, powder-dispensing compositions. US Patent # 837,465,

Robinson, R., A., and Stokes, R., H. (1959). Electrolyte Solutions. Butterworths, London.

Romagnoli, M., Papi, A., Baraldo, S., Fabbri, L., M. (1999). Difficult Asthma and chronic obstructive pulmonary disease (COPD): similarities and discrepancies. In: Holgate S.,T., Boushey H., A., and Fabbri ., L., M. (Eds). Difficult Asthma. Martin Dunitz. London, England.

Sayers, I., Le-Gros, G., and Harper, J., L. (2003). From Hygiene Hypothesis to Novel Allergic Asthma Therapeutics. *Current Medicinal Chemistry-Anti-Inflammatory & Anti-Allergy Agents.* 2; **2**: 143-155.

Sciarra, J., J., Patel, J., M., and Kapoor, A., L. (1972). Synthesis and formulation of a series of epinephrine salts as a dosge form. *J. Pharm. Sci.* Feb 61; **(2** : 219-223.

Scultz, R., K., Dupont, R., L., and Ledoux, K., A. (1994). Issues surrounding metered dose valve technology: past, present and future perspectives. In: Bryon P., R., Dalby R., N., and Farr S., J. (Eds). Proceedings of Respiratory Drug delivery IV . Buffalo Grove IL: Interpharm Press 211-219.

Seaver, M., Peele, J., R., Manuccia, T., J., Reubel, G., O., and Ritchie, G. (1992). Evaporation kinetics of ventilated water droplets coated with octadecanol monolayers. *J. Phys. Chem.* **96**: 6389-6394.

Seville, P., C., Simons, G., Taylor, G., and Dickinson, P., A. (2000). Prodrug to probe solution HFA pMDI formulation and pulmonary esterase activity. *Int. J. Pharm.* **195**: 13-16.

Sirignano, W. (1993). "Fluid Dynamics and Sprays – 1992 Freeman Scholar Lecture", *J. Fluids. Eng.* **115**: 345-378.

Sirignano, W. (1999). In: Fluid dynamics and transport of droplets and sprays. Cambridge University Press.

Smith G., Hiller C., Mazumder M., and Bone R., C. (1980). Aerodynamic size distribution of cromolyn sodium at ambient airway humidities. *Am. Rev. Resp Dis* **121**: 513-517.

Smyth, H., D., C. (2003). The influence of formulation variables on the performance of alternative propellant-driven metered dose inhalers. *Advanced Drug Delivery Reviews.* **55**: 807-828.

Smyth, H., D., C., Meija –Millan, E., A., and Hickey, A., J. (2002). The effect of ethanol on solvency, vapour pressure and emitted droplet size of solution metered dose inhalers containing HFA 134(a) *Proc. from Respiratory Drug Delivery VIII.* Tucson, Arizona. 735-738. Interpharm Press.

Soderholm, S.,C., and Ferron, G., A. (1992). Estimating the effects of evaporation and condensation on volatile aerosols during inhalation exposures. *J.Aer.Sci.* **23**:257.

Soderholm, S.,C., Anderson, D., A., Utell, M., J., and Ferron, G., A. (1991). Method of measuring the total deposition efficiency of volatile aerosols in humans. *J.Aer. Sci.* **22**: 917.

Sollner K. (1936) The mechanism of the formation of fogs by ultrasonic waves. *Trans Faraday Soc.* **32**: 1537-1539.

Solvay Fluor Data (2005) sheet. Solkane 227 and Solkane 134(a) pharma. HFA propellants for medical use.

Stalhofen, W., Rudolf, G., and James, A., C. (1989). Intercomparison of experimental regional aerosol deposition data. *J. Aerosol. Med.* **2**: 285-308.

Staniforth, J., N. (1994). The importance of electrostatic measurements in aerosol formulation and preformulation. In: *Proc from Respiratory Drug Delivery IV.* Deerfield IL.303-311.

Stapleton, K., W., and Finlay, W., H. (1995). Determining the solution concentration within aerosol droplets output by jet nebulisers. *J. Aer. Sci.* **26**:137-145.

Steele, H., M., and Hamill, P. (1981). Effects of temperature and humidity on the growth and optical properties of sulphuric acid water droplkets in the atmosphere. *J.Aerosol. Sci.* **12**: 517-528.

Stein, S., W., and Stefely, J., S. (2003). Reinventing Metered Dose Inhalers: From Poorly Efficient CFC's to highly efficient HFA's. *Drug Delivery Technology.* Article Index. 1-11.

Steventon, R., and Wilson, R. A guide to Apparatus for Home nebuliser Therapy. Allen & Hanbury Ltd, Middlesex, UK, 5-6.

Sturgess, J.,M. (1989) Ciliated cells of the lungs. In: Massaro D. (Ed). Lung Cell Biology. Marcel Dekker, New York. 115-151.

Swfit, D., L. (1996). Use of mathematical models in predicting the distribution of Inhaled therapeutic aerosols. In: Hickey A., J. (Ed.) Inhalation aerosols the physical and biological basis for therapy Marcel Dekker, New York.

Swift, D., L. and Proctor, D., F., (1977). Tempertaure and water vapour adjustment. In: Brain J., D., Proctor D., F., and Greid L., M. (Eds). Respiratory Defense Mechanisms, Part I. 63. Marcel Dekker inc, New York.

Tang, I., N., Munkelwitz, M., R., and Davis, J., G. (1977). Aerosol growth studies II. Preparation and growth measurements of monodisperse salt aerosols. *J. Aerosol. Sci.* **8**: 149-159.

Task Group on Lung Dynamics (1966) Deposition and retention models for internal dosimetry of the human respiratory tract. *Health Physics* **12**: 173-207

The Montréal Protocol on substances that deplete the Ozone layer. (1987). United Nations Environment Programme, The Ozone Secrateriat.

Tzou, T., Z. (1998) Density, excess molar volume, and vapour pressure of propellant mixtures in metered-dose inhalers: deviation from ideal mixtures: In Byron P., R., Dalby R., N., and Farr S., J. (Eds.) Respiratory Drug delivery VI. Interpharm Press, Buffalo Grove, IL. 439-443.

Tzou, T., Z., Pachuta, P., R., Coy R., B., and Schultz, R., K. (1997) Drug form selection in albuterol containing metered dose inhaler formulations and its impact on chemical and physical stability. *J. Pharm. Sci.* **86**: 1352-1357.

Vervaet, C., and Byron, P., R. (1999). Drug surfactant propellant interactions in HFA formulations. *Int. J. Pharm.* 186: 13-30.

Usmani, O., S., Bidescombe, M., F., Nightinglae, J., A., Underwood, S,. R., and Barnes, P,. J. (2003). Effects of broncjodilator size in asthmatic patients using monodisperse aerosols. *J.Appl. Physiol.* Nov, 95; **(5)** : 2016-2112.

Voorhees, P., W. (1985). Theory of Ostwald ripening. *J.Stat. Phys.* **38** ; 231-252.

Wadke, D., A., Serajuddin, A., T., M., and Jacobson, H. (1989). In: Pharamaceutical Dosage Forms. Vol 1 Second Edition. Lieberman H., A., Lachman L., Schawartz J., B. (Eds).Marcel Dekker Inc, New York.

Wagner, J.,G. (1961). Absorption aspects. *Biopharmaceutics*: **50:** 359-387.

Weber, C. (1931). Disintegration of liquid jets. Z. Agnew. Math. Mech. 11; **2**: 136-159.

Weibel, E.R. (1963) Morphometry of the human lung. Springer- Verlag Berlin.

Wildhaber, J., H. (1998). Aerosol Therapy. *Schweiz. Med. Wochenschur.* 128; **(33)**: 1223-1228.

Wells J., I. (1988). Pharmaceutical Preformulation. The physiochemical properties of drug substances. Ellis Horwood , UK.

Williams, R., O., III., Liu, J., and Koleng, J., J. (1997). Influence of Metering Chamber Volume and Water Level on the Emitted Dose of a Suspension- based pMDI Containing Propellant 134(a). *Pharm Res.* **14**: 4:438-434.

Zanen P., Go L., T., and Lammers, J-W. (1994). The optimal particle size for parasympatholytic aerosols in mild asthmatics *Int. J. Pharm.* **114:** 111-115.